UNIVERSIDAD
DE GRANADA

PROGRAMA DE DOCTORADO EN BIOMEDICINA

FACULTAD DE MEDICINA

TESIS DOCTORAL

•

"DEVELOPMENT OF NEW BIOMIMETIC BIOINKS USEFUL IN 3D BIOPRINTING OF CARTILAGE TISSUE"

Memoria presentada por Cristina Antich Acedo

GRANADA, Febrero 2020

Editor: Universidad de Granada. Tesis Doctorales
Autor: Cristina Antich Acedo
ISBN: 978-84-1117-331-5
URI: http://hdl.handle.net/10481/74727

INDEX

SUMMARY

Articular cartilage is a tissue with important functions in preserving and enabling locomotion. However, it has limited intrinsic repair capacity when is damaged, which requires medical intervention. Conventional treatments for cartilage regeneration are not successful enough to repair articular cartilage defects. In the search of alternatives, bioprinting technology approaches are being explored as a promising solution, allowing the fabrication of viable cartilage substitutes by controlled deposition of cells and biomaterials that mimic the native tissue. For this, the selection of a suitable bioink (cell-carrier material), in terms of biological and mechanical properties, is crucial.

Among biomaterials, natural polysaccharides are one of the most attractive, due to structural similarities and high-water retention, that resemble native environment of cartilage. Another approach that has been recently explored is the use of decellularized extracellular matrix derived from tissue (tdECM), which provides unique biochemical cues and microenvironment. However, it entails some issues such as limited donor tissue availability, morbidity or immunogenicity. As alternative source, cell culture is gaining a lot of attention especially with mesenchymal stem cells (MSCs), as these allows to generate easily biomimetic matrices, overcoming limitations that entail extracellular matrix (ECM) derived from tissue.

The first objective of our study was to develop a new biomimetic bioink based on natural biomaterials, such as hyaluronic acid (HA), a main cartilage component, and alginate, which also provides suitable mechanical properties for cartilage tissue 3D bioprinting. The analysis of the main characteristics required for this application revealed an appropriate printability, jellying abilities, stiffness and degradability of this natural biomimetic bioink. In addition, biological assays demonstrated the positive effect of HA, improving the ability of chondrocytes to proliferate and produce ECM components, collagen type II and glycosaminoglycans (GAGs). The analysis of gene expression also indicated that it facilitates phenotype maintenance for long-term culture, increasing the expression of mature chondrocyte genes (collagen type II,

aggrecan and Sox9) and reducing non-specific genes, such as fibrotic (Collagen type I) and hypertrophic (Collagen X) markers.

The second objective was to develop a biomimetic bioink that better resembles chondrogenic environment based on decellularized ECM derived from MSCs in culture (dECM). In this attempt, we first were able to generate a matrix with a composition similar to that in early-step chondrogenic process, proving elements necessaries for tissue development not present in mature cartilaginous ECM. After its effective decellularization, demonstrated by maximal cellular removal and minimal matrix subtraction, it was possible to formulate a bioink with suitable properties to be applied in 3D bioprinting, such as shear thinning behavior, good shear recovery and gelling abilities. In addition to mechanical properties, its biocompatibility and bioactive properties were also demonstrated. We could evidence, by gene expression and histological assays, that this novel biomimetic bioink, at different concentrations, was capable to induce chondrogenesis of MSCs and cartilage tissue formation both *in vitro* e *in vivo*.

Summarizing, here we present a robust and extensive study in which two different biomimetic bioinks suitable for cartilage 3D bioprinting were developed, demonstrating their biological and mechanical properties *in vitro* e *in vivo*, and encouraging its future application in the clinical arena.

RESUMEN

El cartílago articular es un tejido con funciones importantes en la preservación y ejecución de la locomoción. No obstante, tiene una capacidad de reparación intrínseca limitada cuando éste se daña, que requiere intervención médica. Los tratamientos convencionales para la regeneración del cartílago no son suficientemente efectivas para reparar los defectos del cartílago articular. En la búsqueda de alternativas, la tecnología de bioimpresión se está considerando una opción prometedora, puesto que permite la fabricación de sustitutos viables de cartílago mediante la deposición controlada de células y biomateriales, que imitan el tejido nativo. Para ello, la selección de una biotinta (material portador de células) adecuada, en términos biológicos y mecánicos, es crucial.

Entre los biomateriales disponibles actualmente, los polisacáridos naturales son uno de los más atractivos, debido a sus características estructurales y a su alta capacidad de retención de agua que permiten proporcionar un ambiente semejante al del cartílago nativo. Otro posibilidad que se ha explorado recientemente es el uso de la matriz extracelular descelularizada derivada de tejido (tdECM), capaz de proporcionar unas señales bioquímicas y un microambiente únicos. Sin embargo, conlleva algunos problemas, como la disponibilidad limitada de tejido donante, la morbilidad o la inmunogenicidad. Como fuente alternativa, el cultivo celular está recibiendo una gran atención, especialmente de las Células Madre Mesenquimales (MSCs), ya que éstas permiten generar fácilmente matrices biomiméticas, sin presentar las limitaciones que supone la matriz derivada de los tejidos.

El primer objetivo de nuestro estudio fue desarrollar una nieva biotinta biomimética basada en biomateriales naturales, como el ácido hialurónico (HA), uno de los principales componentes del cartílago, y el alginato, que además proporciona una propiedades mecánicas adecuadas para la bioimpresión 3D. El análisis de las características principales requeridas para dicha aplicación determinó que esta biotinta bimimética poseía una adecuada printabilidad, capacidad de gelificación, rigidez y degradabilidad. Además, los ensayos biológicos evidenciaron el efecto positivo de HA, el cual mejoró la capacidad de los condrocitos para proliferar y producir componentes de la matriz extracelular, colágeno tipo II y glucosaminoglicanos. El análisis de la

expresión génica también indicó una mejora en el mantenimiento del fenotipo para el cultivo a largo plazo, aumentando la expresión de los marcadores específicos de condrocitos maduros (colágeno tipo II, agrecano y Sox9) y reduciendo los no específicos de cartílago hialino, como el marcador fibrótico (colágeno tipo I) y el hipertrófico (Colágeno X).

El segundo objetivo fue desarrollar una biotinta biomimética que asemejara mejor el ambiente condrogénico, a partir de matriz derivada de MSCs en cultivo. Para ello, primero se generó una matriz con una composición similar a la establecida durante el proceso condrogénico embrionario, conteniendo los elementos necesarios para el desarrollo del tejido y que no están presentes en la matriz cartilaginosa madura. Después de su efectiva descelularización, demostrada por la eliminación máxima de contenido celular y la sustracción mínima de la matriz, fue posible formular un biotinta con propiedades adecuadas para su aplicación en la bioimpresión 3D, como viscoelasticidad, gran capacidad de recuperación y de gelificación. Además de las propiedades mecánicas, también se demostró su biocompatibilidad y propiedades bioactivas. Mediante el análisis de expresión génica e histológicos se determinó que esta nueva biotinta biomimética, a diferentes concentraciones, fue capaz de inducir la condrogénesis de MSCs y la formación de tejido de cartílago, tanto in vitro como in vivo.

En resumen, aquí presentamos un estudio robusto y extenso en el que se desarrollaron dos bioenlaces biomiméticos diferentes adecuados para la bioimpresión 3D de cartílago, demostrando sus propiedades biológicas y mecánicas in vitro e in vivo, y alentamos su futura aplicación en el ámbito clínico.

I. INTRODUCTION

I.1. ARTICULAR HYALINE CARTILAGE

Articular cartilage is a highly specialized connective tissue that belongs to the group of hyaline cartilages. It is a thin layer of hydrated tissue that covers the ends of long bones at the joints. Its principal function is to provide a smooth, lubricated surface for articulation and to facilitate the transmission of loads with a low frictional coefficient [1].

Unlike most tissues, articular cartilage does not have blood vessels, nerves, or lymphatics. It is composed of a dense and organized ECM with a sparse distribution of highly specialized cells called chondrocytes (2% of tissue volume). The ECM is principally composed of water (68–85%), collagen (15–22%) and proteoglycans (4–7%), with other non-collagenous proteins and glycoproteins present in less amount [2]. All these components, which are continuously synthesized and modified by the chondrocytes, are critical to maintain the unique mechanical properties of cartilage. The collagens, mainly type II, form fibrils that are arranged into a fibrous network and provide tensile strength to the tissue especially at the surface, which is continuously subjected to shear strain during articulation. Meanwhile, proteoglycans, principally aggrecan, forms large aggregates in the matrix, binds to water and provides compressive stiffness to withstand large loads. Minor constituents of the ECM, such as non-fibrillar collagens IX, XI or small proteoglycans biglycan, fibromodulin, decorin and lumican also play an important role in the regulation and formation of this collagen network [3,4].

The elements that constitute articular cartilage are not evenly distributed and organized in the depth of the tissue (Figure 1). Therefore, it can be divided into four distinct zones: superficial, middle, deep and calcified zones. The superficial zone (10%–20% of total thickness) is characterized by tightly packed, tangentially oriented collagen fibrils and a relatively low proteoglycan content. This arrangement provides tensile properties, protecting the deeper layers from stresses and compression. The middle zone (40–60% of cartilage volume) is characterized by randomly oriented collagen fibrils and the highest proteoglycan content, which may contribute to the higher compression modulus in this layer, caused by the larger osmotic water swelling effect. The deep zone (30%–40% of articular cartilage thickness) exhibits radially oriented, larger diameter

collagen fibers and a lower proteoglycan content than the middle zone. The cell density of chondrocytes decreases from the superficial zone to the deep zone, and their morphology changes from a flattened discoidal shape in the superficial zone, to a more spherical shape in the middle zone, to a slightly elongated form in the deep zone. The calcified zone provides a transition between the hyaline cartilage tissue of the overlying zones and the basal subchondral bone. Within this, the cartilage ECM is mineralized and type II collagen is replaced by type X collagen[5–8].

In addition to the zonal division of articular cartilage tissue, the ECM displays some regional variation in the arrangement of its components around the cells (Figure 1). These are defined as the pericellular matrix, territorial matrix and interterritorial matrix [5,6,8]. All the chondrocytes are surrounded by a pericellular region, known as chondron, which is characterized by the absence of collagen network, with the exception of collagen type VI, and a high concentration of other molecules such as proteoglycans (aggrecan, hyaluronan, decorin and biglycan) and glycoproteins (fibronectin, link protein, and laminin). Surrounding the pericellular region, there is a fine fibrillar network of collagen confined to an area defined as territorial region. All these molecules in both regions (around 2-5 µm of thickness each one) allow the chondrocytes to bind to the interterritorial matrix and protect them during mechanical loading. The interterritorial matrix, that is the largest portion of cartilage (more than 5 µm from the surface of chondrocytes) responsible for the zonal architecture of cartilage, contains the most type II collagen and the lowest amount of aggrecan.

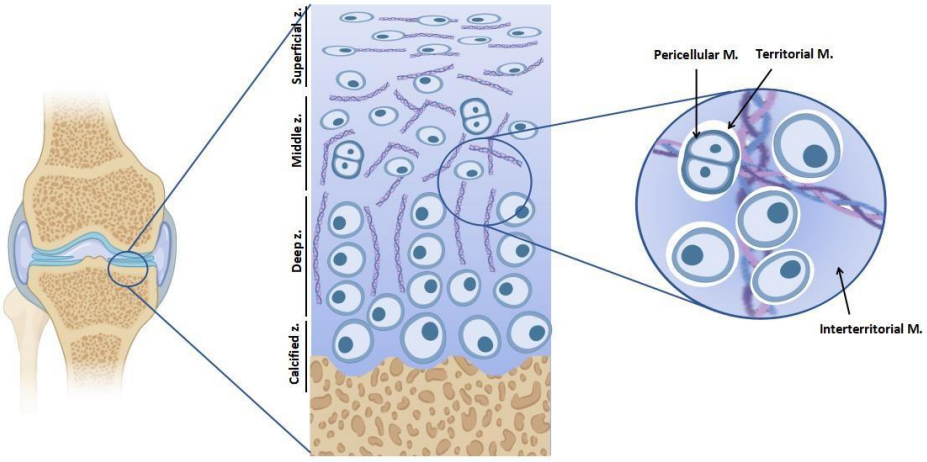

Figure 1. Internal structure of articular cartilage tissue.

I.2. CHONDRAL PATHOLOGY

Due to the unique tissue's structure and physiology (avascular, abneural, low cell density and proliferative activity), healing ability of articular cartilage is extremely limited upon traumatic joint injuries, abnormal joint loading or degenerative joint diseases such as Osteoarthritis [8]. The intrinsic repair response leads to the formation of so-called fibrocartilage, which is functionally and biomechanically inferior to the original hyaline cartilage. This fact makes the tissue more prone to further deterioration, and thus initiates a vicious cycle that eventually results in the dysfunction of the joint [4,9–11] .

I.3. CURRENT TREATMENTS

The defect or injury can be classified as partial thickness defects, confined to cartilage zone, or full thickness defects, also affecting subchondral bone [12–15]. Currently, there are different treatments for patients depending on the severity of damage (Table 1). Nonsurgical treatment that mainly alleviate the pain without correcting the underlying pathology, includes activity modification, physical therapy, dietary supplements, weight loss, anti-inflammatory drugs (e.g., aspirin, ibuprofen, celecoxib) and injections of viscous hyaluronan preparations into the synovial cavity. In an attempt to repair damaged tissue, surgical treatments have been used, involving stimulation and replacement techniques. First procedures take advantage of the natural ability of cells to repair, since they participate in the formation and restore of tissue. It can be conducted by cell implantation, chondrocytes or MSCs (autologous chondrocyte implantation (ACI)-like procedures), or by recruitment from surrounding tissues (abrasion arthroplasty, drilling and microfracture). The other approach represents a means of substituting the defect with healthy tissue (autologous, or mosaicplasty, and allogeneic osteochondral grafting).

Despite these techniques have fairly acceptance in the clinic and are commonly used, they present several limitations [12,13,15,16]. Generally, it still remains full correction of the pathology. None of them have led to tissue formation with structural,

functional and biomechanical properties equivalent to native cartilage and/or subchondral bone. At long term, many cases result in joint deterioration, being total joint replacement with artificial prosthesis the ultimate option at this stage. Currently, researchers are trying to find effective approaches to treat cartilage defects and overcome those drawbacks.

Treatment	*Description*	*Benefits*	*Limitations*
Non-surgical	Oral analgesia, weight loss, physiotherapy	May avoid surgery	Only masks symptoms, chronic use of pain medications
Arthroscopic chondroplasty	Minimally invasive resection of loose cartilage to decrease mechanical joint irritation	Simple procedure, immediate weight bearing	Only masks symptoms
Microfracture	Minimally invasive arthroscopic surgical procedure that breaches the subchondral bone with a pick to release osteoprogenitor cells into a defect to encourage fibrocartilage growth	Minimally invasive, no tissue grafts required, only routine surgical instruments needed, used for lesions <2.5 cm^2	Fibrocartilage biomechanically inferior to hyaline cartilage, brief period of non-weight bearing, unclear impact on development of Arthritis
Mosaicplasty/ osteochondral autograft transfer	Uses multiple osteochondral autografts harvested from the patient's femur to fill an osteochondral defect	No allograft, theoretically fills in with hyaline cartilage. Used to treat lesions from 1-4 cm^2	Graft-site mismatch may not recreate native joint mechanics, graft-site morbidity, cannot treat large lesions, lack of integration with surrounding tissues
ACI	Harvested chondrocytes are cultured prior to being re-implanted into the defect. An evolving procedure due to advances in tissue engineering	May produce hyaline cartilage, can treat lesions 2-10 cm^2	Graft delamination, periosteal hypertrophy, questionable ability to produce hyaline cartilage
Osteochondral allograft transfer	Uses allogenic (cadaveric) osteochondral tissue to fill defect	Can treat large lesions, no graft-site morbidity	Allogenic tissue (potential for disease transmission), size/depth mismatch, questionable chondrocyte viability, lack of integration with surrounding
Joint arthroplasty	Resects and replaces arthritic bone with an artificial joint, most commonly metal implants separated by a polyethylene liner	Pain relief, variable return to function	Variable return to function/activity limitations, infection, Implants wear out over time (need for re-operation), cannot completely recreate native anatomy or mechanics

Table 1. Current clinical options for the treatment of cartilage defects Modified from [17]

I.4. NEW THERAPEUTIC STRATEGIES: TISSUE ENGINEERING

Technological advances in many areas have opened up a new concept to address the previously described current limitations and to provide new and more effective treatments. This area is usually named as tissue engineering [18] and it is included in the novel medical approach known as regenerative medicine. It is a multidisciplinary strategy that applies the principles of engineering, materials sciences and life sciences to develop biological substitutes that restore, maintain, or improve tissue functionality. In cartilage tissue engineering (CTE), the main goal is to create artificially cartilage-like constructs with mechanical and biological characteristics that are reminiscent of native tissue, to promote long-lasting, functional repair of defective articular cartilage lesions.

This approach involves three principal elements: scaffolds, cells and bioactive molecules (i.e., growth factors and proteins), which are combined to produce engineered tissues *in vitro* or as a regenerative medicine strategy *in vivo* [13,17,19] (Figure 2).

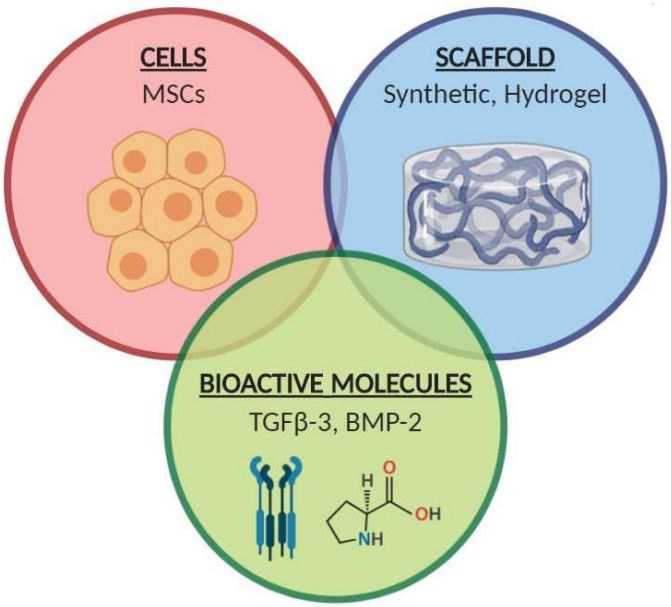

Figure 2. Principal elements of Tissue Engineering: cells, scaffolds and bioactive molecules.

- Cells

Among the various cell types that have been contemplated for CTE, chondrocytes have been considered the logical option, as they are the unique cell type in mature articular cartilage and are responsible for the secretion and maintenance of the ECM [13,19]. These cells are mainly isolated from articular cartilage, although there are other sources such as non-articular sites (e.g. septal or costal sites) or elastic cartilage (e.g. auricular). However, these cells suffer from two major concerns: their instability in monolayer culture and the scarcity of donor tissue [13,20,21]. A potential alternative is the use of stem cells. Particularly, mesenchymal or progenitor stem cells have been considered as an attractive source of cells for cartilage engineering as they have easy availability, have high capacity of *in vitro* expansion and possess ability to differentiate into chondrocyte lineages [22]. They are derived from a variety of tissues including bone marrow, umbilical cord blood, periosteum, adipose tissue and dental pulp, but not all of them have the same chondrogenic potential [9,23]. In this regard, a lot of efforts have been focused on understanding the key signaling that regulates MSC chondrogenesis to consistently generate improved and stable cartilage from MSCs. Similarly, chondrogenic stem/progenitor cells (CSPCs), recently discovered in the superficial zone of articular cartilage, have showed a high therapeutic potential, superior to chondrocytes. However, there are certain issues related with identification and purification of these cells from tissue, due to the lack of well-defined markers. The use of pluripotent stem cells, as embryonic stem cells (ESCs) or induced pluripotent stem cells (iPS), is also a reality, but it remains in an early stage [24]. More studies are needed to solve the problems related with ethical issues, their capacity to develop tumors *in vivo* and antigenicity.

- Scaffolds

The role of the scaffold in tissue engineering is to provide a temporary substrate and microenvironment for cells in order to grow and promote the formation of desired tissue. A considerable amount of materials have been developed and evaluated for CTE [13,16,25,26]. Scaffolds are classified based on the source of material, that can be natural or synthetic. Natural materials are most widely used as they are both biodegradable and biocompatible and provide a more physiological environment for

cells. These materials may be further divided into protein-based matrices, being the most common collagen, gelatin, fibrin or silk; and carbohydrate-based matrices such as alginate, agarose, chitosan, or hyaluronan, although the best candidate currently is the dECM obtained from native tissue. On the other hand, synthetic materials have the advantage of being easily manipulated, with controllable chemical and physical properties, in order to fabricate customized scaffolds that match the features of native tissue or get enhanced chondrogenic potential. They generally include poly (glycolic acid) (PGA), poly(lactic acid) (PLA), poly(lactic-co-glycolic acid) (PLGA), poly-caprolactone (PCL), poly(ethyl glycol) (PEG), poly(vinyl alcohol) (PVA), poloxamers, polyurethane, and self-assembling peptides. Despite this great diversity of biomaterials, the trend in CTE is to combine natural and synthetic biomaterials to exploit the advantages of each one and, therefore, to improve tissue formation.

As tissue formation is affected not only by composition but also architecture and topography, scaffolds have been produced in several forms and different techniques used in order to reproduce the structure of articular cartilage. These fabrication methods include solvent casting, particulate leaching, phase separation, freeze-drying, gas foaming, molding, stereolithography or electrospinning, among others [16,27,28].

- Bioactive molecules

Apart from an appropriate scaffold, cartilage formation will also require the use of signaling factors that will induce specific differentiation pathways toward the chondrogenic lineage or maintenance of chondrogenic phenotype. Several growth and differentiation factors that are involved in regulating cartilage development and homeostasis of mature articular cartilage have been identified and employed in CTE to induce, accelerate, maintain, and/or enhance cartilage formation [17,29,30]. These factors include transforming growth factor family (TGF-βs), bone morphogenetic proteins (BMPs), insulin-like growth factors (IGFs), and fibroblast growth factors (FGFs). Other factors also involved in chondrogenesis are parathyroid hormone-related protein (PTHrP) or thyroid hormone [28,31]. Furthermore, in an attempt to reproduce the complexity of the biological environment, the combination of these factors, dose and release regimes have also been studied. Several methods have been developed such as

the incorporation into scaffolds for spatiotemporal control signaling, programmed delivery by attachment or nanoparticles, or transfection of transcription factors into the cells [28,29,31] .

I.5. 3D BIOPRINTING

Conventional methods that have been previously mentioned to fabricate scaffolds allow to create constructs that may closely match the natural structure of cartilage, by inducing patterns based on fibers or pores. However, most of them lack of precise control of internal structural features and topology. Recently, three dimensional (3D) printing technology has emerged in CTE as a powerful alternative to all these approaches, promising to bridge the divergence between artificially engineered tissue constructs and native tissue [32].

3D printing is a rapid prototyping and additive manufacturing technique used to fabricate complex structures with precise deposition of a material through a layer-by-layer building process [32–34]. Its application in regenerative medicine, known as bioprinting, has enabled to create engineered tissue constructs by controlled delivery of living cells, molecules and biomaterials, often referred as “bioink”, in predefined 3D patterns that mimic native tissues. This technique not only allows to accurately recapitulate microstructural features and complex architecture of target tissue but also produce tailorable scaffolds for patients, based on medical images acquired with non-invasive techniques such as Magnetic Resonance Imaging (MRI) and Computerized Tomography (CT).

I.5.1. 3D Bioprinting Techniques

3D bioprinting was developed in several ways, depending on principles of material releasing and it can be based on jetting, extrusion or laser technology (Figure 3).

- Extrusion-Based 3D Bioprinting:

Among the printing options, this method has been the most utilized for the fabrication of tissue engineering constructs, including cartilage tissue. In a extrusion bioprinting system, the material or bioink is continuously deposited onto the printing platform through a computer-controlled nozzle *via* motor-driven plungers or pneumatic pressure. It has the advantage of printing at high speed a broad range of cell-carrier materials, called bioinks, at different viscosities and minimal cell damage. Once the bioink is printed, it can be crosslinked by ionic, photo, and/or thermal-based mechanisms.

- Jetting-based 3D bioprinting

This technique consists in delivering small droplets of bioink (1–100 picolitres; 10–50 μm diameter) on a platform in a predefined pattern. These droplets are generated by the aid of piezoelectric or thermal actuators, and jellify after deposition by UV light, ionic, thermal or chemical cross-linking methods. Although the main drawback of inkjet bioprinting is the limited bioink selection, only at low viscosities (~ 0.1 Pa), this technique enables to control the small volume of liquid and achieve higher resolutions than extrusion methodology.

- Laser-Based 3D Bioprinting

Laser-based 3D bioprinting is an expensive and complex technique that uses pulsed laser energy to transfer materials to a receiving substrate. Laser pulses are targeted on a layer of a ribbon, creating a high-pressure bubble, which drives the bioink towards a substrate. This is a nozzle-free procedure that allows the fabrication of accurate micro-structured scaffolds. However, its use is restricted due to the high cost, selection of low-viscosity bioinks and poor cell viability in comparison to other techniques.

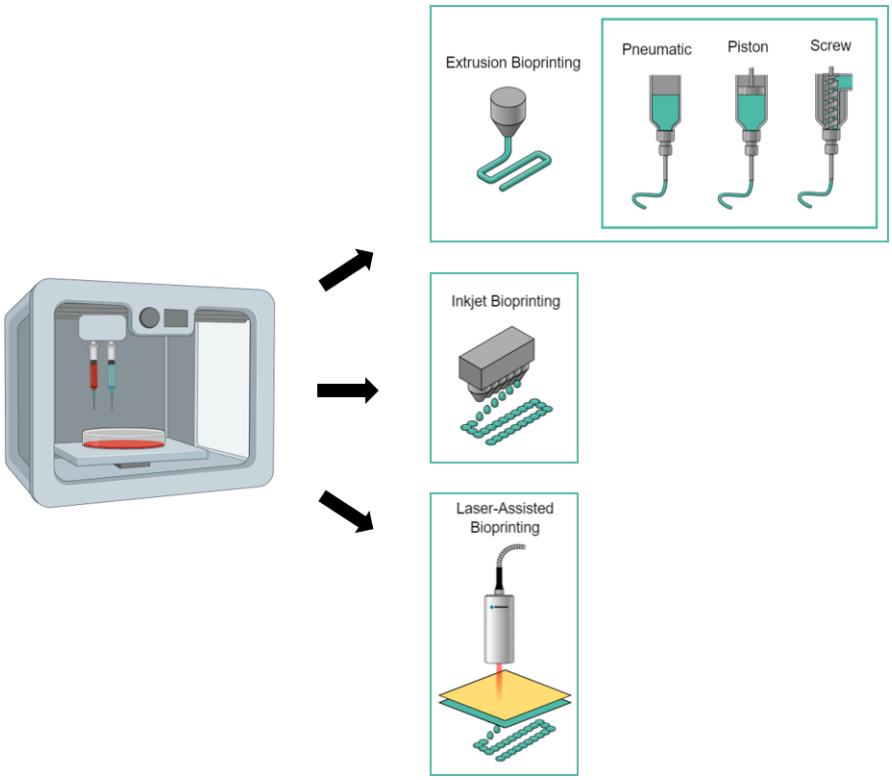

Figure 3. Schematics of the major 3D bioprinting mechanisms.

I.6. 3D BIOPRINTING IN CARTILAGE TISSUE ENGINEERING

To date, there is a lot of research focus on cartilage 3D bioprinting [35,36]. Theoretically, this tissue should be relatively simple to replicate, since it is relatively acellular, avascular, and abneural. For that, a variety of cell and biomaterials have been used, involving mainly extrusion-based techniques.

I.6.1. Bioinks

With the emergence of 3D bioprinting, the role of material in tissue engineering has changed. Now, it acts not only as a suitable substrate for cell adhesion, proliferation and differentiation, in the guidance of tissue generation, but also as a cell-carrier providing a supportive ECM environment that protects cells from printing-associated stresses [37–39].

In general terms, hydrogels are the most common materials used for bioink formulation, as they facilitate homogeneous cell encapsulation in a highly hydrated and mechanically supportive 3D environment, which is similar to that of articular cartilage [39,40]. Ideally, hydrogels should: (i) have good printability; (ii) have a high degree of biocompatibility, without being toxic or eliciting any immunological reactions; (iii) be able to gel by a cell-friendly method; (iv) have good mechanical stability; (v) have good biodegradability and (vi) be able to support cellular activities such as adhesion, migration, proliferation and differentiation. Other important factors to be considered are the price of material, regulatory issues, shelf-life, and easy-handling [38].

I.6.2. Biomaterials used for bioink formulation

Taking inspiration from ECM, which has an important role on cell regulation, researchers have developed bioinks that recreate to some extent the composition or properties of native articular cartilage to guide tissue-specific formation. To date, numerous biomaterials have been explored for bioprinting cartilage constructs [35,41–43] (Table 2).

- Natural components:

Alginate

Alginate, a linear anionic polysaccharide of mannuronic acid and guluronic acid obtained from seaweeds and algae, has been one of the biomaterials mostly used in 3D bioprinting. It has an excellent biocompatibility and properties that are required for a good printability, such as viscosity and instant gelation by mixing with multivalent cations [44,45]. Moreover, the high hydrophilic nature and lack of cell adhesion sites make alginate a good candidate to reproduce cartilaginous ECM. In CTE bioprinting, alginate has been widely used alone or in combination to improve the printability of many biomaterials [19,41,45]. Additionally, it has been chemically modified with

peptides (e.g. RGD) or by oxidation, to improve cellular functions and stability of 3D printed structures [46–48].

Agarose

Agarose is other polysaccharide obtained from seaweed that has been commonly used for CTE bioprinting due to its biocompatibility, gelation properties and mechanical strength. Like alginate, it provides an environment that resemble native tissue, retaining round morphology of cells and inducing chondrogenic differentiation of MSCs [35,43]. Moreover, its gelation is based on a temperature-responsive process, which makes it unnecessary to use another linker.

Collagen

Collagen, as the main protein components in natural cartilage, has been a promising biomaterial for bioink development. Although around 90% of its dry weight is collagen type II, type I collagen has been mostly used for CTE bioprinting because of its easy availability. Collagen-based bioinks display great biocompatibility and biodegradation, related to many RGD domains which facilitates cell adhesion and growth. However, it has some limitations, such as slow gelation rate and poor mechanical properties, that difficult its bioprinting. In addition, collagen is known to decrease in volume up to 20%–30% once gelled due to cellular contractile remodeling [49]. In CTE, these issues have been overcome by additional crosslinking *via* photo-polymerization, enzymatical procedures (genipin and transglutaminase) or other chemical reaction (e.g. with aldehydes, carbodiimides, isocyanates) [50–53]. Its combination with more biomaterials, such as poloxamer, agarose or alginate has also improved tissue formation in 3D-printed cartilage constructs [54–56]. Nevertheless, controversy persists about the perfect source of collagen since most of them come from animals and cadavers, that could entail disease transmission and immunogenicity. Currently, recombinant human collagen based on plant materials provides an alternative. It has been evidenced to play a similar role as natural ECM collagen in the tissue regeneration process.

Gelatin

Gelatin is the denatured form of collagen. It has been widely used in CTE bioprinting due to its inverse thermosensitive properties, which enable the development of shaped fidelity structures at room temperature [38]. However, its low stability at physiological temperatures has led to be chemically modified. In this way, methacryloyl-modified gelatin (GelMA) has gained increasing attention to fabricate cartilage constructs by 3D bioprinting, since it can be photo-crosslinked at mild conditions (e.g., neutral pH, room temperature, in water-based solutions), through exposure to UV light [57]. Like collagen, other approaches have involved the combination of gelatin and derivates with other natural biomaterials such as silk, hyaluronic acid (HA), alginate or chondroitin sulfate (CS) [43,58–60]. Many studies that used gelatin for CTE bioprinting have reported not only to improve mechanical properties of the constructs during printing process but also to promote chondrogenesis [60].

Glycosaminoglycans *(GAGs)*

GAGs (HA, heparin, heparin sulfate -HS- and CS) are linear, anionic and highly heterogeneous carbohydrate polymers composed of repeating disaccharide units, which are commonly uronic acid and hexosamine (glucosamine or galactosamine). Except for HA, such chains are bound to a central protein to form proteoglycans. Along with collagen II, GAGs are the main components in cartilage ECM, where regulate matrix assembly and cell–matrix interactions *via* interacting with various structural proteins (e.g., fibronectin and collagen) and signaling molecules (e.g., growth factors and chemokines) [3,4].

HA, as a main component of aggrecan, is important in regulating not only cartilaginous matrix but also in some key cellular processes of chondrocytes, such as morphogenesis, metabolism and proliferation [61]. However, HA alone is not suitable for 3D printing due to its unstable polymerization properties [62]. In this regard, HA has been widely used as bioink for cartilage 3D bioprinting through chemical modification with crosslinkable groups and/or blending with printable hydrogels (i.e. GelMA) [63–65].

So far, studies that used HA for CTE bioprinting have evidenced its protective and chondro-inductive role. Among these, it is noteworthy the recent approach consisted in combination of HA with collagen and CS, which resulted in an improved ECM-mimicking bioink capable to induce chondrogenesis and cartilage-specific matrix deposition [36].

Other natural materials

Due to the importance of mechanical properties of bioink in the 3D bioprinting field, other polymers such as gellan gum, nanocellulose or fibroin silk has been used in combination with biomaterials described above, to prepare bioinks with attractive rheological properties and to improve the shape fidelity of the bioprinted cartilage constructs. Moreover, such polymers are relatively inexpensive to produce, and has fine processability and tunable mechanical properties that are important for bioprinting processes [35,62].

- Synthetic materials

Poloxamers

Poloxamers, also known by the trade names *Synperonics, Pluronics,* and *Kolliphor*, are nonionic triblock copolymers composed of a central hydrophobic chain of polyoxypropylene flanked by two hydrophilic chains of polyoxymethylene. They are widely used in extrusion-based bioprinting. Like gelatin, its suitable printability is attributed to inverse thermo-gelling properties, which allows to flow at low temperatures and gel at room temperature [38]. In CTE bioprinting, poloxamers have been chemically modified with photo-crosslinkable groups (acrylates) or degradable sequences to improve mechanical stability and degradation of gels [66]. Moreover, it has been used as temporal supportive material of bioink such as GelMA or HA-derivative [67,68]. Although poloxamers have demonstrated to exhibit suitable properties for 3D bioprinting, unsatisfactory results related to long-term cell survival makes necessary to improve its formulation [68].

Poly(ethylene glycol) (PEG)

PEG is a linear polyether hydrophilic compound that can be conjugated with enzymes, liposomes, and other biomolecules [69] . This synthetic polymer is water soluble and its features can be manipulated through variation of its chemistry, being the most common in printing application the addition of diacrylate (DA) and methacrylate (MA) [70,71]. Its non-adhesive properties and great mechanical stiffness, in comparison to naturally-derived polymers, have made PEG very suitable for CTE, therefore, it has been extensively used for bioprinting of cartilage constructs [71] .

Bioink	Cell type	Polymerization	Reference
Alginate	Chondrocytes; ACPCs; MSCs; ATDC5 cell line	$CaCl_2$	[72–76]
Alginate /Agarose	Chondrocytes	$CaCl_2$/Temperature	[77]
Alginate/Methylcellulose	MSC	$CaCl_2$	[78]
Alginate /Collagen I	Chondrocytes	$CaCl_2$/Temperature	[77]
Alginate/ Nanocellulose	Chondrocytes; MSCs; Human iPSC	$CaCl_2$ $CaCl_2/H_2O_2$	[79–81]
Alginate/ Nanocellulose/HA	iPSCs and Chondrocytes	$CaCl_2$	[81]
Alginate/Pluronic F127	MSCs	$CaCl_2$	[82]
Alginate/ dECM	Chondrocytes	$CaCl_2$	[83,84]
Agarose	Chondrocytes; MSC; hMG-63 from osteosarcoma;	Temperature	[73,85]
Collagen	Chondrocytes	Temperature	[86]
Collagen I/ HA	MSCs	$CaCl_2$	[55]
Collagen /Fibrinogen	Chondrocytes	Temperature	[87]
GelMA	Chondrocytes; MSCs	UV	[73,88]
GelMA-Guar Gum	Chondrocytes	UV	[89]
GelMA/HA	MSCs	UV	[90]
GelMA/Pluronic F-127	ACPCs, MSCs, chondrocytes	UV/Temperature	[91]
GelMA/HAMA	ASCs	UV	[92,93]
GelMA/Poloxamer	chondrocytes	UV	[94]
Collagen II	Chondrocytes	Temperature	[95]
GelMA/CS-AEMA/HAMA	MSC	$CaCl_2$	[96]
CSMA/$M_{15}P_{10}$	ATDC5 cells	UV	[97]
CSMA/$M_{15}P_{10}$/HAMA	Chondrocytes	UV	[97]
Atelocollagen/CBDAH	MSCs	-	[98]
Cell ink	Chondrocytes	$CaCl_2$	[99]
PEGDMA	Chondrocytes; MSCs	UV	[100,101]
PEGDMA + GelMA	MSCs	UV	[26,70]
Peptide conjugated PEG	MSCs	-	[26]
polyHPMA-lac-PEG/HAMA	Chondrocytes	UV	[42]
PEG/Partially methacrylated poly(N-(2-hydroxypropyl) methacrylamide mono/ dilactate)	Chondrocytes	UV	[97]

Table 2. Bioinks used in CTE bioprinting

I.6.3. Current approaches

- Internal structure and composition

As it has been previously mentioned, many bioinks based on individual biomaterials have been developed for CTE bioprinting, but the current tendency is the use of composites. The combination of several materials, both natural and/or synthetic, allows to formulate bioinks that reproduce much better zonal composition of articular cartilage [35,86,95,102,103].

To recreate biochemical complexity of ECM, biomaterials have also been loaded or modified with various bioactive factors, sequences and portions from entire protein of ECM, using techniques such as peptide-based self-assembly [19]. More recent strategies have involved the use of dECM obtained from tissues as a novel source of material to formulate a bioink [104–106]. It is a simple way to provide the specific composition of native tissue and, therefore, to create an optimal microenvironment to support biological tissue response. For the bioprinting process, decellularized ECM from tissue (tdMEC) also offers some benefits, as the abundant collagenous proteins that facilitate easy crosslinking through temperature-responsible gelation under physiological conditions. Results from its recent application in CTE bioprinting have revealed that it may contribute to support and guide the generation of articular cartilage better than others materials commonly used. Cartilage dECM bioink has shown to have chondro-inductivity and potential for supporting new matrix synthesis, without the need for further functionalization [62,106] .

- Mechanical properties

The design of hard tissues like articular cartilage, requires mechanical properties that are difficult to reproduce using only bioinks. This fact has promoted the development of

hybrid bioprinting technology [69,107]. In this way, bioinks are reinforced with co-printing of structural degradable polymers in order to match the mechanical properties that are difficult to reproduce only with bioinks [108]. The materials mostly used in CTE as supportive elements have been thermoplastic polymers such as PLA, PCL, poly PGA and combinations such as PLGA or poly (*ε*-caprolactone-*co*-lactide) (PLCL) [26,75,98,106,109].

Polylactic acid is a highly versatile, aliphatic polyester derived 100% from renewable agricultural resources. It has been approved by Federal Drug Administration (FDA, USA) for use in medical applications owing to its mechanical property profile, thermoplastic processability and biological properties, such as biocompatibility and biodegradability. In cartilage and bone tissue engineering, PLA is one of the most favorable matrix materials and provides excellent properties at low price. It has been reported to be an effective scaffold agent alone or in combination with various hydrogels [110,111].

Polycaprolactone (PCL) is another synthetic polyester approved by FDA for clinical use due to its exceptional qualities, including good mechanical properties, biocompatibility, low immunogenicity and non-cytotoxicity of degradation products. Unlike other polymers, PCL has a low melting point, which enable to maintain cellular behavior during the fabrication process [111]. In CTE, this polymer has been widely incorporated with hydrogels in construct designs in order to obtain mechanical reinforcement, similar to that offered by native tissue. Moreover, it has been reported to enable the formation of cartilage-like tissues both *in vitro* and *in vivo*, demonstrated by the deposition of type II collagen and GAGs [26,75,106].

I.7. NEW BIOMATERIALS: CELL-DERIVED EXTRACELLULAR MATRIX

Extracellular matrix derived from tissue (tdECM) has incomparable advantages as biomaterial for 3D bioprinting cartilage constructs. However, there are still some challenges and problems that should be noted. For instance, limited autologous tissue availability or the potential risk of immunogenicity and pathogen transmission when allogenic/xenogeneic sources are used [112,113].

Extracellular matrix can alternatively be obtained from direct secretion of cells in culture. During *in vitro* culture, cells secrete their own ECM depositing beneath them to cover the substrate surface (Figure 3). This matrix consists of a complex assembly of macromolecules, including fibrillar proteins (e.g. collagens, fibronectin, laminin) and glycosaminoglycans (e.g. heparan sulphate), easy to obtain by simple monolayer culture on a larger scale, as cells can be seeded in many flasks and dishes. Second, cell-derived ECM has greater ability for customization by selecting the cell type and culture conditions. In this way, using cells derived from different tissues it is possible to yield matrices that mimic the relative composition of natural tissue matrix. Third, it can be produced from autologous cells, thereby avoiding shortcomings related with immune system [112–116].

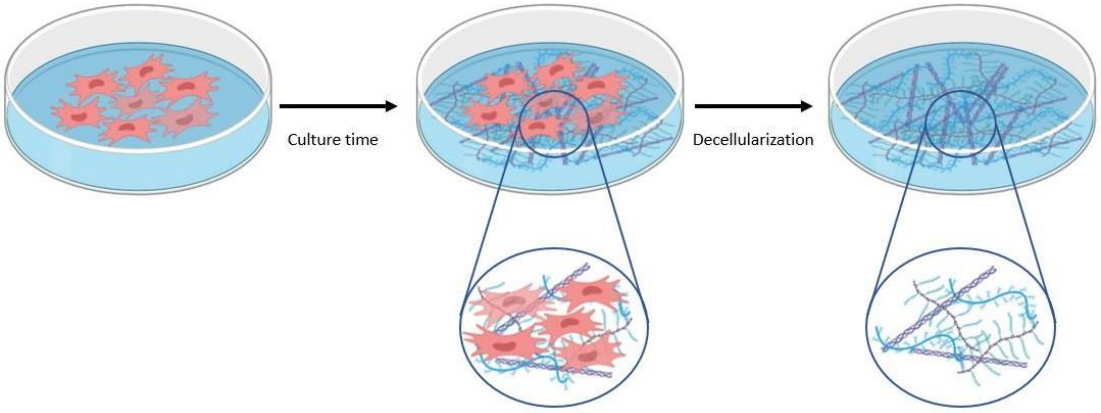

Figure 3. ECM derived from cell cultures.

Based on these benefits, cell-derived ECM has been recently used in tissue engineering as culture substrate, covering 2D culture systems or 3D polymeric templates (PCL, PLGA…) and as a biomaterial to produce scaffolds [115,117,118]. Many studies have evidenced that it provides a more suitable microenvironment for cellular expansion and maintenance, improving cell proliferation, adhesion and decrease senescence or intracellular ROS activity, in comparison to other culture substrates, including those coated with single ECM components (fibronectin, collagen type I, Matrigel), and biomaterials commonly used as scaffolds [119–123]. Moreover, dmECM has demonstrated a significant potential as instructive matrix. It has the ability to induce

specific-lineage differentiation, depending on the cell source, improving differentiation capacity and tissue formation, both *in vitro* and *in vivo* [115,118,124–128].

Specifically, improvements have been evidenced in hyaline cartilage-like tissue generation by using ECM derived from different sources:

- ECM from somatic cells: since chondrocyte is the unique cell type that constitutes articular cartilage, responsible for the secretion and maintenance of the ECM, it has been the first option for researchers, which reported to be an excellent support for chondrocyte, able to preserve and promote chondrogenic phenotype, and for differentiation of MSCs, inducing chondrogenesis even without external signaling factors, or improving this process in comparison to standard methods (pellet) [125,129].
- ECM from stem cells: this type of cells has gained a great attraction in recent years as source of ECM for its easy availability, self-renewal properties that allows an unlimited production of ECM, and its ability to differentiate into several cell lineages, which endows flexibility to generate a wide variety of matrices depending on culture conditions. Among cell sources, MSCs is the most common, although there are other very popular such as synovium-derived stem cells (SDSCs). Studies that used their matrices as coatings or to produce fiber mesh scaffolds in CTE indicated to be a potential system to enhance the quantity and quality of seeded chondrocytes as well as the chondrogenesis of MSCs, in comparison to those seeded on TP plates or other scaffolds [127,130].

  Additionally, stem cell culture has enable the obtention of tissue development-mimicking matrices by controlling their stepwise differentiation to better reproduce the dynamically changing microenvironment, which is known to sustain ECM during tissue development [131–134]. Hence, recent evidences, not only in CTE but also in bone and adipose tissue, have shown that ECM at early stage of maturity directs tissue-specific cell lineage commitment and facilitate the creation of *de novo* specific tissue better than those at late state of maturity [124,135–137].

II. HYPOTHESIS

3D bioprinting has been a step forward in the treatment of articular cartilage by the creation of patient-specific engineered constructs with the structural and functional features of native tissue. In this attempt, it has been required the identification of biomaterials suitable to produce bioinks that provide the physiological conditions for development of cartilage-like engineered constructs.

This thesis is based on the following hypothesis:

1) Natural polysaccharides are one of the most attractive materials for design of bioinks in CTE due to structural similarities and high-water retention that resemble native environment of cartilage. We hypothesize that the combination of natural polymers such as hyaluronic acid, main component in cartilaginous matrix, and alginate, which also exhibit ideal features for bioprinting, would enable the production of a biomimetic bioink with biological and mechanical properties suitable for CTE 3D bioprinting.

2) The best approach for the obtaining of biomimetic bioinks has been attained recently by the use of dECM derived from native tissue. However, it entails some issues such as limited donor tissue availability, morbidity or immunogenicity. As alternative option, we hypothesize that ECM derived from cells, specifically from MSCs, would be an ideal biomaterial to produce more affordably a new biomimetic bioink suitable for CTE 3D bioprinting, since it can be easily synthetized in large scales and customized by manipulation of culture conditions.

III. OBJECTIVES

Main objective

To develop biomimetic bioinks with suitable biological and mechanical properties to be applied in CTE by 3D bioprinting technique.

Specific objectives:

1. To produce a biomimetic bioink based on natural polymers, HA and alginate, and to characterize its biocompatibility, functionality and rheology.

2. To obtain 3D bioprinted cartilage constructs based on co-printing of biomimetic bioink based on natural polymers and PLA.

3. To synthesize and characterize biomimetic ECM derived from MSCs previously induced to the chondrogenic lineage.

4. To produce a bioink based on biomimetic decellularized MSC-derived ECM (dmECM) through decellularization and solubilization processes.

5. To evaluate, in vitro and in vivo, the biocompatibility, functionality and mechanical properties of the biomimetic dmECM.

IV. MATERIALS AND METHODS

IV.1. CELLS

IV.1.1. Isolation and culture of chondrocytes

Articular cartilage was obtained from patients with osteoarthritis (OA) during joint replacement surgery after informed consent from all patients and approval from the Ethics Committee of Clinical University Hospital of Málaga, Spain. Sample was isolated from the femoral side, selecting the non-overload compartment: lateral condyle in varus knees and medial condyle in the valgus cases. None of the patients had a history of inflammatory arthritis or crystal-induced arthritis and only cartilage that macroscopically looked relatively normal was used for this study. Articular cartilage was minced and digested overnight in 0.08% collagenase IV (Sigma) at 37°C with gentle agitation. Cells were centrifuged and rinsing to remove the collagenase. The remaining cells were then plated in cultured flasks with chondrocytes media: Dulbecco's Modified Eagle's Medium (DMEM, Sigma) supplemented with 20% fetal bovine serum (FBS, Gibco), 5 ml of 1% ITS (Insulin-Transferrin-Selenium, Gibco), 50 µg/µL of l-ascorbic acid 2-phosphate (Sigma), 40 µg/µL of l-proline (Sigma) and 100 U/ml penicillin and 100 µg/ml streptomycin at 37°C in a humidified atmosphere of 5% carbon dioxide (CO_2). After 24 hours, the medium was replaced with fresh medium supplemented with 10% FBS. At 80% of confluency cells were detached with TrypLE (Invitrogen) and sub-cultured.

IV.1.2. Isolation and culture of adipose derived stem cells (ASCs)

Subcutaneous adipose tissue was obtained from patients undergoing liposuction procedure after informed consent from all patients and approval from the Ethics Committee of Clinical University Hospital of Málaga, Spain. Samples of adipose tissue from lipoaspirates was minced and digested using an enzymatic solution of 1 mg/ml collagenase type IA (Sigma) at 37°C for 1 h on a shaker. After digestion, collagenase was removed by a single wash in sterile PBS, followed by two further washes in DMEM supplemented with 10% FBS. The cell pellet was resuspended in DMEM (Sigma) containing 10% FBS and 1% penicillin/streptomycin and cultured at 37°C in 5% CO_2. After

48 hours, the medium was removed to discard non adherent cells. At 80% of confluency the cells were released with TrypLE (Invitrogen) and sub-cultured.

IV.1.3. Flow cytometry analysis of ASCs

The immunophenotype of ASCs was analyzed by flow cytometry (FACS). Cells were washed and resuspended in PBS with 2% bovine serum albumin (BSA, Sigma, St. Louis, MO), and 2 mM ethylenediaminetetraacetic acid (EDTA, Sigma). Cells were incubated in dark for 30 minutes at 4°C with the appropriate fluorochrome-conjugated monoclonal antibodies. Markers used were: CD73-APC, CD90-FITC, CD105-PE, CD34-PE, CD45-PerCP, and CD133-APC (Miltenyi). All cells were washed in PBS and analyzed in a FACS Canto II cytometer (BD Biosciences).

IV.1.4. Differentiation assays of adipose derived stem cells

ASCs isolated from lipoaspirates were plated at 2 x 10^3 cells/cm^2 in DMEM (Sigma) containing 10% FBS (Gibco) with penicillin and streptomycin at 100 µg/ml (Sigma) and allowed to adhere for 24 hours. The culture media was then replaced with specific inductive media. For adipogenic, osteogenic and chondrogenic differentiation, cells were cultured for two weeks in Adipogenic MSCs Differentiation Bullet Kit, Osteogenic MSCs Differentiation Bullet Kit (Lonza) and NH ChondroDiff Medium (Miltenyi), respectively. Differentiated cell cultures were stained with Oil Red O (Amresco) for adipogenic differentiation, Alizarin Red (Lonza) for osteogenic differentiation or Toluidine Blue (Sigma) for chondrogenic differentiation.

IV.2. BIOINKS

IV.2.1. Biomimetic bioink based on natural polymers

IV.2.1.1. Preparation of bioink based on natural polymers, Hyaluronic acid and Alginate.

The bioink was prepared by dissolving alginate (A) (2 % (w/v)) and HA (0,1; 0,5; 1 or 5%(w/v)) in deionized water. The range of HA concentrations were selected based on what's reported in literature about HA-based hydrogels for cartilage tissue engineering. Finally, to obtain the bioink, chondrocytes were suspended at the desired concentration (1×10^6 cells/mL) in the solutions. Two other hydrogels consisting of A at 2% (w/v) and HA at 1% (w/v) respectively, were also prepared as a control.

IV.2.1.2. Bioprinting of cartilage construct using biomimetic bioink based on natural polymers

The design of the construct was based on the combination of the positive attributes of the PLA synthetic polymer, that confers superior mechanical properties, and natural biopolymers (Hyaluronic acid and Alginate), which provide a supportive native-like environment for cell encapsulation. It was fabricated using the REGEMAT V1 bioprinter (REGEMAT, Spain). The bioprinting process involves a dual step procedure: deposition of a thermoplastic polymer framework and injection of the bioink and $CaCl_2$ solution into that structure. First, PLA was deposited by head (at 200°C) in a layer-by-layer manner to generate the framework that was previously designed using software REGEMAT 3D designer (porous cylinder-type structure, 10 x 10 mm; 600 µm pore size). After printing 4 layers, the HA-based bioink with chondrocytes loaded in a syringe (3 cc) was injected into the pores of PLA structure. Then, it was physically cross-linked by following injection of 100 mM Calcium chloride ($CaCl_2$), loaded in another syringe. This procedure was repeated until the scaffold was completely built. There were bioprinted as many cell-laden scaffolds as we needed for following analytical studies. Finally, hybrid constructs were cultured in growth medium at 37°C and 5% CO_2 atmosphere.

IV.2.2. Bioink based on biomimetic ECM from mesenchymal stem cells in culture

IV.2.2.1. Production of the early chondrogenic matrix derived from MSCs

At complete confluence, MSCs were released with TriPLE (Invitrogen) and sub-cultured in Petri dishes at the cell density of $1 \cdot 10^4$ cells/cm^2. To allow the formation of ECM membrane, they were cultured in monolayer during 1, 2, 3 or 4 weeks in

chondrocytes media supplemented with dexamethasone (100 nM) and TGF-β3 (10 ng/mL) at 37°C humidified atmosphere containing 5% CO_2. The medium was refreshed every 2 or 3 days. As a control, chondrocyte-derived ECM was generated in the same way, but without using supplements in the culture medium.

IV.2.2.2. Decellularization of the early chondrogenic matrix derived from MSCs

At the completion of culture period, cells were removed from the underlying matrix by exposition to a decellularization treatment, selected from a variety of methodologies that have been reported to prepare cultured cell-derived ECM scaffolds [138]. The chemical procedure consisted on incubation in a detergent solution containing 0.25% Triton X-100 and 10 mM ammonium hydroxide (NH_4OH) at 37°C for 5 min, followed by treatment with 50 units/mL Deoxyribonuclease (DNase) I and 50 mg/mL Ribonuclease (RNase) A (Invitrogen) for 2h. After several washes with PBS, culture plates were examined by optical microscopy to ensure that all cellular material had been removed. Finally, the supernatant was removed and matrix remaining on the plate was scraped and lyophilized.

IV.2.2.3. Preparation of bioink based on early chondrogenic matrix derived from MSCs

Lyophilized decellularized early chondrogenic matrix derived from MSCs (dmECM) was crushed into powder with the help of liquid N_2. Required amount of dmECM powder was weighed and digested in a solution of 0.5M acetic acid with 10 mg of pepsin for 100 mg dECM (P7125, Sigma-Aldrich) for 48 h. After complete solubilization of dmECM, the pH of the solution was neutralized with dropwise addition of cold 1M NaOH and 10X PBS (to 1X final dilution), while maintaining the temperature below 10°C to avoid gelation of the dmECM. The pH-adjusted pre-gel was stored in refrigerator at 4°C.

IV.3. MOLECULAR ANALYSIS

IV.3.1. Rheological study

All the rheological tests were carried out in a torsional rheometer MCR302 (Anton Paar, Austria) using a cone-plate geometry (50 mm diameter and 1° angle). For analysis of biomimetic bioink based on natural polymers, tests were performed at 25°C, while for analysis of biomimetic bioink based on matrix derived from MSCs, tests were performed at 15°C, except temperature sweep test.

IV.3.1.1. Steady shear and linear viscoelasticity of bioinks

The shear viscosity was obtained in a three-step protocol. First, the bioink was pre-sheared at 1000 s^{-1} during 1 min. Then, it was allowed to rest (without a shear rate applied) for another min. Finally, the shear rate was logarithmically increased from 0.1 to 1000 s^{-1} (acquisition time of 5 s) during 5 min.

The viscoelastic properties were also investigated in dynamic oscillatory shear. We performed strain amplitude and frequency sweeps, again, in a three-step process. The first and second steps were similar to those for steady shear tests, while the third one consisted in either increasing the strain amplitude from 10 to 1000% at a constant frequency of 1 Hz, or decreasing the excitation frequency from 100 to 0.1 Hz at a constant strain amplitude of 10%.

IV.3.1.2. Dynamic oscillatory shear behavior of the crosslinked bioinks

The mechanical properties were measured using a plate-plate geometry with 20 mm diameter and 5 mm gap. The viscoelastic properties were determined as follows. After the specimen was placed on top of the lower base of the rheometer, the rheometer head was displaced downwards at a constant velocity of 10 µm/s. Once the head registers a normal force that is larger than 0.5 N, the rheometer head stops and the normal force is kept constant at 0.5 N during 30 more seconds. Finally, the sample is subjected to an oscillatory shear of 0.1% strain amplitude and an excitation frequency of 1 Hz at a constant normal force of 0.5 N to quantify the viscoelastic properties.

IV.3.1.3. Degradation rate of bioinks using linear viscoelasticity

The degradation rate of crosslinked bioink based on natural polymers was studied through the evolution of their viscoelastic moduli as a function of time over a month. We prepared as many identical samples as time points, keeping them under the same culture conditions up to the measure time point. For the experiments, we followed the same rheological protocol as described before.

IV.3.1.4. Gelation kinetics of bioinks

Viscoelastic moduli were measured at each temperature by exposing bioinks to oscillatory shear stress (setting the strain and angular frequency to 1% and 10 rad s^{-1}, respectively) during heating up from 20 to 37°C with an increment rate of 1°C/min. In addition, there were two incubation periods at 20°C and 37°C for 5 min.

IV.3.1.5. Recoverability of bioink

The recovery test was performed to determine the recovering abilities of bioinks by oscillatory time sweeps in 200 s intervals at alternating 100 and 1% strains performed at 1 Hz. Flow rate sweeps were run with a shear rate from 10^{-3} to 10^{3} s^{-1}.

IV.4. Biocompatibility assays

IV.4.1. Cell viability

The Live/Dead assay (Thermo Fisher Scientific) was used to evaluate cell viability. Briefly, samples were washed and stained with 4 µL of 2 µM calceine AM and 8 µL of 4 µM EthD-I in 4 mL of sterile PBS, incubated in the dark for 30 min. After washing with PBS, samples were observed using confocal microscope and imaged. Green fluorescence was visualized in live cells and red fluorescence in dead cells using two different filters. Images were analyzed with Image J software (v. 1.52i, USA). For each cell type, six regions were counted to obtain an average value of the percent of viable cells (n=3).

IV.4.2. Cell proliferation

The proliferation rate of cells embedded in bioinks were assessed by colorimetric alamar Blue (aB) assay (Thermo Fisher Scientific) at different time points. Data were normalized to the appropriate control without cells. Briefly, at each time point, samples

were incubated with 10 µL of aB solution per each 100 µL of medium and incubated for 3 h. The fluorescence intensity was measured using a plate reader (Synergy HT, BIO-TEK) with excitation and emission wavelengths of 570 and 600 nm, respectively. The absorbance data were represented as fold increase to day 0. Experiments were performed in triplicate (n =3).

IV.4.3. Karyotype Analysis

Karyotype analysis was performed before and after bioprinting process by G band techniques. In order to obtain chromosomal preparations, cells were treated with 0.8 mg/mL colchicine and incubated at 37°C for 1.15 h. Then, cells were collected and digested in 0.05% trypsin, continued with a hypotonic treatment using 0.075 mol/L KCl and fixation in a mixture of methanol and glacial acetic acid. Mitosis metaphase spreads were stained with Giemsa dye and imaged under the optical microscope. Approximately 20 metaphases were analyzed under the microscope. The final result was described to account the recommendations from the International System for Human Cytogenetic Nomenclature.

IV.5. Gene expression analysis

IV.5.1. Ribonucleic acid extraction

Total cellular Ribonucleic acid (RNA) was isolated using Trizol Reagent (Invitrogen) according to the manufacturer's recommendations. Briefly, 1 ml of Trizol by sample was added and homogenized by pipetting or vortex and then 0.2 ml of chloroform added and leaved 15 minutes at room temperature (RT) to ensure complete dissociation of nucleoprotein complexes. The resulting mixture was centrifuged at 12,000 × g for 15 minutes at 4°C. Then, the supernatant was transferred (colorless upper aqueous phase) to a fresh tube and added 0.5 ml of 2-propanol, allowing the sample to stand for 10 minutes at RT and centrifuged at 12,000 x g for 10 minutes at 4°C. The RNA precipitated will form a pellet on the side and bottom of the tube. After that, the supernatant was removed and the RNA pellet washed by adding a minimum of 1 ml of 75% ethanol, and then centrifuged at 7,500 × g for 5 minutes at 4°C. The RNA pellet was dried for 5–10 minutes by air-drying and add 20 µl of free-RNAse water.

IV.5.2. Reverse transcription–polymerase chain reaction

Total RNA was reverse transcribed using the Reverse Transcription System kit (Promega, Madison, WI, USA). Briefly, 1 µg of RNA was incubated in a final volume of 10 µl (dilution in distilled water) at 70°C for 10 minutes. Then, we added the following reagents: Magnesium chloride ($MgCl_2$) 25 mM (4 µl), Reverse Transcription 10X Buffer (2 µl), deoxyribonucleotide triphosphate (dNTP) Mixture 10 mM (2 µl), Recombinant RNasin Ribonuclease Inhibitor (0.5 µl), Avian Myeloblastosis Virus Reverse Transcriptase (High Conc.) (15 µl), and Random Primers (0.5 µg). Then, the reaction was incubated at RT for 10 minutes, and incubated at 42°C for 15 minutes, heated at 95°C for 5 minutes, and then incubated at 0–5°C for 5 minutes.

IV.5.3. Real-time Polymerase Chain Reaction (RT-PCR) analysis

RT-PCR was performed using the SYBR-Green PCR Master mix (Promega) according to the manufacturer's recommendations. PCR reactions were performed as follows: an initial denaturation at 95°C for 2 min, 40 cycles of 95°C for 5 s and 60°C for 30 s, and a final cycle of dissociation of 60 – 95°C. The gene expression levels were normalized to the corresponding GAPDH values and are shown as fold change relative to the value of the control sample. All the samples were done in triplicate for each gene. Primers used are shown in Table 3.

GENE	FORWARD	REVERSE
GADPH	TGCACCACCAACTGCTTAGC	GGCATGGACTGTGGTCATGAG
COL II	GAGACAGCATGACGCCGAG	GCGGATGCTCTCAATCTGGT
AGGRECAN	AGGATGGCTTCCACCAGTGC	TGCGTAAAAGACCTCACCCTCC
SOX9	ACTCCGAGACGTGGACATC	TGTAGGTGACCTGGCCGTG
COL I	ATGGATGAGGAAACTGGCAACT	GCCATCGACAAGAACAGTGTAAGT
COL X	GCCCACTACCCAACAC	TGGTTTCCCTACAGCTGA

Table 3. Sequences of the primers used in the RT-PCR reactions

IV.6. Histological analysis

Samples were immersed in 4% paraformaldehyde in 0.1 M Phosphate Buffered Saline (PBS) for 4 hours at 4°C, washed in 0.1 M PBS and embedded in paraffin in an automatic tissue processor (TP1020, Leica, Germany). The paraffin blocks were cut into 4 µm sections for staining. Tissue sections were deparaffinized in Xylene, 4 changes of 5 min per change, then hydrated in 100% ethanol, 1 change of 3 min, hydrated in 95% ethanol, 1 change of 3 min, and washed in tap water for 3 min. After the staining, the slides were dehydrated in 95% ethanol, 2 changes of 2 min per change, and in 100% ethanol, 1 change of 2 min. After that, tissue sections were cleaned in Xylene, 2 changes of 2 min per change. Finally, tissue sections were mounted and observed under microscope.

IV.6.1. Hematoxilyn-Eosin staining

The following protocol was used:

1. Stain in hematoxylin (Panreac) for 3 minutes. Always filter before each use to remove oxidized particles

2. Rinse in running tap water for 10 minutes

3. Counterstain in Aqueous Eosin 1 min: 1 g of eosin (Panreac) + 100 ml of distillated water + 1 ml of acetic acid (add in the moment of the staining)

4. Wash gently in top water, approximately 4 changes or until excess dye stops leaching out of tissue for 10 minutes

IV.6.2. Toluidine Blue staining

The following protocol was used:

1. Stain with 0.04% Toluidine O Blue solution for 20 min.

a. 0.1M Sodium Acetate Buffer: 13.6 g of Sodium Acetate anhydrous + 1 L of deionized water. Adjust final pH at 4 using glacial acetic acid. Store at RT or 4°C for longer storage

b. 0.4% Toluidine O Blue Solution: 0.4 g of Toluidine Blue O (Sigma) + 100 ml of 0.1 M Sodium Acetate Buffer

2. Rinse gently with 3 changes of deionized water (30 sec each)

For Toluidine blue stain in monolayer, cells were washed twice in PBS and fixed with 4% paraformaldehyde for 20 min at RT. Cells were stained in Toluidine Blue (Sigma) solution (0.1% in distillated water) for 5 minutes at RT, and rinsed with deionized water until the excess stain washed away. Finally, stained monolayer was kept in PBS.

IV.6.3. Masson´s Trichrome staining

The following protocol was used:

1. Bouin´s solution during 24h

a. Picric solution: 2 g of Picric acid (Fluka) + 100 ml of distillated water

b. 75 ml of Picric solution + 25 ml of formaldehyde (37 – 40%) + 5 ml of glacial acetic acid.

2. Rinse running tap water for 5-10 minutes to remove the yellow color.

3. Stain in Weigert's iron hematoxylin working solution for 10 minutes.

a. Stock Solution A: 1 g of Hematoxylin (Panreac) + 100 ml of 95% alcohol. Not expired

b. Stock Solution B: 4 ml of 29% Ferric chloride in water (Merk) + 95 ml of distillated water + 1 ml of Hydrochloric acid concentrated. Not expired

c. Mix equal parts of stock solution A and B. This working solution is stable for about 4 weeks.

4. Rinse in running warm tap water for 10 minutes

5. Stain in Biebrich scarlet-acid fuchsin solution for 3 minutes (Add glacial acetic acid). Solution can be saved for future use.

6. Wash in distilled water.

7. Differentiate in phosphomolybdic-phosphotungstic acid solution for 15 minutes or until collagen is not red: 5 g of Phosphomolybdic acid x-hydrate (Panreac) + 5 g of Phosphotungstic acid hydrate PA (Panreac) + 200 ml of distilled water. Not expire.

8. Transfer sections directly (without rinse) to 0.02% light green solution and stain for 7-10 minutes: 2 g of Light green SF yellowish (Merck) + 98 ml of distilled water + 1 ml of glacial acetic acid (add in the moment of the staining)

9. Wash in distilled water.

IV.6.4. Safronin O staining

The following protocol was used:

1. Stain in Weigert's iron hematoxylin working solution for 10 minutes.

2. Rinse in running tap water for 10 minutes

3. Differentiate in 1% Acid-Alcohol for 2 seconds.

4. Rinse gently with 3 changes of deionized water (30 sec each)

3. Counterstain in 0,02% Fast Green Solution (0,02g Fast Green (Sigma) in 100ml distilled water) for 1 minute

4. Rinse in 1% Acetic Acid for 2-10 seconds.

5. Stain in 0.1% Safronin O staining solution (0.1 g Safronin O (Sigma) in 100 ml distilled water) for 30 minutes.

IV.6.5. Sirius Red straining

The following protocol was used:

1. Stain in Sirius Red (Sigma) solution (0.1% in picric acid) for 30 minutes

2. Rinsed with 0.1% acetic acid until the excess stain washed away.

For staining in monolayer, cells were washed twice in PBS and fixed with 4% paraformaldehyde for 20 min at RT. Cells were stained in Sirius Red (Sigma) solution (0.1% in picric acid) for 30 minutes at RT, and rinsed with 0.1% acetic acid until the excess stain washed away. Finally, stained monolayer was keept in PBS.

IV.6.6. Alizarin Red staining

The following protocol was used:

1. Stain in Alizarin Red (Sigma) solution (2 g of Alizarin Red + in 100 ml of deionized water, and pH was adjusted to 4.3 with ammonium hydroxide) for 5 minutes.
2. Counterstain in Fast Green (0.02% in distilled water) for 1 min
3. Rinse in acetone for 20 seconds
4. Rinse in acetone : xilene (50:50) for 20 seconds
5. Rinse in xilene for 20 seconds

IV.7. Immunostaining assay

All samples were fixed with 4% paraformaldehyde (PFA) in PBS for 20 min at RT. For inmunofluorohistochemistry, samples were embedded in Optimal cutting temperature compound (OCT) and sectioned using cryotome in 10-mm thickness. Samples were washed repeatedly with PBS solution to remove OCT compound. Then, it was permeabilized with 0.1% Triton X-100 for 15 min and blocked in 3% Bovine Serum Albumin for 1 h at RT. Primary antibodies were incubated overnight at 4°C, and secondary antibodies were incubated at RT for 2 hours. Afterwards, they were washed three times in PBS and the slides were mounted using Vectashield containing 4',6-Diamidino-2-Phenylindole Dihydrochloride (DAPI,Thermo Fisher). Photographs were taken with a Leica DM 5500B (Solms, Germany) fluorescent microscope, software Meta Systems Isis, or confocal microscopy (Nikon Eclipse Ti-E A1, USA) and analyzed using NIS-Elements software. Primary antibodies used for immunocytochemistry were: i) anti-collagen type I (Santa Cruz Biotechnology), anti-collage type II (Santa Cruz

Biotechnology) and anti-Aggrecan (Sigma). All antibodies were diluted 1:100. Secondary antibodies used were: Fluorescein Iso-thiocyanate (FITC) or Phycoerythrin (PE) (Santa Cruz Biotechnology) diluted 1:200.

IV.8. Quantitative biochemistry assay

IV.8.1. Glycosaminoglycans quantification assay

GAGs content was estimated via quantifying the amount of sulphated glycosaminoglycans by Dimethyl Methylene Blue (DMMB) colorimetric assay. With that aim, samples were digested in 1 ml of papain solution (125 mg/ml papain in 0.1 M sodium phosphate with 5 mM Na_2-EDTA and 5 mM cysteine-HCl at pH 6.5) for 16 h at 60°C. The resulting extract was mixed with DMMB solution to bind GAG. The content was calculated based on a standard curve of sulphate chondroitin from shark cartilage (Sigma) at 570 nm on a microplate spectrophotometer.

IV.8.2. General Collagen quantification assay

Total collagen content was measured by picrosirius red staining. For this, it was firstly solubilized by incubation matrix with pepsin in acetic acid 0.5 M (2 mg/ml) and stained with 1 mL of Sirius red dye for 30 min at room. Then, the stain was dissolved using 0.5 N Sodium Hydroxide (0.5 N NaOH) and the absorbance was measured at 560 nm using a Microplate Reader (Berthold technologies, USA). Collagen type I (rat tail) was used as standard for the biochemical assays.

IV.8.3. Collagen Type II quantification assay

Type II collagen content was determined using a commercially available Type II collagen ELISA kit (Chondrex). For this, samples were digested by pepsin (1 mg/ml) in 0.5 N acetic acid for 48h at 4°C followed by adding 1 mg/ml pancreatic elastase solution at 4°C for 24 h. Finally, these were neutralized with 1 M Tris base. Insoluble material was

removed by centrifugation at 10,000 rpm at room temperature for 5 min, and the supernatant was collected for assay. Quantitative analysis was performed according to manufacturer's instruction and measured on micro-plate Spectrophotometer at 490 nm.

IV.8.4. Deoxyribonucleic acid quantification assay

DNA content was quantified by fluorometric assay using DAPI staining. For this, samples were digested in papain solution for 16 h at 60°C. The resulting extract was stained with DAPI. The fluorescence intensity was measured in fluorescence spectrophotometer (excitation wavelength: 360 nm, emission wavelength: 450 nm). The standard curve for DNA was generated in advance using calf thymus DNA and used for quantifying the DNA in samples.

IV.9. Analysis by Mass Spectrometry (MS)

To more fully characterize the protein content of samples, tandem mass spectroscopy (MS/MS) was performed. Proteins were extracted from culture dish with 5 M guanidine buffer containing 10 mM DTT (Sigma) and protease inhibitors (protease inhibitor mix M, Serva) at 4°C over night (ON). The extracts were mechanically homogenized on ice for 60 s followed by 2 h rotation at 4°C. The sample buffer was exchanged using cellulose-membrane spin columns with an exclusion size of 3 kDa (AmiconUltra-4, Millipore) against tissue protein extraction buffer (T-PER buffer, Pierce) supplemented with 20 mM β-mercaptoethanol (Sigma). After washing in an equal volume of T-PER buffer, samples were concentrated to a final volume of 500 µl. Proteins were precipitated with four volumes of ice-cold acetone at −20 °C for 2 h. A pellet was obtained after centrifugation at 18,000 g and was dissolved in 20 µl 4× sample buffer (0.25 M Tris-HCl, 6% SDS, 40% glycerol, 0.04% bromophenol blue, 20% β-mercaptoethanol). Samples were separated by sodium dodecyl sulfate PAGE (SDS-PAGE) on 1-mm-thick, 7% acrylamide gels at 120 V. Protein bands were visualized by Coomassie brilliant blue stain (Coomassie G-250, Sigma). SDS-PAGE gels were imaged using a LAS 3000 Bioimager (Fujifilm Life Sciences) before subsequent processing for

mass spectrometry. SDS-PAGE–separated extracts were cut into 17–20 slices according to major bands. In-gel digestion of proteins was performed using standard protocols.

IV.10. Scanning Electron Microscope (SEM) analysis

The internal microstructure of samples was examined using SEM. The specimens were fixed in cold 2.5% glutaraldehyde and rinsed in PBS, followed by a dehydration process through a graded series of ethanol (30-100%), and finally critically point dried in an Emscope CPD 750 critical point dryer. The samples were attached to aluminum SEM specimen mounting stubs (Electron Microscopy Sciences) and sputter coated with a gold palladium alloy using a Sputter Coater 108 Auto. Finally, samples were examined using a scanning electron microscope (Quanta 400 (FEI)). Images were taken at a 5,000 and 10,000x magnification.

IV.11. In vivo study

In-vivo biocompatibility was assessed in immunocompetent CD1(ICR) mice. Acellular gels were introduced in PCL scaffolds, for easy localization, and transplanted into the back subcutaneous tissue of mice anesthetized by isoflurane inhalation (n=6). Animals were maintained in a micro-ventilated cage system with a 12-h light/dark cycle with food and water *ad libitum*. Mice were manipulated in a laminar air-flow to maintain specific pathogen-free conditions. Two and four weeks later, mice were sacrificed via an overdose injection of anesthetics, and gels were excised for further histologic analysis.

In vivo tissue formation was evaluated in immunodeficient NOD SCID gamma (NOD.Cg-Prkdcscid Il2rgtm1Wjl/SzJ, NSG) mice. dmECM gels and pellets cultured during 2 weeks were transplanted into the back subcutaneous tissue of mice anesthetized by isoflurane inhalation (n=8). Animals were maintained in a micro-ventilated cage system with a 12-h light/dark cycle with food and water *ad libitum*. Mice were manipulated in a laminar air-flow to maintain specific pathogen-free conditions. Two and four weeks later, mice were sacrificed via an overdose injection of anesthetic, and dmECM gels and pellets were excised for further histologic analysis.

In vivo assays were carried out in accordance with the approved guidelines of University of Granada following institutional and international standards for animal welfare and experimental procedure. All experimental protocols were approved by the Research Ethics Committee of the University of Granada.

IV.12. Statistical analysis

Statistical analysis was performed using SPSS software (version 17.0). Unpaired t-test was used for single comparison between groups. All results are shown as means and standard deviations. A difference between the mean values for each group was considered statistically significant when the *p* value was lower than 0.05.

V. RESULTS AND DISCUSSION

V.1. CHAPTER I:

Development of bio-inspired hydrogel composed of hyaluronic acid and alginate as a potential bioink with application in 3D bioprinting of cartilage-like engineered constructs.

V.1.1. Results

V.1.1.1. Preparation of biomimetic bioink based on natural polymers, Hyaluronic acid and Alginate

To formulate the biomimetic bioink based on natural polymers, first we determined the optimal HA concentration for preservation and improvement of chondrogenic phenotype. It was analyzed by gene expression of chondrocytes embedded in hydrogels of alginate (2% w/w) and HA, at different concentrations (0.1, 0.5, 1 and 5% w/w) after 14 days in culture. These concentrations were selected based on that is reported in the literature about HA-based hydrogels for CTE[139–141][139–141][139–141][139–141]. As Figure 4 indicates, the addition of HA to alginate hydrogel caused an overall increased expression of chondrogenic markers such as Collagen type II (COL2A1), aggrecan (ACAN) and SOX9, especially in 1% HA. It showed significantly higher levels for all these genes in comparison to the rest of conditions, although in the case of ACAN and SOX9 were similar to 0.5% and 5%, respectively. Moreover, there was a trend towards a reduction of dedifferentiation markers, such as fibrotic marker collagen type I (COL1A1) and hypertrophic marker (COL10A1), in presence of HA, without significant differences among concentrations. Altogether, these results indicated that 1% HA provided the most favorable environment to preserve and enhance the phenotype of chondrocytes. Therefore, this combination was chosen to formulate the biomimetic bioink.

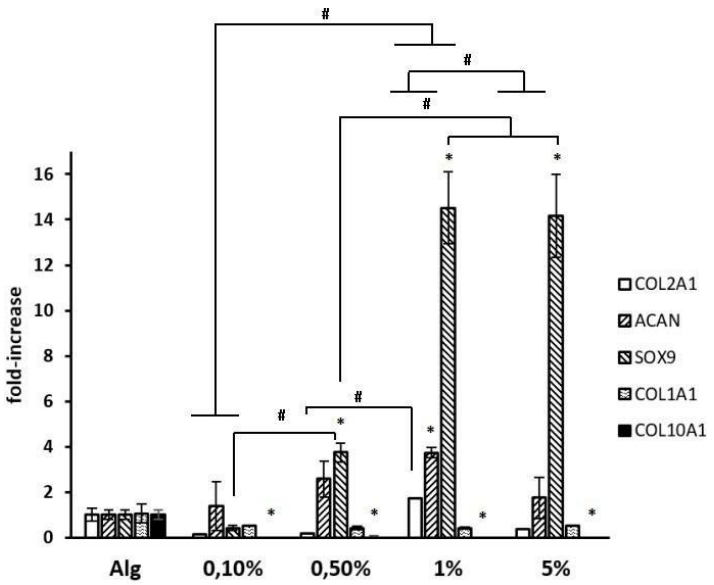

Figure 4. Expression of chondrogenic (SOX9, COL2A1, ACAN), non-chondrogenic (COL1A) and hypertrophy (COL10A) markers, after 14 days in culture, represented as fold increase compared to the house keeping gene GADPH. The different concentrations of HA are indicated in the x-axis. Statistical significance is indicated with different symbols ($p < 0.05$): (*) between chondrocytes in alginate hydrogel (Alg) and chondrocytes in alginate hydrogel containing HA; (#) between chondrocytes in alginate hydrogel with different concentrations of HA.

V.1.1.2. Characterization of biomimetic bioink based on natural polymers

The rheological properties of the bioink are crucial for an optimal performance in the extrusion process through the syringe. For this reason, both steady shear and dynamic oscillatory properties were investigated.

As it is observed in the viscosity curve (Figure 5A), the biomimetic bioink based on HA and alginate exhibited a shear thinning behavior. It was evidenced by a decrease in viscosity with shear rate that is characteristic of large molecular weight HA. Figure 5A also indicated that the presence of alginate in the composition of biomimetic bioink produced an increase in its viscosity in comparison to HA solution.

The measurement of storage and loss modulus versus a wide range of strains indicated viscous fluid behavior (G''> G') of the bioink (Figure 5B). Frequency sweep test also shows that bioink acted as viscous material in a wide range of frequencies (G'' > G') (Figure 5C). After crosslinking with calcium, the storage modulus G' of bioink became larger than the loss modulus G'' and clearly above those measured in non-crosslinked bioink. The storage modulus reached a value of approximately 3 kPa.

The long-term stability of the crosslinked HA-based bioink was investigated through changes in material rheological behavior with time. Compression and viscoelastic moduli were recorded over a culture period of 4 weeks, exhibiting similar trends. As shown in Figures 5E and 2F, there was a significant decrease in both moduli after 1 week, but then they were kept unchanged until the end of the test.

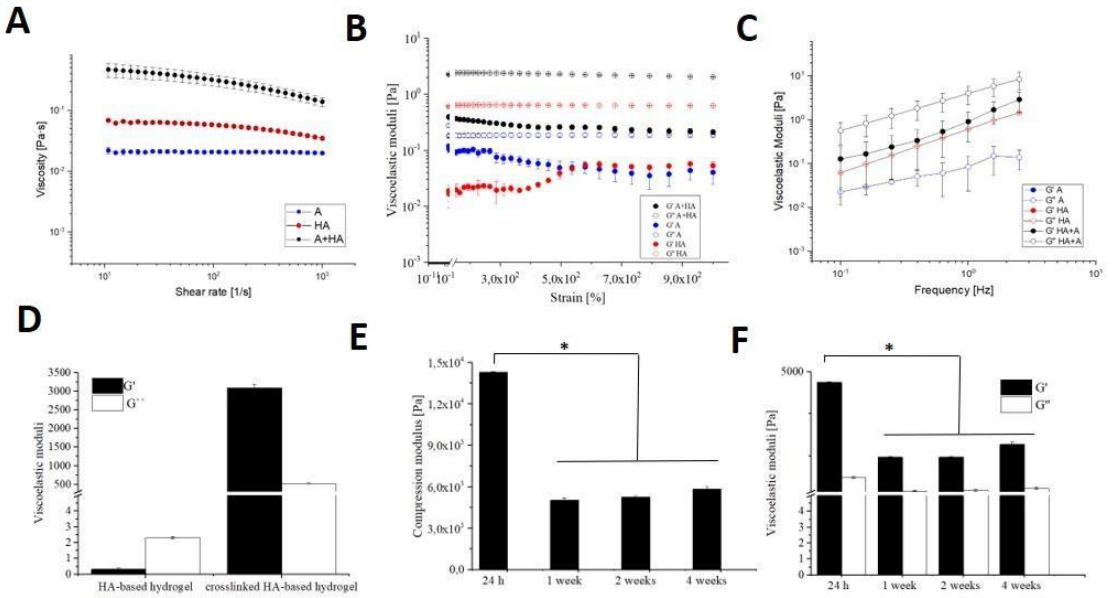

Figure 5. Rheological characterization. (A) Viscosity curves of alginate (A), hyaluronic acid (HA) and A+HA hydrogels. (B) Strain amplitude sweeps in dynamic oscillatory shear of the three hydrogels. Frequency 1 Hz. (C) Frequency sweep in dynamic oscillatory shear of the three hydrogels. Strain amplitude 0.1%. (D) Viscoelastic moduli of HA-based hydrogels and crosslinked HA-based hydrogel (A+HA). Compression (E) and viscoelastic moduli (F) of the crosslinked HA-based hydrogel after 1 month in culture. Mean ± SD, n=3, Student's t-test, *p <0.05.

V.1.1.3. Fabrication of cartilage construct using biomimetic bioink based on natural polymers

Cartilage construct was successfully produced using the bioprinter REGEMAT 3D V1. Figure 6 shows the 3D printing system and bioprinting procedure, respectively. It was obtained through simultaneous deposition, layer by layer, of a porous PLA thermoplastic framework, that confers superior mechanical properties, and bioink injection into these pores. This bioink was immediately gelled by following injection of ionic crosslinker (calcium chloride) at the same position. Eventually, it resulted in a 10 mm high × 10 mm wide structure.

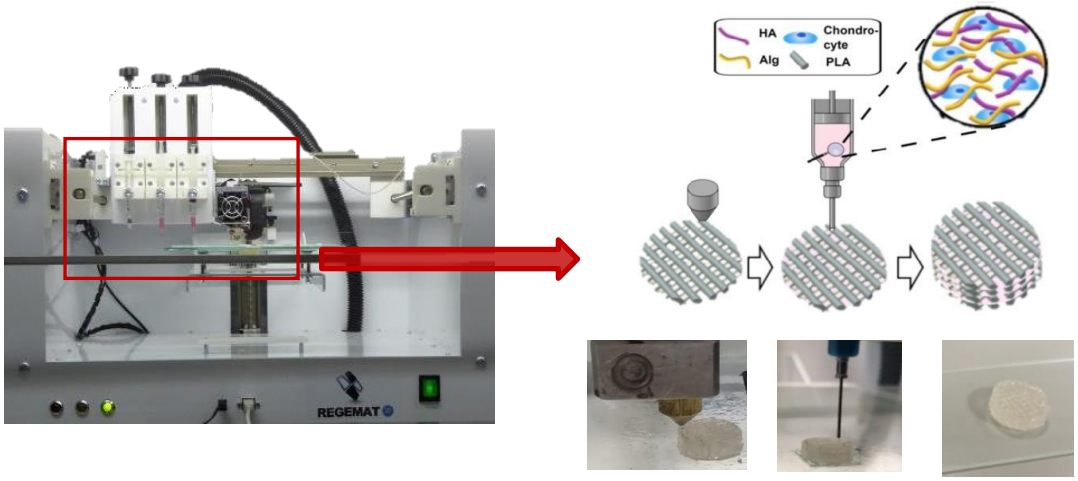

Figure 6. Scheme of 3D bioprinting process of articular cartilage engineering.

V.1.1.4. Cell viability in biomimetic bioink based on natural polymers after 3D bioprinting

The viability of chondrocytes was examined by live/dead staining (Figure 7 A and B). The bioink was found to retain more than 85% of cell viability with no significant changes, prior to, and after bioprinting. Results from karyotyping analysis of chondrocytes also revealed no changes during this process, obtaining a typical diploid karyotype (46, XX) (Figure 7 C and D).

Cell viability was slightly decreased after 1 day, but steadily recovered afterwards (Figure 8 A-F), evidenced by predominant green fluorescence of chondrocytes over 1 month in the biomimetic bioink. These results were confirmed by the proliferation assay that indicated cell growth over this period with a significant increase in biomimetic bioink in comparison to control constructs with A ($p < 0.05$) (Figure 8G).

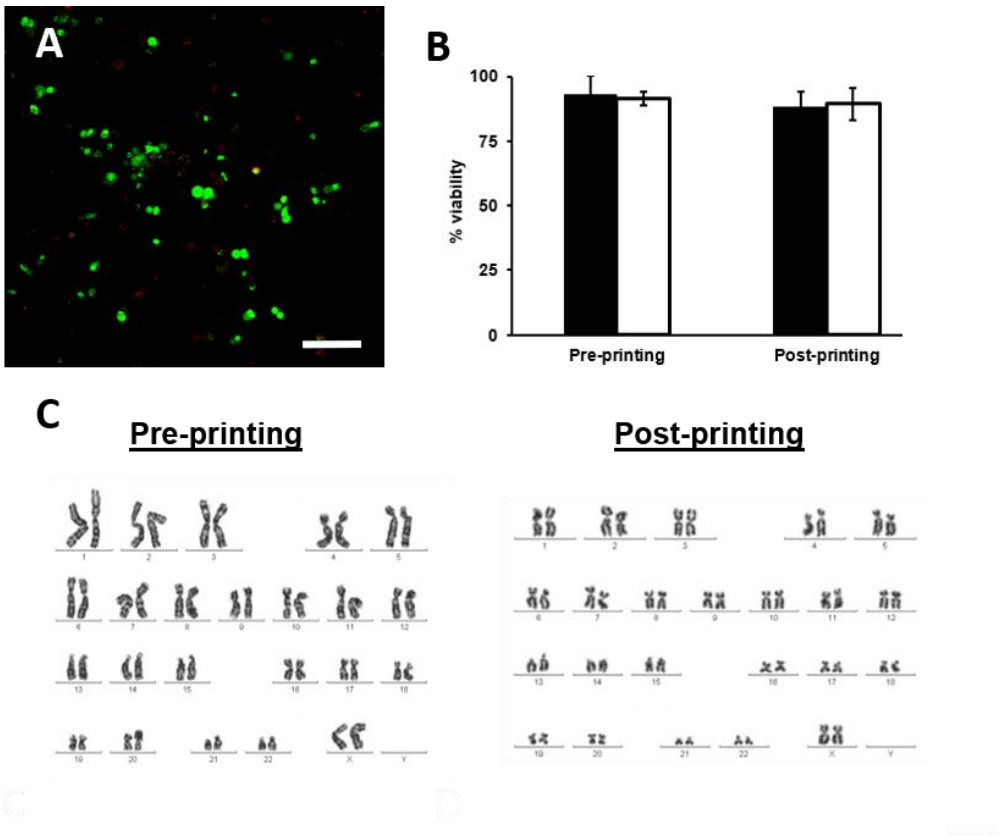

Figure 7. Cell viability during bioprinting process. Live/Dead cell imaging analysis. (A) Representative image of bioprinted human chondrocytes in HA-based bioink, showing live (green) and dead (red) cells. (B) Percent of chondrocytes viability in HA-based bioinks before and after the bioprinting process. (C) Karyotype of chondrocytes before and after bioprinting process.

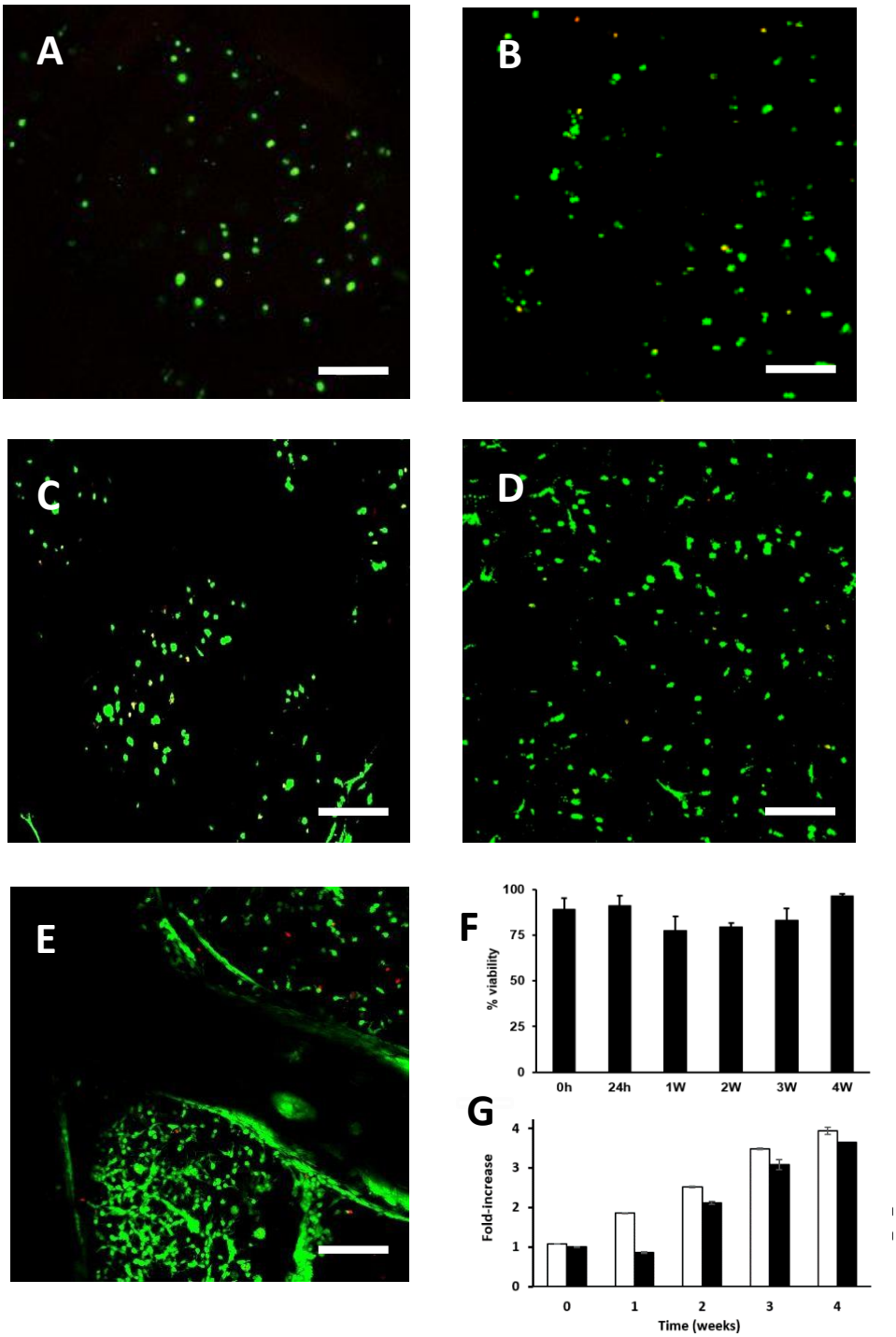

Figure 8. Cell viability of chondrocytes in bioprinted construct along time in culture. Representative images of bioprinted human chondrocytes in HA-based bioink after 24 h (a), 1 (b), 2 (c), 3 (d) and 4 weeks (e) in culture, showing live (green) and dead (red) cells. (f) Percent of chondrocytes viability in HA-based bioinks along time in culture. (g) Cell proliferation inside the HA-based (white) and alginate bioink (black). Error bars represent standard deviations (n = 3). Scale bar: 100 µm.

V.1.1.5. Functionality of hybrid 3D bioprinted constructs of HA-based biomimetic bioink

We investigated the capacity of HA-based biomimetic bioink to enhance chondrogenic phenotype and, therefore, cartilage formation in hybrid constructs. Figure 9C shows gene expression of chondrocytes in biomimetic bioink, after 4 weeks in culture, compared to chondrocytes in control alginate bioink. We observed an increased expression of hyaline cartilage-specific genes such as SOX9, COL2A1 and ACAN (9.7, 2.3 and 3.2-fold, respectively), while the expression of the fibrotic marker gene COL1A1 was significantly decreased. The hypertrophic marker gene COL10A1 were undetectable in both conditions. Quantification of hyaline cartilage-specific ECM components also revealed a higher content of Collagen type II and GAGs in matrix formed by chondrocytes after 4 weeks in biomimetic bioink (18.32 ng and 41.37 µg/scaffold, respectively). In both cases, values were significantly higher than controls (Figure 9A and 9B).

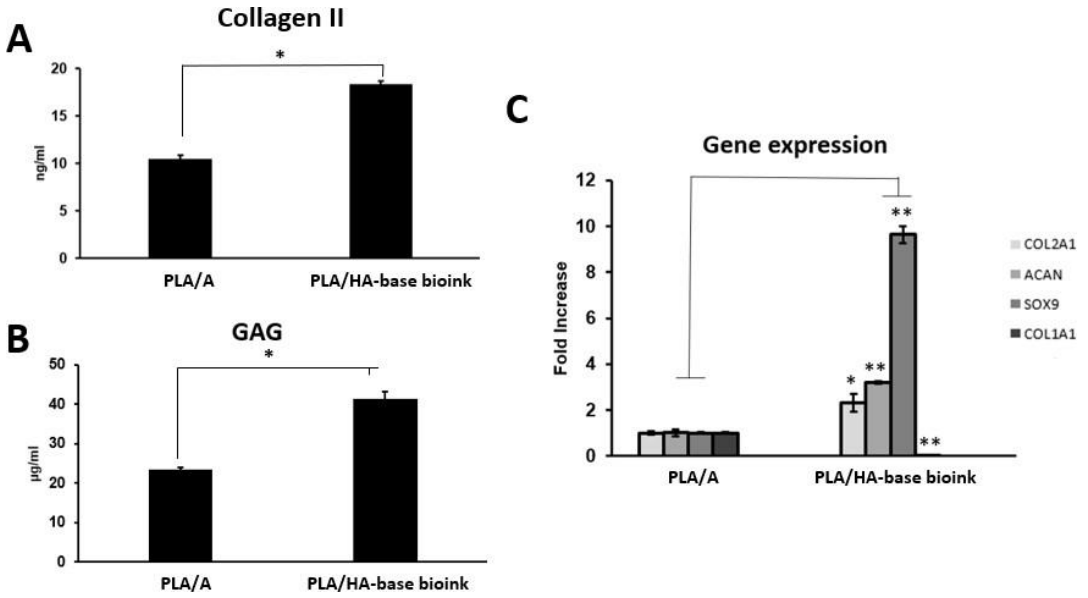

Figure 9. Cartilage formation in hybrid 3D bioprinted constructs after 1 month in culture. Quantitative analysis of type II collagen (a) and GAG (b) in the total extract per scaffold (in 1 mL). (c) Gene expression levels of hyaline-specific chondrogenic marker genes (COL2A1, ACAN and SOX9) and fibrotic maker (COL1A1) in bioprinted 3D hybrid construct (mean ± SD, n=3, Student's t-test, *p <0.05, **p <0.01).

V.1.2. Discussion

3D bioprinting represents an advantage in CTE and this technology has enabled the creation of biomimetic constructs by spatial distribution of living cells and supporting biomaterials at pre-defined sites [34]. In this field, bioinks play a critical role, providing the desired 3D environment to embedded cells, which is essential to achieve a functional construct. Natural polymers are particularly attractive as material to formulate bioink for CTE due to features such as biochemical structure and high capacity of water uptake that resemble the natural environment of cartilage [40,142]. Here, we have developed a biomimetic bioink using a combination of natural polysaccharides to produce cartilage constructs by 3D bioprinting. One of these components was HA, a main element of articular cartilage ECM. It is involved in the maintenance of cartilage homeostasis by regulating cell functions that includes promotion of chondrogenic phenotype, and synthesis and retention of cartilaginous matrix elements [61]. The other component was alginate, a biostable material outstanding in CTE bioprinting. It exhibits bioinert properties, that allow retaining phenotype of embedded chondrocytes, and fast gelation kinetics, suitable for 3D printing [19,41,44,45].

Physical properties of bioinks are important to be considered since they are directly correlated with printability. For extrusion-based bioprinting, it is required that the material retains cells but also remains sufficiently fluid to be extruded through the nozzle[143,144]. Results from rheological analysis indicated that our biomimetic bioink based on natural polymers was a viscous solution, exhibiting shear thinning behavior characteristic of HA. This polymer facilitates the flow through fine nozzles during the bioprinting process and, therefore, reduces cell damage caused by extrusion forces. Many studies have reported the use of HA as “building block” in various bioinks formulations for cartilage bioprinting because of its viscoelastic properties [145]. The presence of alginate also allowed rapid gelation, evidenced by the increase in G’ when it was exposed to calcium, helping to maintain 3D structure after bioprinting and keeping cells in a 3D environment adequately for long-term culture. In accordance with *Honghyun Park et al*, the reached value for G’ is sufficient to hold the cells in place, still allowing them to proliferate and grow [146]. Results from long term stability shows that there was a significant decrease in both moduli after 1 week, probably due to the gel

dissociation by ionic exchange of the Ca^{+2} with Na^{+} in the culture medium and the degradation of HA by hyaluronidases secreted from cells [147–149]. Over time, a slight increase was observed that could be correlated with new tissue synthesis.

In addition to physical properties, another essential condition for a bioink is to exhibit biocompatibility and cell protection during the printing process [143,150]. Hyaluronic acid and alginate are some of the materials that have been approved by FDA. Their excellent biocompatibility has been well documented in many studies [151]. In accordance, we evidenced high cell viability in our biomimetic bioink (>85%), which was maintained even after extrusion. This fact could be explained through the shear thinning behavior described previously, which reduces shear stress causative of cell disruption. Observations at long time confirmed that bioink offered a cell-friendly environment, maintaining a high percentage of viability over 3 weeks in culture. Moreover, it was evidenced the positive effect of HA on cell proliferation that has been reported in several studies [152–154].

A cartilage construct generated by 3D bioprinting has an ultimate objective, i.e. the replacement of damaged tissue. Therefore, it is required to assure the correct maturation of this bioprinted construct in order to achieve a better approach to native articular cartilage. Here, we could evidence how a bioink based on natural polymers improved cartilage-like tissue formation by embedded chondrocytes. So far, alginate has been a gold standard for CTE, promoting growth of chondrocytes and the chondrogenic phenotype [155–157]. In this study, the combination with HA to formulate this biomimetic bioink led to an increase in hyaline-specific ECM production as well as an improvement in the quality of chondrocytes embedded into it after the 3D bioprinting process. We determined a significant higher content of cartilage-specific ECM components, Collagen type II and GAGs, compared to a control of alginate. Gene expression analysis also revealed that there were an up-regulation of chondrogenic genes, such as COL2A1, ACAN and SOX9, and a down-regulation of non-chondrogenic marker, COL1A1. The beneficial effect of hyaluronate on chondrogenic matrix production has been extensively reported in numerous studies [73,154,158]. In

accordance with our results, it has been evidenced a stimulatory effect on the synthesis of collagen type II, glycosaminoglycan (particularly aggrecan) and hydroxyproline, according to various mechanisms. This effect is expected to be the result of cell receptor binding with HA (i.e. CD44, hyaluronan mediated motility receptor). Chondrocytes and MSCs have membrane receptors capable of binding with HA and, thus, being influenced by its presence [61].

Taking all data together, we concluded that hyaluronic acid-alginate forms a promising combination to produce a biomimetic bioink for CTE bioprinting, providing a suitable environment for cartilage formation *in vitro*.

V.2. CHAPTER II:

Development of a new biomimetic bioink based on extracellular matrix derived from MSCs in culture

V.2.1. Results

V.2.1.1. Isolation and characterization of Adipose tissue-derived Stem Cells

Stem cells used as source of ECM to produce a new biomimetic bioink were isolated from adipose tissue of patients undergoing a liposuction surgery for aesthetic issues. Following the recommendation of the International Society for Cellular Therapy (ISCT), Adipose tissue-derived Stem Cells (ASCs) were characterized according to the minimal criteria to define multipotent mesenchymal stromal cells. Freshly isolated ASCs presented a typical spindle shape fibroblastic morphology when they were cultured on plastic surfaces under standard culture conditions. At passage 4, cells were tested for specific surface human MSCs markers (CD73, CD90, CD105), and endothelial and hematopoietic markers (CD133, CD34, CD45) expression. Fluorescence-activated cell sorting analysis in MSCs showed a high expression of CD73 (100%), CD90 (98%) and CD105 (95,7%), while there was a low expression of endothelial and hematopoietic markers: CD45 (4,6%), CD133 (3,7%) and CD34 (6.4%) (Figure 10A).

We further tested the plasticity potential of the isolated cells checking their differentiation capacity towards chondrocytes, adipocytes and osteoblasts. ASCs were cultured under standard *in vitro* culture-differentiating conditions during 3 weeks. The acquisition of an adipocyte-like phenotype was confirmed by the lipid deposits stained with Oil Red. Osteogenic differentiation was confirmed by calcific deposition using Alizarin Red staining. Finally, chondrogenic differentiation was assessed by the presence of proteoglycans stained with Toluidine Blue. In conclusion, cells isolated from adipose tissue were capable of differentiating into other mesenchymal tissue types, including adipocytes, chondrocytes and osteoblasts (Figure 10B).

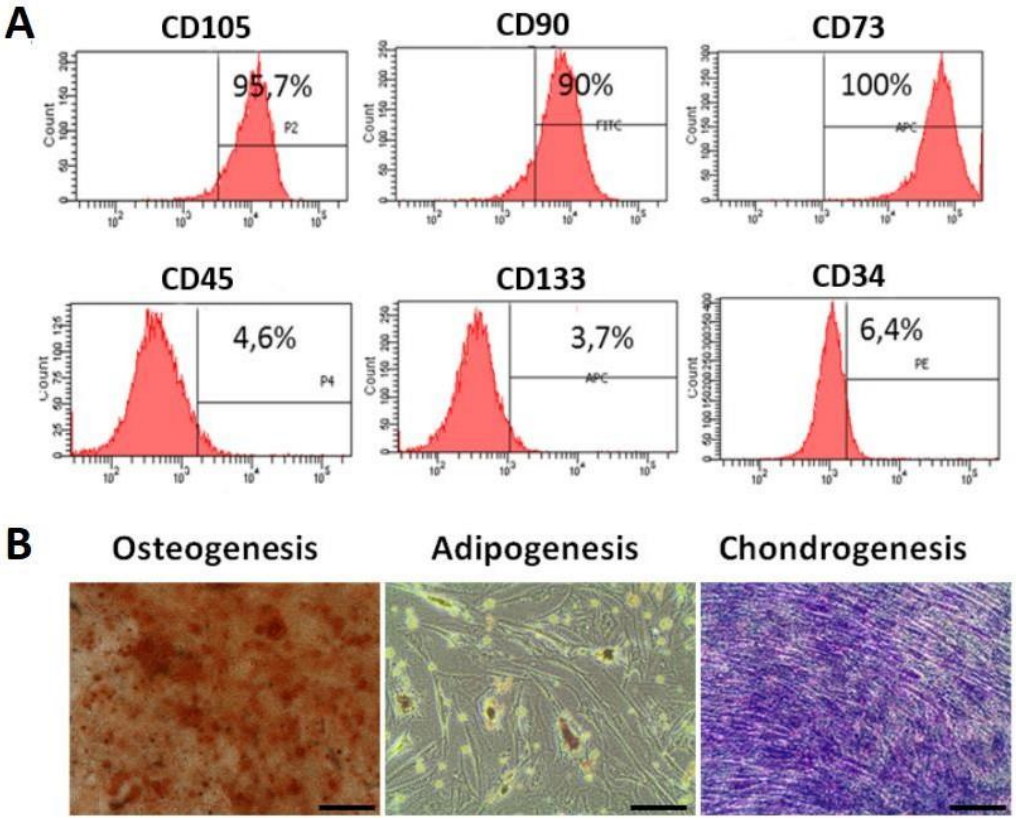

Figure 10. Phenotypic characterization and differentiation potential of MSCs. **(A)** FACS characterization of MSCs showed a positive expression of the surface markers CD105, CD90, CD73 and negative or low expression of CD45, CD133 and CD34. **(B)** The differentiation potential of MSCs obtained from lipoaspirate towards osteogenic, adipogenic and chondrogenic lineage was confirmed by alizarin red S, oil red O, and toluidine blue staining, respectively. Scale bar: 100 µm.

V.2.1.2. Production and characterization of biomimetic ECM derived from MSCs

In an attempt to produce a bioink that better recreates the environment during chondrogenesis, we synthetized an early chondrogenic matrix from MSCs, since it contains the factors that are necessary for tissue development, not present in mature ECM.

Firstly, we determined the culture time necessary to obtain an early chondrogenic matrix. For this, MSCs were cultured under chondrogenic media during different time periods (1, 2, 3 and 4 weeks). Quantification of main components of

articular cartilage, Collagen type II and Sulfated glycosaminoglycans, were performed to investigate the different stages of chondrogenesis. As it can be appreciated in Figure 11A, after 1 week in conditioned culture, the content of GAGs per µg DNA of MSCs was at the same level as that cultured in normal conditions (growth medium). The GAGs/DNA ratio raised significantly with increasing culture time. Similar situation was observed for Collagen type II, whose levels were inappreciable in the first week, but remarkably detected after 2 weeks in culture (Figure 11B). Since a high content in collagen and GAG is characteristic of mature cartilaginous matrix, we considered 2 weeks as the culture time required to generate an early chondrogenic matrix.

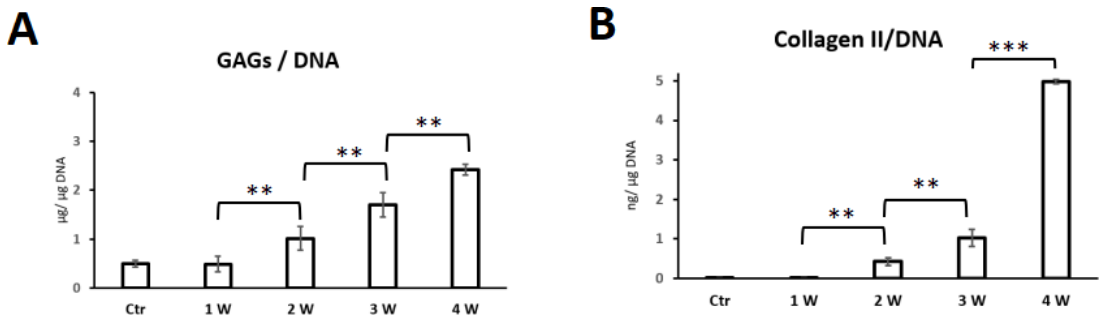

Figure 11. Quantitative analysis of cartilage-specific components, Glycosaminoglycans (GAGs) **(A)** and Collagen II **(B)** in ECM derived from MSCs cultured under chondrogenic culture conditions during 4 weeks in vitro. Data represent mean ± S.D. (n = 3). **, $p < 0.01$; ***, $p < 0.001$.

To confirm these observations, we compared 2 week MSC-derived ECM and mature chondrogenic matrix derived from chondrocytes in culture. Histology and immunofluorescence staining revealed differential presence and distribution of the main ECM components. Figure 12 shows that both ECMs expressed similar levels of collagen and GAGs, however, only ECM-derived from chondrocytes showed high expression of collagen type II. These observations were in accordance with quantitative results, which revealed that matrices were rich in collagen (430 µg/mg for chondrocyte-derived matrix and 760 µg/mg for MSCs-derived matrix), being 70% of this content collagen type II in matrix from chondrocytes, in contrast to MSC-derived ECM that was only 2,45%. Meanwhile, GAGs content expressed values around 60 µg/mg in chondrocyte-derived ECM, and 47 ug/mg in MSC-derived ECM.

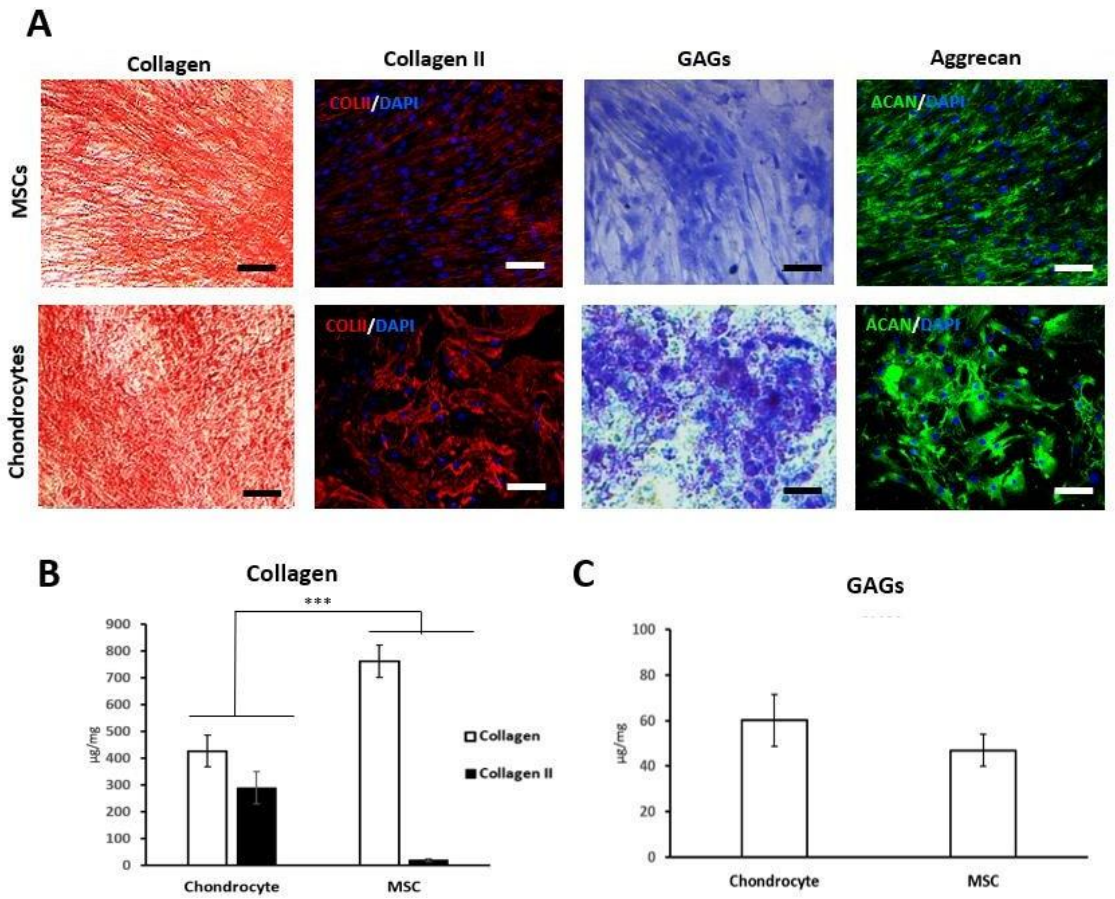

Figure 12. Characterization of matrix derived from MSCs and Chondrocytes after 2 weeks in culture. **(A)** Qualitative analysis of main components, Collagen and GAGs, by histological staining (Sirius Red, Toluidine O) and immunofluorescence (Collagen type II and Aggrecan). Quantitative analysis of collagen **(B)** and GAGs **(C)** content. Scale bar: 50 µm. Data represent mean ± S.D. (n = 3). ***, $p < 0.001$.

In order to get more details about the composition of this matrix, we performed the characterization by mass spectrometry. Results revealed the presence of a complex protein matrix, identifying 100 proteins that included core matrisome and matrisome associated proteins. Core matrisome, consisting of structural proteins that confer mechanical properties and cell adhesion to the ECM, was the main presence. It includes collagens, glycoproteins and proteoglycans. A large variety of collagens were identified, most of them constituents of cartilaginous ECM. There were some members of fibrillar family (collagen type I, III and V), fibril associated collagens with interrupted triple helices (FACIT) (collagens type XII, XIV and XIV) and network-forming collagens (collagen type IV and VIII). Other subtypes of collagen such as Collagen VI, which is the primary collagen located in the pericellular matrix of cartilage, was also present. Between glycoproteins, it was found some MSC matrix markers like Emilin-1 but also typical

structural proteins of cartilage matrix such Cartilage Oligomeric Matrix Protein (COMP), Tenascin-C, Lumican (LUM), Chondroitin sulfate proteoglycan core protein 2 (CSPG2 or Versican), Prolargin (PRELP) and Transforming growth factor-beta-induced protein, although the mostly detected was fibronectin. Biglycan, Decorin and Versican core protein, which are also very common in cartilage, were the principal proteoglycans in our MSC-derived ECM. In less abundance were identified other affiliated proteins including regulators e.g. matrix metalloproteinases (MMP) and their inhibitors (TIMPs), ECM-associated proteins (i.e. Annexins and Galectins) and signaling ligands (Table 4).

Table 4. Detectable proteins in early chondrogenic matrix derived from MSCs.

Extracellular matrix proteins	
COLLAGENS	**REGULATORS**
Collagen I	Matrix metallopeptidase-3
Collagen III	Matrix metallopeptidase-14
Collagen V	Matrix metallopeptidase inhibitor 1
Collagen VI	Matrix metallopeptidase inhibitor 3
Collagen VII	Type IV collagenase
Collagen VIII	Matrix-remodelling-associated protein 5
Collagen XI	Cell migration-inducing and hyaluronan-binding protein
Collagen XII	Interstitial collagenase
Collagen XXII	Disintegrin and metalloproteinase with thrombospondin motifs 2 (ADAMTs)
GLYCOPROTEINS	Disintegrin and metalloproteinase with thrombospondin motifs 3 (ADAMTs)
Fibulin 1	Disintegrin and metalloproteinase with thrombospondin motifs 4 (ADAMTs)
Fibulin 2	Adipocyte enhancer-binding protein 1
Filamin	14-3-3 protein eta
Emilin 1	Collagen triple helix repeat-containing protein 1
Emilin 2	Dermcidin
Fibronectin	Serine protease HTRA1
Fibromodulin	Cartilage intermediate layer protein 1
Cartilage intermediate layer protein 2	Cathepsin B
Chitinase-3-like protein 1	**ECM-AFFILIATED PROTEINS**
Perioscin	Latent-transforming growth factor beta-binding protein 1
Thrombospondin 1	Transforming growth factor-beta-induced protein ig-h3
Tenascin	Cartilage-associated protein
Cartilage oligomeric matrix protein (COMP)	Prolargin
Laminin	Procollagen C-endopeptidase enhancer 1
SPARC	Microfibrillar-associated protein 2
EGF-containing fibulin-like extracellular matrix protein 1	Microfibrillar-associated protein 5
EGF-containing fibulin-like extracellular matrix protein 2	Annexin A1
Vitronectin	Annexin A2
Lactadherin	Annexin A4
Podocan	Annexin A5
Olfactomedin-like protein 3	Annexin A6
Secretoglobin family 1D member 2	Annexin A7
Semaphorin-3C	Galectin 1
Thyroglobulin	Galectin 3
	Protein CYR61
	Elastin
PROTEOGLYCANS	**SECRETED FACTORS**
Byglican	Connective tissue growth factor
Decorin	Guanylate-binding protein 1
Heparin sulphate core protein (Perlecan)	Pentraxin-related protein PTX3
Lumican (keratan sulphate)	Myeloid-derived growth factor
Versican Core Protein	Hepatoma-derived growth factor
Mimecan	Leukocyte elastase inhibitor
	Mesencephalic astrocyte-derived neurotrophic factor
	Spondin-1
	Sushi repeat-containing protein 1
	Sushi repeat-containing protein 2

V.2.1.3. Decellularization of biomimetic ECM derived from MSCs.

Early chondrogenic MSC-derived ECM was decellularized according to a protocol that has been widely used to treat ECM from monolayer culture. The goal was to maximize the removal of cellular material, while minimizing ECM loss and damage. Treatment containing Triton X-100 and NH_4OH successfully reduced cellular content, that was estimated by the absence of nuclei on phase-contrast images and H&E-stained sections of decellularized matrix (Figure 13A), as well as the reduction in ~98% in DNA content (Figure 13B). In parallel, it was demonstrated that ECM composition was properly preserved. Comparative information about protein content by MS revealed similar patterns before and after decellularizing treatment (Supplementary Table 1). Similarly, histological analysis using Masson's Trichrome and Toluidine O staining also showed the persistence in dmECM of collagen and GAGs, respectivelywith non-significative differences in remaining content, in terms of quantification (Figure 13C-D).

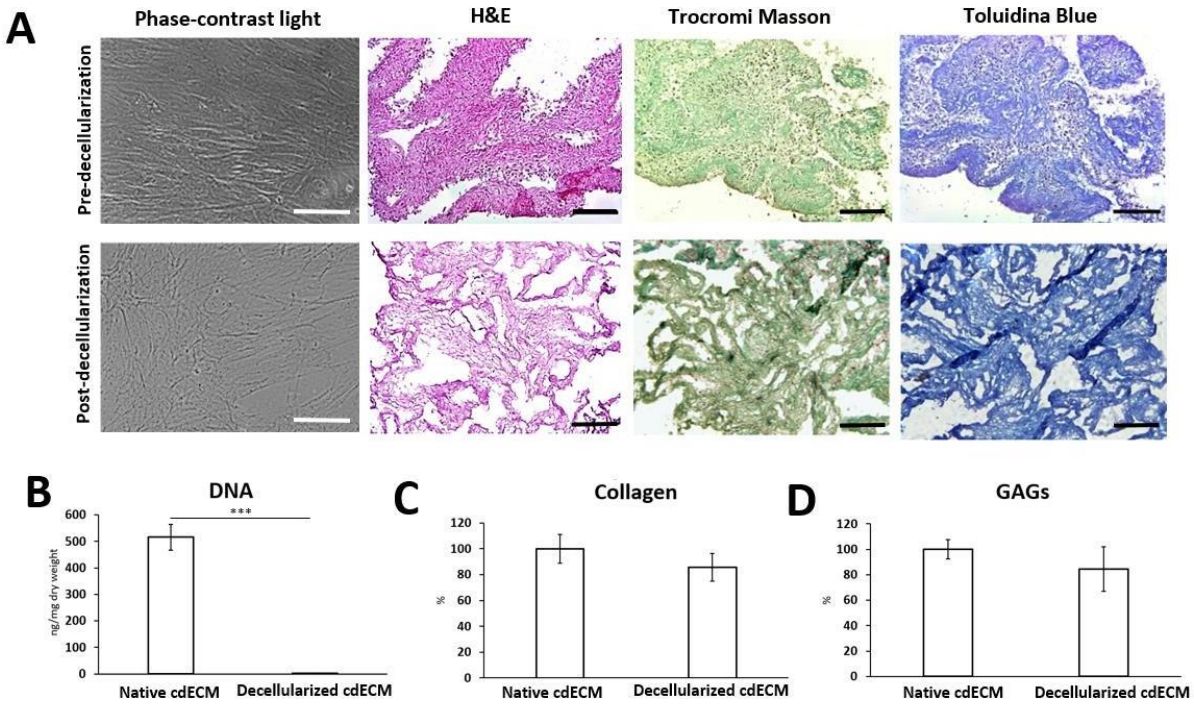

Figure 13. Decellularization of early chondrogenic matrix derived from MSCs. **(A)** Qualitative analysis by Optical microscope image (Phase-contrast light) and histological staining: H&E (cellular content), Masson's Trichrome(Collagen) and Toluidine Blue (GAGs) staining. Quantitative analysis of DNA **(B)**, Collagen **(C)** and GAGs **(D)** content. Scale bar: 50 µm (phase-contrast) and 200 µm (histological staining). Data represent mean ± S.D. (n = 3). ***, $p < 0.001$.

V.2.1.4. Preparation of bioink based on biomimetic ECM derived from MSCs

After decellularization, the early chondrogenic dmECM was lyophilized, milled into a fine powder and then solubilized with pepsin to liquify it at final concentrations of 3 and 6% w/v. (Figure 14). The resulting solubilized acidic biomimetic matrix solutions were adjusted to physiological pH before encapsulating cells. At low temperatures, biomimetic dmECM was freely flowing and slightly viscous but formed a stable gel once incubated at 37º C.

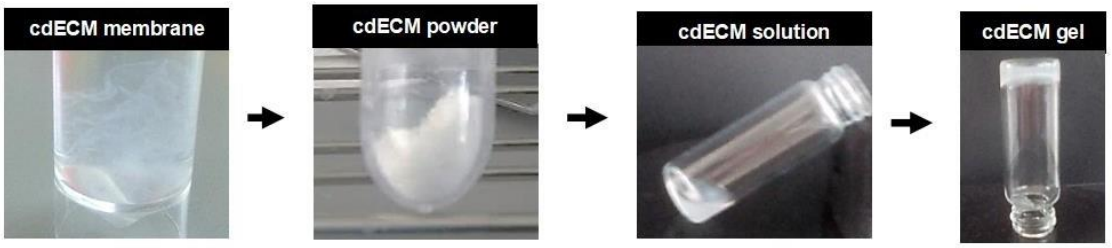

Figure 14. Schematic elucidating preparation of bionk based on early chondrogenic decellularized matrix derived from MSCs.

V.2.1.5. Characterization of bioink based on biomimetic ECM derived from MSCs

V.2.1.5.1. Rheological characterization

The flow behavior and gelling abilities of dmECM bioink were investigated through measurement of steady shear and dynamic oscillatory properties.

In Figure 15A, viscosity curve indicated that dmECM bioink exhibited a shear thinning behavior. It was evidenced by a decrease of viscosity with shear rate, ranging values from 3,96 Pa·s and 4,9 Pa·s at 0.01 s^{-1} shear rate to 0.005 Pa·s and 0.0126 Pa·s at 1000 s^{-1} shear rate for 3 and 6%, respectively. We also observed that a higher content of matrix produced a slight increase in bioink viscosity.

Shear recovery test determined that bioink was capable to recover after being exposed to cycles of large shear deformation. As it is observed in Figure 15B, viscosity of

dmECM bioink at both concentrations drops when they were subjected to large amplitude oscillatory strain, while it was quickly reestablished when returned to the low amplitude oscillatory strain, with no significant difference from the initial value.

In Figure 15C, temperature sweep test shows that storage modulus G' and loss modulus G'' of ECM bioinks changed significantly after raising the temperature from 20°C to 37°C. We observed that, for both concentrations, storage modulus exceeded loss modulus even at the lower temperature, indicating that bioink was acting as a gel-like material. At 37°C values of both moduli raised, especially for storage modulus. The higher value exhibited at 6% indicated that a more robust gel was generated in comparison to that formed at a lower concentration.

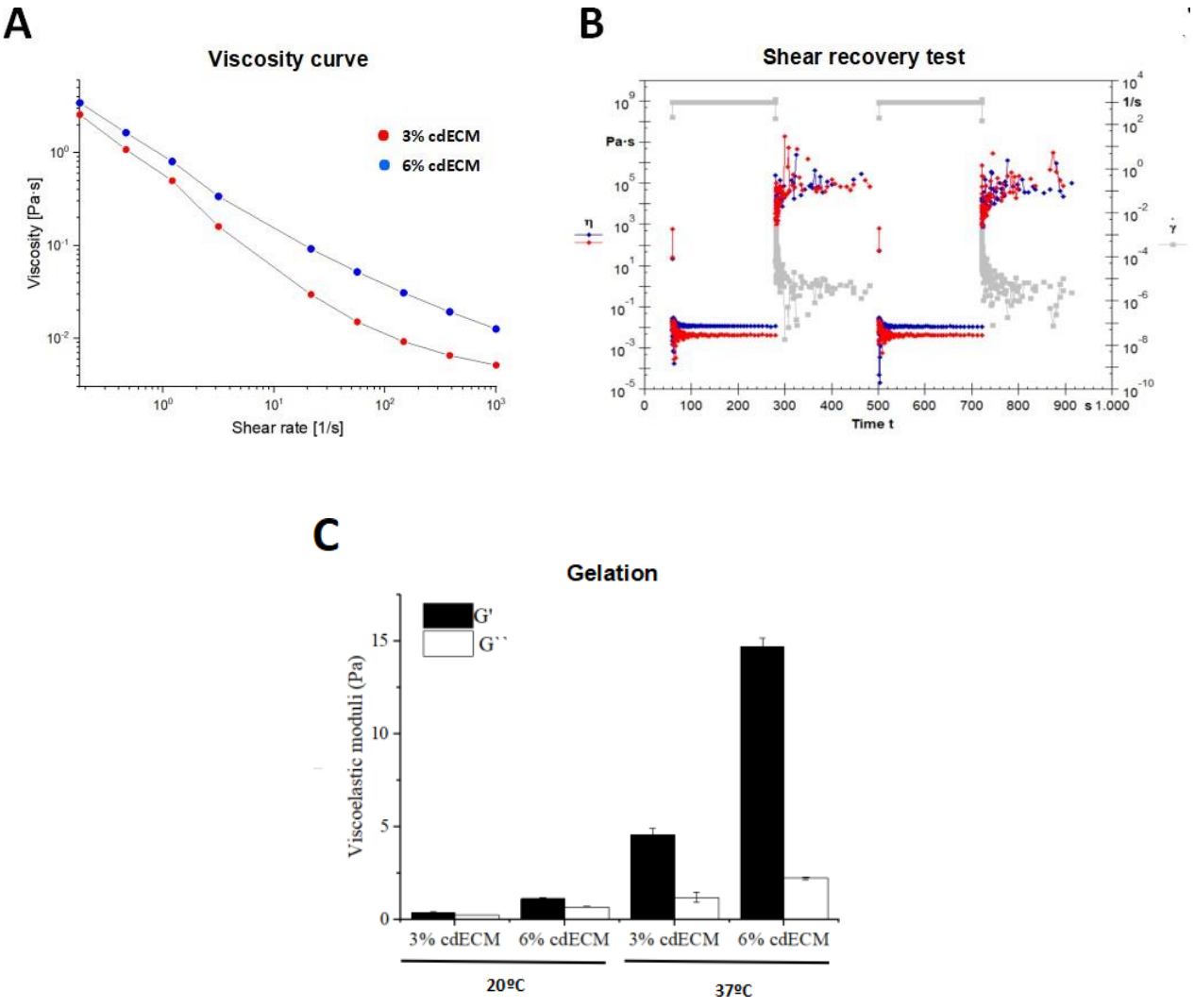

Figure 15. Rheological characterization of dmECM bioink with two concentrations (3 and 6%). **(A)** Flow curves of bioink viscosity as a function of shear rate. **(B)** Recovery behavior of the bioink at different shear rates. (C) Gelation of the bioink determined by monitoring viscoelastic moduli (Storage modulus G' and loss modulus G'') at 20°C and 37°C.

V.2.1.5.2. Biocompatibility

Cell survival of MSCs encapsulated inside 3% and 6% dmECM bioinks was determined using a live/dead staining during 28 days in culture. As it is shown in Figure 16, more than 90% of embedded cells were viable along this period in both gels, without significative differences between them. In addition to the good viability of the bioink, Alamar Blue assay revealed a tendency to maintain cell proliferation along culture time in both concentrations, although it showed an increase during the first days in the 6% dmECM bioink, remaining significatively higher than in the case of the 3% sample until 2 weeks. Nonetheless, at day 14 similar cell proliferation were found (Figure 16C).

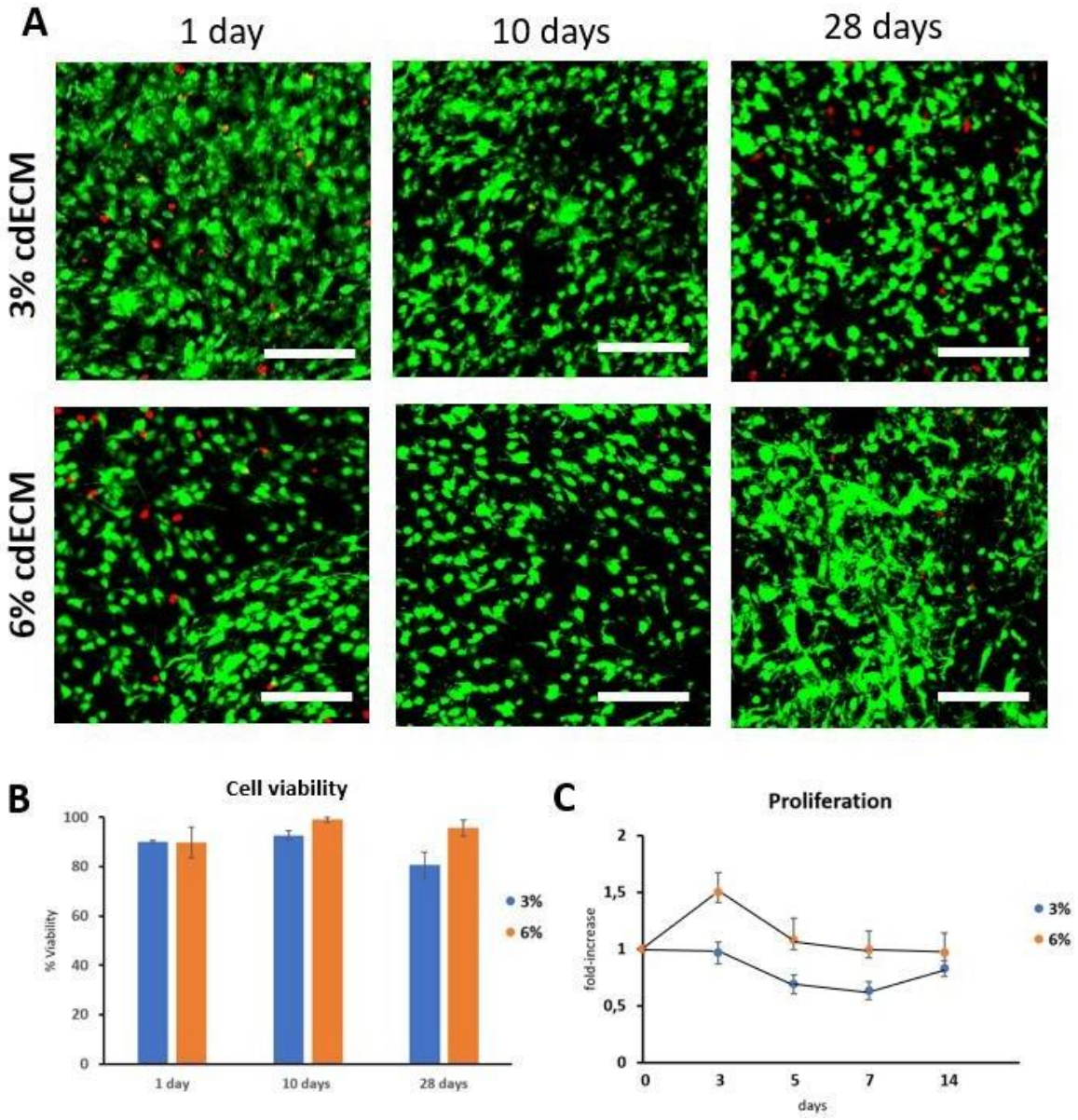

Figure 16. Cell viability inside the dmECM bioink at different concentrations. **(A)** Representative images from live/dead assay at 1, 10 and 28 days (green for live cells, red for dead cells). **(B)** Survival rates of MSCs inside the dmECM bioink. **(C)** Proliferation rate of MSCs cultured in dmECM bioink in comparison to day 0 of culture. Scale bar: 100 µm. Data represent mean ± S.D., n=3.

V.2.1.5.3. Functional characterization

To investigate the chondro-inductivity of dmECM bioink, gene expression from MSCs were analyzed during 1 month in culture without any inductive factor (Figure 17A). qPCR results evidenced a constant increase in the expression of chondrogenic markers and decrease on non-chondrogenic markers over time. High levels in COL2A1, ACAN and

SOX9 genes were observed by day 14 in both gels, although it was more significative in 3% than in 6% dmECM. At day 28, this upregulation was even more evident, in a concentration dependent manner. The decrease in fibrotic marker gene COL1A1 was also significant from day 14, and much more after 28 days, in both gels, whereas the expression of hypertrophic marker gene COL10A1 was undetectable from the beginning.

To confirm results from gene expression, we evaluated chondrogenesis in dmECM bioink using histological techniques (Figure 17B). Immunofluorescence staining revealed the presence of Collagen type II and Collagen type I after 14 days in culture. In accordance with the qPCR results previously described, it was observed a good evolution of the hyaline cartilaginous matrix over time, with more positive staining for Collagen type II and less for Collagen Type I by day 28, without appreciable differences between concentrations.

Altogether these results indicated that dmECM environment promoted chondrogenic commitment of MSCs and tissue-specific formation, more efficiently at higher concentrations.

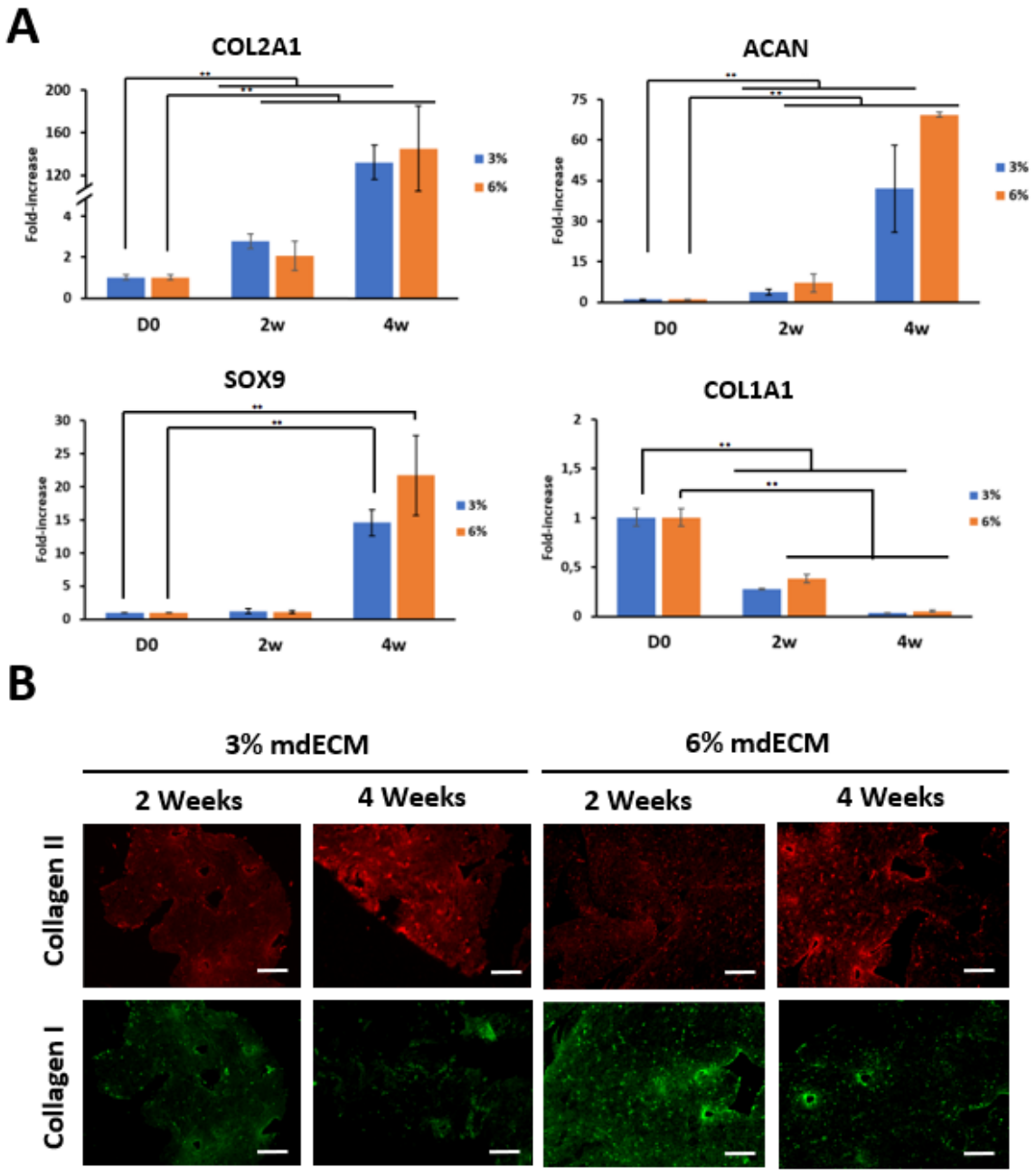

Figure 17. Evaluation of chondro-inductivity of dmECM bioink *in vitro*. **(A)** Gene expression analysis of specific (COL2A1, ACAN, SOX9) and non-specific chondrogenic (COL1A1) genes of MSCs in 3 and 6% dmECM after 2 and 4 weeks. **(B)** Histological analysis of chondrogenic and non-chondrogenic markers in MSCs-dmECM gel using safranin O staining (GAGs) and immunostaining for Collagen II and Collagen I. Scale bar 100 µm. Data are expressed as mean ± S.D.; n=3; **p < 0.01.

V.2.1.5.4. Morphological characterization

To examine the internal ultrastructure of the dmECM bioink, SEM was performed. Our results show that it had a 3D sponge-like appearance with a randomly oriented fibrillar structure (Figure 18). Both concentrations appeared visually similar, although interconnectivity was higher with increasing concentration.

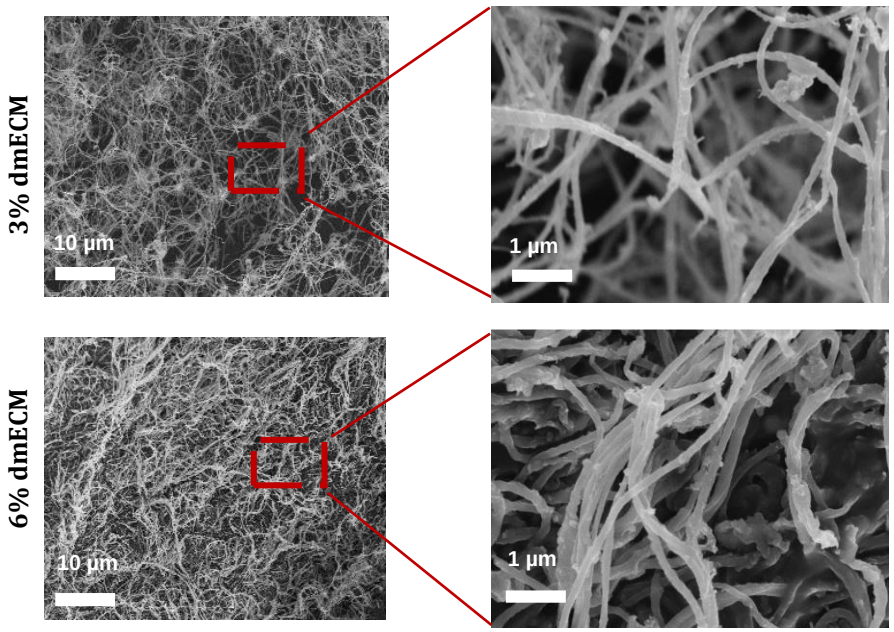

Figure 18. Scanning electron micrographs of crosslinked dmECM bioink at varying magnifications from 5,000x to 23,000x.

V.2.1.5.5.* Evaluation of dmECM bioink *in vivo

To evaluate the *in vivo* maintenance of chondrogenic properties, dmECM bioinks were subcutaneously injected into mouse dorsal regions at two concentrations. Previously to implantation, dmECM gels were inserted in 3D-printed PCL scaffolds in order to easy localization once in mice.

Biocompatibility was assessed by subcutaneous implantation of the scaffold-based on acellular bioink in subcutaneous pockets along the dorsal skin of immunocompetent mice. After 2- and 4-weeks post-implantation, animals were

euthanized, and the constructs containing dmECM gels were retrieved for analysis. During the retrieval process, we found no red or swelling appearance, and the scaffolds were well integrated with surrounding tissues (Figure 19A). DAPI staining demonstrated the distribution of cells in the acellular gel, suggesting infiltration of surrounding cells. The increasing number of nucleus over time indicated that cells were able to attach, penetrate, and grow into the 3D structure of the bioink (Figure 19B).

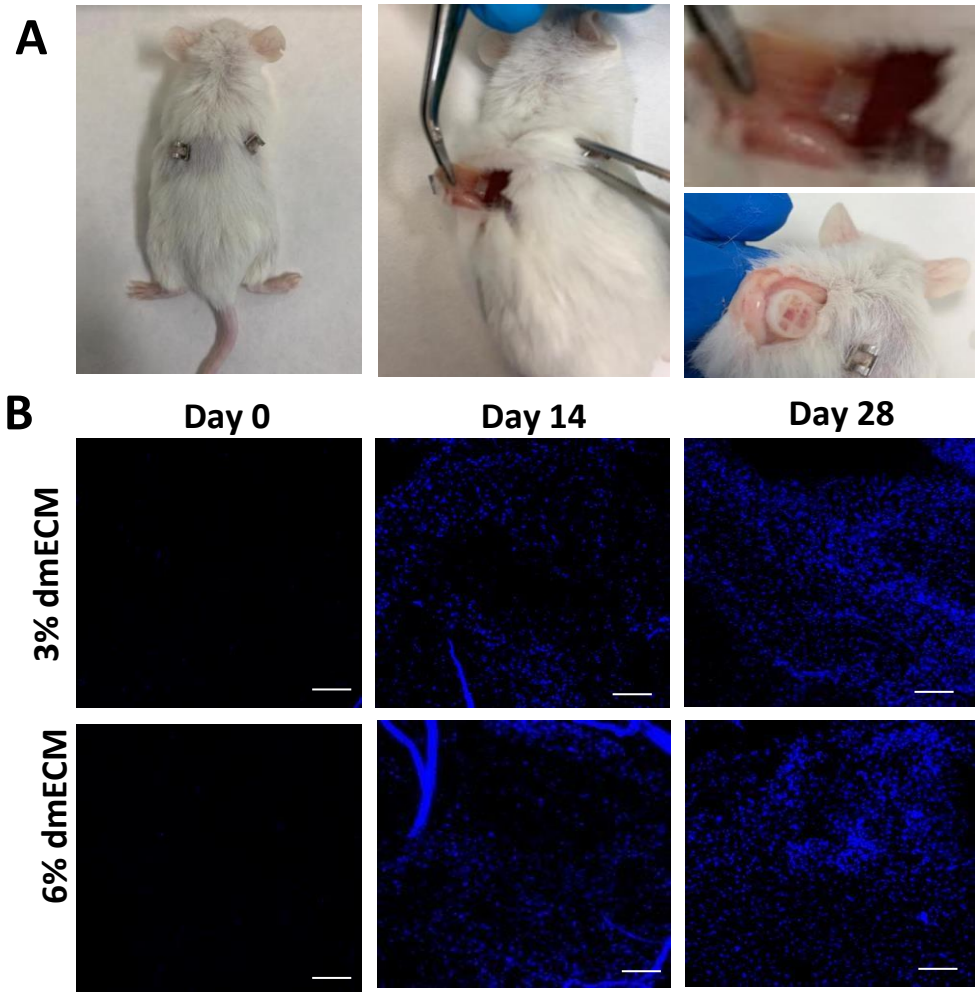

Figure 19. Biocompatibility of dmECM bioink *in vivo*. **(A)** Images at 4 weeks of post-implantation. ***(B)*** DAPI staining to show cell infiltration in subcutaneously implanted acellular dmECM gels after 2 and 4 weeks.

Tissue formation after implantation was examined by histology (Figure 20). H&E staining showed that cells in dmECM gel, especially at the highest concentration, acquired the typical shape of chondrocytes embedded in lacunas after 2 weeks *in vivo*.

Using Safranin O and Toluidine O staining it is also evidenced an increase in the deposition of GAGs, showing an intense staining in four-week implanted 3% and 6% dmECM gels. Although these results from both concentrations of dmECM were comparable to that produced by implanting a control pellet, which is the current methodology to promote chondrogenesis; however, it can be observed that dmECM was able to induce a more dense and compact matrix.

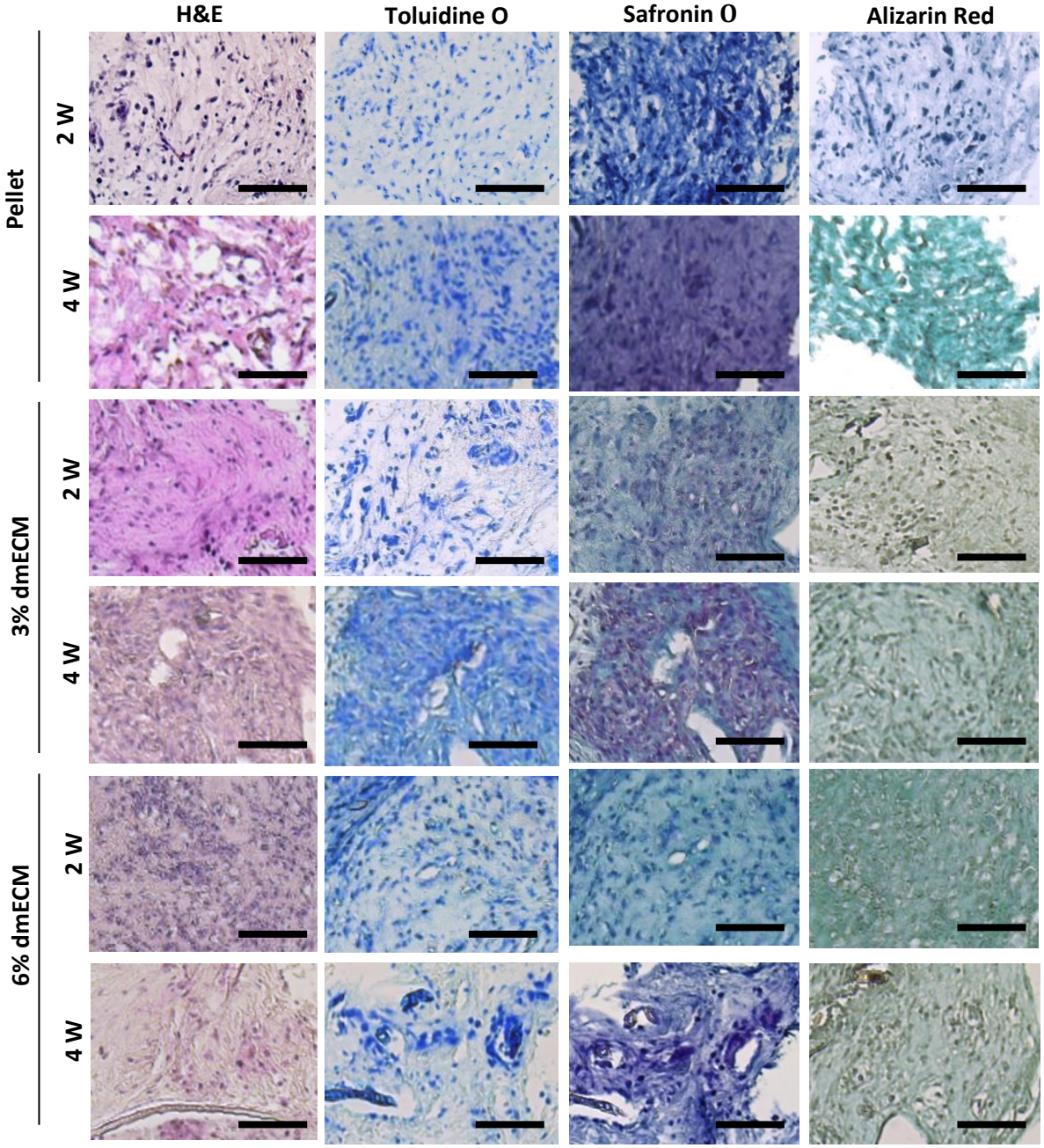

Figure 20. Tissue formation in dmECM gels *in vivo*. Histological analysis of dmECM gels and pellet at 2 and 4 weeks after subcutaneous implantation in mice.

V.2.2. Discussion

Cell-derived ECM offers an alternative option to produce ECM-based bioink as it contains a complex assembly of macromolecules, including fibrillar proteins and glycosaminoglycans, and it is easy to obtain on a larger scale by simple monolayer culture. Especially, an advantage for those derived from MSCs is that they are able to be customized depending on culture conditions [112–116].

During tissue development, including chondrogenesis, the composition of extracellular microenvironments is constantly changing in order to regulate the process and provide appropriated signals at each development state [131–134]. Studies that compared several states of maturity have evidenced different effects on cells, such as in MSCs differentiation, which was more favorable in early matrices [124,137]. These better results were related to biochemical composition, as early matrix contain factors that are not present in the mature one.Taking all this in consideration, we generated an early chondrogenic matrix that was confirmed by the initial expression of major components of native tissue, collagen type II and GAGs, as well as proteins that have been linked to the first steps of chondrogenesis such as fibronectin, collagen type I, versican or tenascin-C [133]. In addition to those markers, mass spectrometry also allows the identification of other components that constitute this rich and complex matrix, including structural proteins that confer mechanical properties and cell adhesion, as well as affiliated proteins that contribute to ECM function and dynamics. Among structural proteins, collagens such as type III, V, VIII or XII, which are involved in formation and assembly of the main collagen in cartilage (collagen type II) were detected, or collagen VI, which is the primary collagen located in the pericellular matrix of that tissue. Also, we found glycoproteins, including MSC matrix markers like Emilin-1 but also typical structural proteins of cartilage matrix such as COMP, LUM, CSPG2 or PRELP; and proteoglycans such as Biglycan or Decorin. As affiliated proteins we found regulators, which maintain a balance between ECM stability and remodeling by degrading proteins, such as MMPs and its inhibitors, TIMPs; and ECM-associated proteins, such as Annexins and Galectins, involved in the assembly of ECM structural elements, as well as cell-adhesion proteins ([133,159,160]. For example, annexin A2 is bound to the tenascin-C and has a role in regulating cell functions by inducting signaling pathways such as migration and mitogenesis. Since ECM serves as a reservoir for

numerous secreted factors that bind to core matrisome proteins, as well as ECM-associated proteins, we could identify some like hepatoma-derived growth factor responsible for mitogenic activity, or connective tissue growth factor implicated in various cellular processes such as cell proliferation and differentiation of chondrocytes, among others [10,114,133,161].

The formulation of the cell-derived ECM bioink, as in the case of tissue-derived ECM, involves a process that includes decellularization and solubilization of matrix. The first step was the most important, since it should ensure that the minimum possible cellular material remains while preserving the most ECM components, which provide matrix functionality. In the literature, there are several protocols that have been applied to decellularize ECM from monolayer culture [138]. Among these, the most frequent has been the combination of Triton X-100 (mild detergent) and ammonium hydroxide (alkaline reagent), to break down cellular and nuclear membranes, followed by enzymatic treatment based on nucleases, to disrupt cytoplasmatic content and break down remnant DNA and RNA [162,163]. Using this method, researchers have demonstrated decellularization efficiency without influencing ECM intactness. Here, we also effectively decellularized the early chondrogenic matrix derived from MSCs. The absence of nuclei and DNA content, which was lower than the upper limit content considered (<50 ng/mg DNA) [164], confirmed the complete removal of cellular content, while similar patterns in terms of composition indicated minimal subtraction of ECM elements.

A biomimetic bioink based on MSCs-derived ECM was finally attained after solubilization and neutralization of the decellularized matrix at different concentrations (3 and 6% w/v). Due to the high presence of collagen, it showed thermo-sensitivity, remaining in solution state at low temperatures, but becoming gel when incubated at 37°C.

There are fundamental aspects to be considered when designing bioinks for 3D bioprinting. Material requirements include mainly printability and gelling abilities [143,165–167]. Results from rheological analysis revealed that dmECM bioink could have suitable properties to be applied in 3D bioprinting. On the one hand, it had a

viscosity in the range required for extrusion-based bioprinting [165], that could be improved by increasing matrix concentration. Moreover, it exhibited shear-thinning behavior, which is essential to assure good extrusion and cell protection during the printing process. The bioink also demonstrated quick shear recovery, which would ensure shape retention after extrusion. On the other hand, the rheological study also showed that dmECM bioink was capable to jellify at 37°C, more strongly at the highest concentration, although it exhibited a gel-like behavior even at low temperature [168]. This feature was expected due to the presence of self-assembling molecules responsible for the gelation such as collagens, laminins, and proteoglycans, and it would assure stability of printed bioink for long time [104,106,150].

In addition to mechanical properties, an ideal bioink have to satisfy some biological requirements, which include biocompatibility and bioactivity [143,150]. Here, we showed that dmECM bioink provided a cell-friendly environment, supporting a high cell viability at different concentrations of 3% and 6%, which were evidenced by the live/Dead assay. These results are in line with many other studies, which previously reported the benefits of ECM as biomaterial in tissue engineering, including improvement cell maintenance, cell adhesion, reduction of apoptosis, and intracellular ROS activity decrease [119–122]. In terms of functionality, dmECM bioink was capable to induce chondrogenic differentiation of MSCs and cartilage tissue formation without any external stimuli. These effects were observed by an increase in cartilage-specific markers, both at genetic (COL2A1, ACAN and SOX9 genes) and proteomic (collagen type II and proteoglycans) levels using qPCR and histological techniques, respectively. These results highlight the role that ECM plays on cell behavior and, therefore, the importance of its structural composition. There are many studies that have evidenced the capacity of specific ECMs, from tissue or cells isolated from these, to direct stem cell fate toward particular cell lineages [124,126,169–172]. Promising results have been recently reported by using stepwise-mimicking matrices derived from stem cells, as it presents a composition that reproduce better the environment and contain adequate factors necessaries for tissue development [117,124]. Otherwise, cell differentiation could also explain the maintenance of proliferation that was observed along the culture period in both concentrations, although 6% showed an increase during the first days. This fact

could be related to a higher content in fibronectin, which is involved in the promotion of cell survival and proliferation during the first stage of chondrogenesis [133] and/or by restriction of cell migration and viability due to the high density of the fibrillar structures.

As a follow-up step, we evaluated the potential of dmECM bioink *in vivo* by its subcutaneous implantation in a mice model. Similar to the *in vitro* study, it was demonstrated the biocompatibility by the high cell infiltration and no immune reaction or inflammation. Although it is known that ECM can cause this adverse effects, however, our results could be explained by the presence of immunomodulatory factors, secreted by MSC during matrix production, and retained in dmECM after decellularization [173,174]. Histological analysis also revealed that dmECM bioink was supportive of hyaline cartilage development once *in vivo*, showing an increased deposition of cartilage components (GAGs and Collagen) over 4 weeks, in a concentration-dependent way. The neo-cartilage tissue formed in both concentrations of dmECM gels was better that control pellet, which is the current methodology to promote chondrogenesis.

In conclusion, we have demonstrated that MSCs are an attractive source of ECM useful to produce biomimetic bioinks. Its stem cell properties, such as self-renewal and capacity to commit towards several cell lineages, allowed the generation of a stepwise biomimetic cartilaginous ECM easily and at low cost. It was useful to formulate a new bioink capable to induce chondrogenesis and further hyaline cartilage formation. Although it has been addressed to cartilage regeneration, our results encourage applying this strategy for engineering other tissues and organs by 3D bioprinting.

VI. CONCLUSIONS

1. To produce a biomimetic bioink based on natural polymers, 1% HA (w/v) and 2% alginate (w/v) shows the most effective formulation for CTE application.
2. The biomimetic bioink based on natural polymers exhibits good mechanical properties, including easy extrusion ability, shear thinning behavior and gelling capabilities to be applied to 3D bioprinting.
3. The co-bioprinting of biomimetic bioink based on natural polymers and PLA enable to generate 3D cartilage-like constructs.
4. The biomimetic bioink based on natural polymers preserves cell viability and genomic stability during the 3D bioprinting process and, then, in the cartilage-like constructs.
5. The biomimetic bioink based on natural polymers provides a suitable environment for cartilage development, by promoting chondrogenic phenotype in cartilage-like constructs.
6. *In vitro* cultures of MSCs enable the production of a biomimetic matrix that better reproduce the environment established during chondrogenesis.
7. The ECM derived from MSCs in culture allows the production of a new biomimetic bioink for cartilage tissue 3D bioprinting after its complete decellularization and solubilization.
8. The biomimetic bioink based on dmECM exhibits suitable mechanical properties, including shear thinning behavior, good shear recovery and gelling abilities useful to be applied to 3D bioprinting.
9. The biomimetic bioink based on dmECM offers a suitable environment for cells, preserving high viability at long time in culture.
10. The biomimetic bioink based on dmECM has high bioactive properties, including chondrogenesis of MSCs *in vitro*.
11. The biomimetic bioink based on dmECM is biocompatible and provoke well integration in immunocompetent mice.

12. The biomimetic bioink based on dmECM allows cartilage-specific tissue formation *in vivo*.

13. Our results clearly suggest the great potential of bioinks based on dmECM to generate other mature tissues and encourage further studies to translate 3D bioprinting technology based on these conditioned dmECM to the clinical arena.

VII. CONCLUSIONES

1. Para la producción de una biotinta biomimética basada en polímeros naturales, el 1% HA (p/v) y 2% alginato (p/v) resulta la formulación más eficaz para la aplicación de CTE.

2. La biotinta biomimética basada en polímeros naturales exhibe buenas propiedades mecánicas, incluyendo la capacidad de extrusión fácil, propiedades viscoelásticas y rápida gelificación, para ser aplicada a la bioimpresión 3D.

3. La co-impresión de la biotinta biomimética basada en polímeros naturales y PLA permiten generar constructos en 3D similares al cartílago.

4. La biotinta biomimética basada en polímeros naturales preserva la viabilidad celular y la estabilidad genómica durante el proceso de bioimpresión 3D y, posteriormente, en los constructos 3D.

5. La biotinta biomimética basada en polímeros naturales proporciona un entorno adecuado para el desarrollo del cartílago, mediante la promoción del fenotipo condrogénico en los constructos 3D.

6. El cultivo de células madre mesenquimales in vitro permite la producción de una matriz biomimética que reproduce mejor el entorno establecido durante la condrogénesis.

7. La matriz derivada de células madre mesenquimales en cultivo permite la producción de una nueva biotinta biomimética útil para la bioimpresión 3D de cartílago, tras su completa descelularización y solubilización.

9. La biotinta biomimética basada en matriz de células en cultivo exhibe propiedades mecánicas adecuadas, incluyendo viscoelasticidad, buena recuperación tras un esfuerzo y capacidades de gelificación, para su aplicación en la bioimpresión 3D.

10. La biotinta biomimética basada en matriz de células en cultivo ofrece un entorno adecuado para las células, preservando la alta viabilidad durante todo el tiempo del cultivo in vitro.

11. La biotinta biomimética basada en matriz de células en cultivo tiene altas propiedades bioactivas, incluyendo la condrogénesis de las células madre mesenquimales in vitro.

12. La biotinta biomimética basada en matriz de células en cultivo es biocompatible y provoca una buena integración en ratones inmunocompetentes.

13. La biotinta biomimética basada en matriz de células en cultivo permite la formación de tejido específico del cartílago in vivo.

14. Nuestros resultados sugieren claramente el gran potencial de los bioinks basados en dmECM para generar otros tejidos maduros y alentar más estudios para traducir la tecnología de bioimpresión 3D basada en estos dmECM condicionados a la arena clínica.

VIII. ABREVIATIONS LIST

3D: Three-Dimensional

A: Alginate

ACI: Autologous Chondrocytes Implantation

ADAMTS: A Disintegrin-like and Metalloproteinase-like Domain Thrombospondin Domain

ASC: Adipose derived Stem Cell

BMP: Bone Morphogenetic Protein

COMP: Cartilage Oligomeric Matrix Protein

CS: Chondroitin sulfate

CSPCs: Chondrogenic Stem Progenitor Cells

CSPG2: Chondroitin Sulfate Proteoglycan Core Protein 2

CT: Computerized Tomography

CTE: Cartilage Tissue Engineering

CTG: Cell tracker Green

DAPI: 4',6-Diamidino-2-Phenylindole Dihydrochloride

dECM: Decellularized Extracellular Matrix

dmECM: Decellularized MSC-derived extracellular matrix

DMMB: 1,9-Dimethylmethylene Blue

DMEM: Dulbecco's Modified Eagle's Medium

DNA: Deoxyribonucleic Acid

DNase: Deoxyribonuclease

dNTP: Deoxyribonucleotide Triphosphate

ECM: Extracellular Matrix

EDTA: Ethylenediaminetetraacetic Acid

ESC: Embryonic Stem Cells

FACIT: Fibril Associated Collagens with Interrupted Triple Helices

FACS: Fluorescence-activated Cell Sorting

FBS: Fetal Bovine Serum

FDA: Federal Drug Administration

FITC: Fluorescein Iso-thiocyanate

FGF: Fibroblast Growth Factor

G': storage modulus

G'': loss modulus

GAPDH: Glyceraldehyde-3-Phosphate Dehydrogenase

GAGs: Glycosaminoglycans

GelMA: Methacryloyl-modified Gelatin

H&E: Hematoxylin and Eosin

HA: Hyaluronic Acid

HS: Heparin Sulfate

IGF: Insulin-like Growth Factor

iPS: Induced Pluripotent Stem Cell

ISCT: International Society for Cellular Therapy

LUM: Lumican

MMP: Metalloproteinases

MRI: Magnetic Resonance Imaging

mRNA: messenger RNA

MS: Mass Spectroscopy

MSC: Mesenchymal Stem Cell

OA: Osteoarthritis

OCT: Optimal cutting temperature compound

PBS: Phosphate Buffered Saline

PCL: Poly-caprolactone

PCR: Polymerase Chain Reaction

PE: Phycoerythrin

PEG: Poly(ethyl) Glycol

PEGDA: Poly(Ethylene Glycol) Diacrylate

PEGDMA: Poly(Ethylene Glycol) Dimethacrylate

PFA: Paraformaldehyde

PGA: Poly (glycolic acid)

PLA: Poly(lactic acid)

PLCL: Poly (*ε*-caprolactone-*co*-lactide)

PLGA: Poly(lactic-co-glycolic acid)

PRELP: Prolargin

PTHrP: Parathyroid Hormone-related Protein

PVA: Poly(vinyl alcohol)

qPCR: Quantitative Polymerase Chain Reaction

RNA: Ribonucleic acid

RNase: Ribonuclease

RT: Room Temperature

RT-PCR: Reverse Transcription Polymerase Chain Reaction

SEM: Scanning Electron Microscope

tdECM: Decellularized Extracellular Matrix derived from Tissue

TE: Tissue Engineering

TIMPs: Metalloproteinases Inhibitors

TGF-β: Transforming growth factor

IX. BIBLIOGRAPHY

[1] D. Heinegård, M. Paulsson, Cartilage, Methods Enzymol. 145 (1987) 336–363. doi:10.1016/0076-6879(87)45020-9.

[2] M. Stockwell, R. A., Meachim, G., & Freeman, Adult articular cartilage., London Med. P. (1979).

[3] M.I. Froimson, A. Ratcliffe, T.R. Gardner, V.C. Mow, Differences in patellofemoral joint cartilage material properties and their significance to the etiology of cartilage surface fibrillation, Osteoarthr. Cartil. 5 (1997) 377–386. doi:10.1016/S1063-4584(97)80042-8.

[4] A.R. Poole, T. Kojima, T. Yasuda, F. Mwale, M. Kobayashi, S. Laverty, Composition and structure of articular cartilage: A template for tissue repair, in: Clin. Orthop. Relat. Res., Lippincott Williams and Wilkins, 2001. doi:10.1097/00003086-200110001-00004.

[5] I. Onyekwelu, M.B. Goldring, C. Hidaka, Chondrogenesis, joint formation, and articular cartilage regeneration, J. Cell. Biochem. 107 (2009) 383–392. doi:10.1002/jcb.22149.

[6] J.S. Temenoff, A.G. Mikos, Review: Tissue engineering for regeneration of articular cartilage, Biomaterials. 21 (2000) 431–440. doi:10.1016/S0142-9612(99)00213-6.

[7] A.J. Sophia Fox, A. Bedi, S.A. Rodeo, The basic science of articular cartilage: Structure, composition, and function, Sports Health. 1 (2009) 461–468. doi:10.1177/1941738109350438.

[8] A.M. Bhosale, J.B. Richardson, Articular cartilage: Structure, injuries and review of management, Br. Med. Bull. 87 (2008) 77–95. doi:10.1093/bmb/ldn025.

[9] S. Boeuf, W. Richter, Chondrogenesis of mesenchymal stem cells: Role of tissue source and inducing factors, Stem Cell Res. Ther. 1 (2010). doi:10.1186/scrt31.

[10] R.O. Hynes, A. Naba, Overview of the matrisome-An inventory of extracellular matrix constituents and functions, Cold Spring Harb. Perspect. Biol. 4 (2012). doi:10.1101/cshperspect.a004903.

[11] J. Ryu, B. V. Treadwell, H.J. Mankin, Biochemical and metabolic abnormalities in normal and osteoarthritic human articular cartilage, Arthritis Rheum. 27 (1984) 49–57. doi:10.1002/art.1780270109.

[12] P. Abdel-Sayed, D.P. Pioletti, Strategies for improving the repair of focal cartilage defects, Nanomedicine. 10 (2015) 2893–2905. doi:10.2217/nnm.15.119.

[13] B. Zylińska, P. Silmanowicz, A. Sobczyńska-Rak, Ł. Jarosz, T. Szponder, Treatment of articular cartilage defects: Focus on tissue engineering, In Vivo (Brooklyn). 32 (2018) 1289–1300. doi:10.21873/invivo.11379.

[14] M. Tamaddon, L. Wang, Z. Liu, C. Liu, Osteochondral tissue repair in osteoarthritic joints: clinical challenges and opportunities in tissue engineering, Bio-Design Manuf. 1 (2018) 101–114. doi:10.1007/s42242-018-0015-0.

[15] R. Lyon, X.-C. Liu, Future Treatment Strategies for Cartilage Repair, Clin. Sports Med. 33 (2014) 335–352. doi:10.1016/j.csm.2013.12.003.

[16] A.R. Armiento, M.J. Stoddart, M. Alini, D. Eglin, Biomaterials for articular cartilage tissue engineering: Learning from biology, Acta Biomater. 65 (2018) 1–20. doi:10.1016/j.actbio.2017.11.021.

[17] B. Mollon, R. Kandel, J. Chahal, J. Theodoropoulos, The clinical status of cartilage tissue regeneration in humans, Osteoarthr. Cartil. 21 (2013) 1824–1833.

doi:10.1016/j.joca.2013.08.024.

[18] J.P. Vacan~, R. Langer, Tissue engineering: the design and fabrication of living replacement devices for surgical reconstruction and transplantation, n.d.

[19] K. Kim, D.M. Yoon, A. Mikos, F.K. Kasper, Harnessing cell-biomaterial interactions for osteochondral tissue regeneration., Adv. Biochem. Eng. Biotechnol. 126 (2012) 67–104. doi:10.1007/10_2011_107.

[20] H. Chiang, C.-C. Jiang, Repair of Articular Cartilage Defects: Review and Perspectives, n.d. doi:10.1016/S0929-6646(09)60039-5.

[21] L. Danišovič, I. Varga, R. Zamborský, D. Böhmer, The tissue engineering of articular cartilage: cells, scaffolds and stimulating factors, Exp. Biol. Med. 237 (2012) 10–17. doi:10.1258/ebm.2011.011229.

[22] M. Dominici, K. Le Blanc, I. Mueller, I. Slaper-Cortenbach, F.C. Marini, D.S. Krause, R.J. Deans, A. Keating, D.J. Prockop, E.M. Horwitz, Minimal criteria for defining multipotent mesenchymal stromal cells. The International Society for Cellular Therapy position statement, Cytotherapy. 8 (2006) 315–317. doi:10.1080/14653240600855905.

[23] L. Song, D. Baksh, R.S. Tuan, Mesenchymal stem cell-based cartilage tissue engineering: Cells, scaffold and biology, Cytotherapy. 6 (2004) 596–601. doi:10.1080/14653240410005276-1.

[24] M. Bhattacharjee, J. Coburn, M. Centola, S. Murab, A. Barbero, D.L. Kaplan, I. Martin, S. Ghosh, Tissue engineering strategies to study cartilage development, degeneration and regeneration, Adv. Drug Deliv. Rev. 84 (2015) 107–122. doi:10.1016/j.addr.2014.08.010.

[25] M.J. Lammi, J. Piltti, J. Prittinen, C. Qu, Challenges in fabrication of tissue-engineered cartilage with correct cellular colonization and extracellular matrix assembly, Int. J. Mol. Sci. 19 (2018). doi:10.3390/ijms19092700.

[26] Z. Izadifar, T. Chang, W. Kulyk, X. Chen, B.F. Eames, Analyzing biological performance of 3D-printed, cell-impregnated hybrid constructs for cartilage tissue engineering, Tissue Eng. - Part C Methods. 22 (2016) 173–188. doi:10.1089/ten.tec.2015.0307.

[27] P. Bajaj, R.M. Schweller, A. Khademhosseini, J.L. West, R. Bashir, 3D Biofabrication Strategies for Tissue Engineering and Regenerative Medicine, Annu. Rev. Biomed. Eng. 16 (2014) 247–276. doi:10.1146/annurev-bioeng-071813-105155.

[28] J. Yang, Y.S. Zhang, K. Yue, A. Khademhosseini, Cell-laden hydrogels for osteochondral and cartilage tissue engineering, Acta Biomater. 57 (2017) 1–25. doi:10.1016/j.actbio.2017.01.036.

[29] V.E. Santo, M.E. Gomes, J.F. Mano, R.L. Reis, Controlled release strategies for bone, cartilage, and osteochondral engineering-part i: Recapitulation of native tissue healing and variables for the design of delivery systems, Tissue Eng. - Part B Rev. 19 (2013) 308–326. doi:10.1089/ten.teb.2012.0138.

[30] D.A. Yu, J. Han, B.S. Kim, Stimulation of chondrogenic differentiation of mesenchymal stem cells, Int. J. Stem Cells. 5 (2012) 16–22. doi:10.15283/ijsc.2012.5.1.16.

[31] M. Demoor, D. Ollitrault, T. Gomez-Leduc, M. Bouyoucef, M. Hervieu, H. Fabre, J. Lafont, J.M. Denoix, F. Audigié, F. Mallein-Gerin, F. Legendre, P. Galera, Cartilage tissue engineering: Molecular control of chondrocyte differentiation for proper cartilage matrix reconstruction, Biochim. Biophys. Acta - Gen. Subj. 1840 (2014) 2414–2440.

doi:10.1016/j.bbagen.2014.02.030.

[32] A. Arslan-Yildiz, R. El Assal, P. Chen, S. Guven, F. Inci, U. Demirci, Towards artificial tissue models: Past, present, and future of 3D bioprinting, Biofabrication. 8 (2016). doi:10.1088/1758-5090/8/1/014103.

[33] I.T. Ozbolat, W. Peng, V. Ozbolat, Application areas of 3D bioprinting, Drug Discov. Today. 21 (2016) 1257–1271. doi:10.1016/j.drudis.2016.04.006.

[34] A. Munaz, R.K. Vadivelu, J. St. John, M. Barton, H. Kamble, N.T. Nguyen, Three-dimensional printing of biological matters, J. Sci. Adv. Mater. Devices. 1 (2016) 1–17. doi:10.1016/j.jsamd.2016.04.001.

[35] L. Roseti, C. Cavallo, G. Desando, V. Parisi, M. Petretta, I. Bartolotti, B. Grigolo, Three-Dimensional Bioprinting of Cartilage by the Use of Stem Cells: A Strategy to Improve Regeneration, Materials (Basel). 11 (2018) 1749. doi:10.3390/ma11091749.

[36] V.H.M. Mouser, R. Levato, L.J. Bonassar, D.D. D'Lima, D.A. Grande, T.J. Klein, D.B.F. Saris, M. Zenobi-Wong, D. Gawlitta, J. Malda, Three-Dimensional Bioprinting and Its Potential in the Field of Articular Cartilage Regeneration, Cartilage. 8 (2017) 327–340. doi:10.1177/1947603516665445.

[37] J. Groll, J.A. Burdick, D.W. Cho, B. Derby, M. Gelinsky, S.C. Heilshorn, T. Jüngst, J. Malda, V.A. Mironov, K. Nakayama, A. Ovsianikov, W. Sun, S. Takeuchi, J.J. Yoo, T.B.F. Woodfield, A definition of bioinks and their distinction from biomaterial inks, Biofabrication. 11 (2019). doi:10.1088/1758-5090/aaec52.

[38] P.S. Gungor-Ozkerim, I. Inci, Y.S. Zhang, A. Khademhosseini, M.R. Dokmeci, Bioinks for 3D bioprinting: An overview, Biomater. Sci. 6 (2018) 915–946. doi:10.1039/c7bm00765e.

[39] S.K. Williams, J.B. Hoying, Bioinks for bioprinting, in: Bioprinting Regen. Med., Springer International Publishing, 2015: pp. 1–31. doi:10.1007/978-3-319-21386-6_1.

[40] Y. Luo, X. Wei, P. Huang, 3D bioprinting of hydrogel-based biomimetic microenvironments, J. Biomed. Mater. Res. - Part B Appl. Biomater. 107 (2019) 1695–1705. doi:10.1002/jbm.b.34262.

[41] J. Jang, J.Y. Park, G. Gao, D.W. Cho, Biomaterials-based 3D cell printing for next-generation therapeutics and diagnostics, Biomaterials. 156 (2018) 88–106. doi:10.1016/j.biomaterials.2017.11.030.

[42] V.H.M. Mouser, A. Abbadessa, R. Levato, W.E. Hennink, T. Vermonden, D. Gawlitta, J. Malda, Development of a thermosensitive HAMA-containing bio-ink for the fabrication of composite cartilage repair constructs, Biofabrication. 9 (2017). doi:10.1088/1758-5090/aa6265.

[43] Z.M. Jessop, N. Gao, S. Manivannan, A. Al-Sabah, I.S. Whitaker, 3D bioprinting cartilage, in: 3D Bioprinting Reconstr. Surg. Tech. Appl., Elsevier Inc., 2018: pp. 277–304. doi:10.1016/B978-0-08-101103-4.00034-X.

[44] K.Y. Lee, J.A. Rowley, P. Eiselt, E.M. Moy, K.H. Bouhadir, D.J. Mooney, Controlling Mechanical and Swelling Properties of Alginate Hydrogels Independently by Cross-Linker Type and Cross-Linking Density, Macromolecules. 33 (2000) 4291–4294. doi:10.1021/ma9921347.

[45] E. Axpe, M.L. Oyen, Applications of alginate-based bioinks in 3D bioprinting, Int. J. Mol.

Sci. 17 (2016). doi:10.3390/ijms17121976.

[46] J.T. Connelly, A.J. García, M.E. Levenston, Inhibition of in vitro chondrogenesis in RGD-modified three-dimensional alginate gels, Biomaterials. 28 (2007) 1071–1083. doi:10.1016/j.biomaterials.2006.10.006.

[47] J.C. Chang, S. hui Hsu, D.C. Chen, The promotion of chondrogenesis in adipose-derived adult stem cells by an RGD-chimeric protein in 3D alginate culture, Biomaterials. 30 (2009) 6265–6275. doi:10.1016/j.biomaterials.2009.07.064.

[48] A. Grigore, B. Sarker, B. Fabry, A.R. Boccaccini, R. Detsch, Behavior of encapsulated MG-63 cells in RGD and gelatine-modified alginate hydrogels, Tissue Eng. - Part A. 20 (2014) 2140–2150. doi:10.1089/ten.tea.2013.0416.

[49] D.O. Visscher, E.J. Bos, M. Peeters, N. V. Kuzmin, M.L. Groot, M.N. Helder, P.P.M. van Zuijlen, Cartilage Tissue Engineering: Preventing Tissue Scaffold Contraction Using a 3D-Printed Polymeric Cage, Tissue Eng. Part C Methods. 22 (2016) 573–584. doi:10.1089/ten.tec.2016.0073.

[50] S. Ibusuki, A. Papadopoulos, M.P. Ranka, G.J. Halbesma, M.A. Randolph, R.W. Redmond, I.E. Kochevar, T.J. Gill, Engineering cartilage in a photochemically crosslinked collagen gel., J. Knee Surg. 22 (2009) 72–81. doi:10.1055/s-0030-1247729.

[51] N.S. Kajave, T. Schmitt, T.U. Nguyen, V. Kishore, Dual crosslinking strategy to generate mechanically viable cell-laden printable constructs using methacrylated collagen bioinks, Mater. Sci. Eng. C. 107 (2020). doi:10.1016/j.msec.2019.110290.

[52] N. Diamantides, L. Wang, T. Pruiksma, J. Siemiatkoski, C. Dugopolski, S. Shortkroff, S. Kennedy, L.J. Bonassar, Correlating rheological properties and printability of collagen bioinks: The effects of riboflavin photocrosslinking and pH, Biofabrication. 9 (2017). doi:10.1088/1758-5090/aa780f.

[53] Y.B. Kim, H. Lee, G.H. Kim, Strategy to Achieve Highly Porous/Biocompatible Macroscale Cell Blocks, Using a Collagen/Genipin-bioink and an Optimal 3D Printing Process, ACS Appl. Mater. Interfaces. 8 (2016) 32230–32240. doi:10.1021/acsami.6b11669.

[54] Y. Zhang, X. Cheng, J. Wang, Y. Wang, B. Shi, C. Huang, X. Yang, T. Liu, Novel chitosan/collagen scaffold containing transforming growth factor-β1 DNA for periodontal tissue engineering, Biochem. Biophys. Res. Commun. 344 (2006) 362–369. doi:10.1016/j.bbrc.2006.03.106.

[55] J.Y. Park, J.C. Choi, J.H. Shim, J.S. Lee, H. Park, S.W. Kim, J. Doh, D.W. Cho, A comparative study on collagen type i and hyaluronic acid dependent cell behavior for osteochondral tissue bioprinting, Biofabrication. 6 (2014). doi:10.1088/1758-5082/6/3/035004.

[56] C.M. Homenick, G. de Silveira, H. Sheardown, A. Adronov, Pluronics as crosslinking agents for collagen: novel amphiphilic hydrogels, Polym. Int. 60 (2011) 458–465. doi:10.1002/pi.2969.

[57] J.W. Nichol, S.T. Koshy, H. Bae, C.M. Hwang, S. Yamanlar, A. Khademhosseini, Cell-laden microengineered gelatin methacrylate hydrogels, Biomaterials. 31 (2010) 5536–5544. doi:10.1016/j.biomaterials.2010.03.064.

[58] A. Abbadessa, M.M. Blokzijl, V.H.M. Mouser, P. Marica, J. Malda, W.E. Hennink, T. Vermonden, A thermo-responsive and photo-polymerizable chondroitin sulfate-based hydrogel for 3D printing applications, Carbohydr. Polym. 149 (2016) 163–174.

doi:10.1016/j.carbpol.2016.04.080.

[59] P.A. Levett, F.P.W. Melchels, K. Schrobback, D.W. Hutmacher, J. Malda, T.J. Klein, A biomimetic extracellular matrix for cartilage tissue engineering centered on photocurable gelatin, hyaluronic acid and chondroitin sulfate, Acta Biomater. 10 (2014) 214–223. doi:10.1016/j.actbio.2013.10.005.

[60] W. Schuurman, P.A. Levett, M.W. Pot, P.R. van Weeren, W.J.A. Dhert, D.W. Hutmacher, F.P.W. Melchels, T.J. Klein, J. Malda, Gelatin-methacrylamide hydrogels as potential biomaterials for fabrication of tissue-engineered cartilage constructs, Macromol. Biosci. 13 (2013) 551–561. doi:10.1002/mabi.201200471.

[61] C.B. Knudson, Hyaluronan and CD44: Strategic players for cell-matrix interactions during chondrogenesis and matrix assembly, Birth Defects Res. Part C - Embryo Today Rev. 69 (2003) 174–196. doi:10.1002/bdrc.10013.

[62] M. Kesti, M. Müller, J. Becher, M. Schnabelrauch, M. D'Este, D. Eglin, M. Zenobi-Wong, A versatile bioink for three-dimensional printing of cellular scaffolds based on thermally and photo-triggered tandem gelation, Acta Biomater. 11 (2015) 162–172. doi:10.1016/j.actbio.2014.09.033.

[63] M. Kesti, C. Eberhardt, G. Pagliccia, D. Kenkel, D. Grande, A. Boss, M. Zenobi-Wong, Bioprinting Complex Cartilaginous Structures with Clinically Compliant Biomaterials, Adv. Funct. Mater. 25 (2015) 7406–7417. doi:10.1002/adfm.201503423.

[64] D. Petta, A.R. Armiento, D. Grijpma, M. Alini, D. Eglin, M. D'Este, 3D bioprinting of a hyaluronan bioink through enzymatic-and visible light-crosslinking., Biofabrication. 10 (2018) 044104. doi:10.1088/1758-5090/aadf58.

[65] S. Sakai, K. Mochizuki, Y. Qu, M. Mail, M. Nakahata, M. Taya, Peroxidase-catalyzed microextrusion bioprinting of cell-laden hydrogel constructs in vaporized ppm-level hydrogen peroxide, Biofabrication. 10 (2018). doi:10.1088/1758-5090/aadc9e.

[66] M. Müller, J. Becher, M. Schnabelrauch, M. Zenobi-Wong, Nanostructured Pluronic hydrogels as bioinks for 3D bioprinting, Biofabrication. 7 (2015). doi:10.1088/1758-5090/7/3/035006.

[67] H.W. Kang, S.J. Lee, I.K. Ko, C. Kengla, J.J. Yoo, A. Atala, A 3D bioprinting system to produce human-scale tissue constructs with structural integrity, Nat. Biotechnol. 34 (2016) 312–319. doi:10.1038/nbt.3413.

[68] N.E. Fedorovich, I. Swennen, J. Girones, L. Moroni, C.A. Van Blitterswijk, E. Schacht, J. Alblas, W.J.A. Dhert, Evaluation of photocrosslinked lutrol hydrogel for tissue printing applications, Biomacromolecules. 10 (2009) 1689–1696. doi:10.1021/bm801463q.

[69] J.K. Carrow, P. Kerativitayanan, M.K. Jaiswal, G. Lokhande, A.K. Gaharwar, Polymers for bioprinting, in: Essentials 3D Biofabrication Transl., Elsevier Inc., 2015: pp. 229–248. doi:10.1016/B978-0-12-800972-7.00013-X.

[70] G. Gao, T. Yonezawa, K. Hubbell, G. Dai, X. Cui, Inkjet-bioprinted acrylated peptides and PEG hydrogel with human mesenchymal stem cells promote robust bone and cartilage formation with minimal printhead clogging, Biotechnol. J. 10 (2015) 1568–1577. doi:10.1002/biot.201400635.

[71] A. De Mori, M.P. Fernández, G. Blunn, G. Tozzi, M. Roldo, 3D printing and electrospinning of composite hydrogels for cartilage and bone tissue engineering, Polymers (Basel). 10 (2018). doi:10.3390/polym10030285.

[72] Y. Zhang, Y. Yu, H. Chen, I.T. Ozbolat, Characterization of printable cellular micro-fluidic channels for tissue engineering, Biofabrication. 5 (2013). doi:10.1088/1758-5082/5/2/025004.

[73] A.C. Daly, S.E. Critchley, E.M. Rencsok, I.A.D. Mancini, V.H.M. Mouser, A. Abbadessa, R. Levato, W.E. Hennink, T. Vermonden, D. Gawlitta, J. Malda, Development of a thermosensitive HAMA- containing bio-ink for the fabrication of composite cartilage repair constructs Fixation of Hydrogel Constructs for Cartilage Repair in the Equine Model: A Challenging Issue Fixation of hydrogel constructs for cartil, Biofabrication. 9 (2017). https://doi.org/10.1088/1758-5090/aa6265.

[74] N.E. Fedorovich, J.R. De Wijn, A.J. Verbout, J. Alblas, W.J.A. Dhert, Three-dimensional fiber deposition of cell-laden, viable, patterned constructs for bone tissue printing, Tissue Eng. - Part A. 14 (2008) 127–133. doi:10.1089/ten.a.2007.0158.

[75] J. Kundu, J.H. Shim, J. Jang, S.W. Kim, D.W. Cho, An additive manufacturing-based PCL-alginate-chondrocyte bioprinted scaffold for cartilage tissue engineering, J. Tissue Eng. Regen. Med. 9 (2015) 1286–1297. doi:10.1002/term.1682.

[76] A.D. Olubamiji, N. Zhu, T. Chang, C.K. Nwankwo, Z. Izadifar, A. Honaramooz, X. Chen, B.F. Eames, Traditional Invasive and Synchrotron-Based Noninvasive Assessments of Three-Dimensional-Printed Hybrid Cartilage Constructs in Situ, Tissue Eng. - Part C Methods. 23 (2017) 156–168. doi:10.1089/ten.tec.2016.0368.

[77] X. Yang, Z. Lu, H. Wu, W. Li, L. Zheng, J. Zhao, Collagen-alginate as bioink for three-dimensional (3D) cell printing based cartilage tissue engineering, Mater. Sci. Eng. C. 83 (2018) 195–201. doi:10.1016/j.msec.2017.09.002.

[78] K. Schütz, A.-M. Placht, B. Paul, S. Brüggemeier, M. Gelinsky, A. Lode, Three-dimensional plotting of a cell-laden alginate/methylcellulose blend: towards biofabrication of tissue engineering constructs with clinically relevant dimensions, J. Tissue Eng. Regen. Med. 11 (2017) 1574–1587. doi:10.1002/term.2058.

[79] T. Möller, M. Amoroso, D. Hägg, C. Brantsing, N. Rotter, P. Apelgren, A. Lindahl, L. Kölby, P. Gatenholm, In Vivo Chondrogenesis in 3D Bioprinted Human Cell-laden Hydrogel Constructs, in: Plast. Reconstr. Surg. - Glob. Open, Lippincott Williams and Wilkins, 2017. doi:10.1097/GOX.0000000000001227.

[80] K. Markstedt, A. Mantas, I. Tournier, H. Martínez Ávila, D. Hägg, P. Gatenholm, 3D Bioprinting Human Chondrocytes with Nanocellulose–Alginate Bioink for Cartilage Tissue Engineering Applications, Biomacromolecules. 16 (2015) 1489–1496. doi:10.1021/acs.biomac.5b00188.

[81] D. Nguyen, D.A. Hgg, A. Forsman, J. Ekholm, P. Nimkingratana, C. Brantsing, T. Kalogeropoulos, S. Zaunz, S. Concaro, M. Brittberg, A. Lindahl, P. Gatenholm, A. Enejder, S. Simonsson, Cartilage Tissue Engineering by the 3D Bioprinting of iPS Cells in a Nanocellulose/Alginate Bioink, Sci. Rep. 7 (2017). doi:10.1038/s41598-017-00690-y.

[82] J.P.K. Armstrong, M. Burke, B.M. Carter, S.A. Davis, A.W. Perriman, 3D Bioprinting Using a Templated Porous Bioink, Adv. Healthc. Mater. 5 (2016) 1724–1730. doi:10.1002/adhm.201600022.

[83] S. Rathan, L. Dejob, R. Schipani, B. Haffner, M.E. Möbius, D.J. Kelly, Fiber Reinforced Cartilage ECM Functionalized Bioinks for Functional Cartilage Tissue Engineering, Adv. Healthc. Mater. 8 (2019). doi:10.1002/adhm.201801501.

[84] F. You, X. Wu, N. Zhu, M. Lei, B.F. Eames, X. Chen, 3D Printing of Porous Cell-Laden Hydrogel Constructs for Potential Applications in Cartilage Tissue Engineering, ACS Biomater. Sci. Eng. 2 (2016) 1200–1210. doi:10.1021/acsbiomaterials.6b00258.

[85] D.F.D. Campos, A. Blaeser, A. Korsten, S. Neuss, J. Jäkel, M. Vogt, H. Fischer, The stiffness and structure of three-dimensional printed hydrogels direct the differentiation of mesenchymal stromal cells toward adipogenic and osteogenic lineages, Tissue Eng. - Part A. 21 (2015) 740–756. doi:10.1089/ten.tea.2014.0231.

[86] S. Rhee, J.L. Puetzer, B.N. Mason, C.A. Reinhart-King, L.J. Bonassar, 3D Bioprinting of Spatially Heterogeneous Collagen Constructs for Cartilage Tissue Engineering, ACS Biomater. Sci. Eng. 2 (2016) 1800–1805. doi:10.1021/acsbiomaterials.6b00288.

[87] T. Xu, K.W. Binder, M.Z. Albanna, D. Dice, W. Zhao, J.J. Yoo, A. Atala, Hybrid printing of mechanically and biologically improved constructs for cartilage tissue engineering applications, Biofabrication. 5 (2013). doi:10.1088/1758-5082/5/1/015001.

[88] W. Schuurman, V. Khristov, M.W. Pot, P.R. Van Weeren, W.J.A. Dhert, J. Malda, Bioprinting of hybrid tissue constructs with tailorable mechanical properties, Biofabrication. 3 (2011). doi:10.1088/1758-5082/3/2/021001.

[89] V.H.M. Mouser, F.P.W. Melchels, J. Visser, W.J.A. Dhert, D. Gawlitta, J. Malda, Yield stress determines bioprintability of hydrogels based on gelatin-methacryloyl and gellan gum for cartilage bioprinting, Biofabrication. 8 (2016). doi:10.1088/1758-5090/8/3/035003.

[90] C. Di Bella, S. Duchi, C.D. O'Connell, R. Blanchard, C. Augustine, Z. Yue, F. Thompson, C. Richards, S. Beirne, C. Onofrillo, S.H. Bauquier, S.D. Ryan, P. Pivonka, G.G. Wallace, P.F. Choong, In situ handheld three-dimensional bioprinting for cartilage regeneration, J. Tissue Eng. Regen. Med. 12 (2018) 611–621. doi:10.1002/term.2476.

[91] R. Levato, W.R. Webb, I.A. Otto, A. Mensinga, Y. Zhang, M. van Rijen, R. van Weeren, I.M. Khan, J. Malda, The bio in the ink: cartilage regeneration with bioprintable hydrogels and articular cartilage-derived progenitor cells, Acta Biomater. 61 (2017) 41–53. doi:10.1016/j.actbio.2017.08.005.

[92] C. Di Bella, S. Duchi, C.D. O'Connell, R. Blanchard, C. Augustine, Z. Yue, F. Thompson, C. Richards, S. Beirne, C. Onofrillo, S.H. Bauquier, S.D. Ryan, P. Pivonka, G.G. Wallace, P.F. Choong, *In situ* handheld three-dimensional bioprinting for cartilage regeneration, J. Tissue Eng. Regen. Med. 12 (2018) 611–621. doi:10.1002/term.2476.

[93] C.D. O'Connell, C. Di Bella, F. Thompson, C. Augustine, S. Beirne, R. Cornock, C.J. Richards, J. Chung, S. Gambhir, Z. Yue, J. Bourke, B. Zhang, A. Taylor, A. Quigley, R. Kapsa, P. Choong, G.G. Wallace, Development of the Biopen: A handheld device for surgical printing of adipose stem cells at a chondral wound site, Biofabrication. 8 (2016). doi:10.1088/1758-5090/8/1/015019.

[94] F.P.W. Melchels, M.M. Blokzijl, R. Levato, Q.C. Peiffer, M. De Ruijter, W.E. Hennink, T. Vermonden, J. Malda, Hydrogel-based reinforcement of 3D bioprinted constructs, Biofabrication. 8 (2016). doi:10.1088/1758-5090/8/3/035004.

[95] X. Ren, F. Wang, C. Chen, X. Gong, L. Yin, L. Yang, Engineering zonal cartilage through bioprinting collagen type II hydrogel constructs with biomimetic chondrocyte density gradient, BMC Musculoskelet. Disord. 17 (2016). doi:10.1186/s12891-016-1130-8.

[96] M. Costantini, J. Idaszek, K. Szöke, J. Jaroszewicz, M. Dentini, A. Barbetta, J.E.

Brinchmann, W. Święszkowski, 3D bioprinting of BM-MSCs-loaded ECM biomimetic hydrogels for in vitro neocartilage formation, Biofabrication. 8 (2016). doi:10.1088/1758-5090/8/3/035002.

[97] A. Abbadessa, V.H.M. Mouser, M.M. Blokzijl, D. Gawlitta, W.J.A. Dhert, W.E. Hennink, J. Malda, T. Vermonden, A Synthetic Thermosensitive Hydrogel for Cartilage Bioprinting and Its Biofunctionalization with Polysaccharides, Biomacromolecules. 17 (2016) 2137–2147. doi:10.1021/acs.biomac.6b00366.

[98] J.H. Shim, K.M. Jang, S.K. Hahn, J.Y. Park, H. Jung, K. Oh, K.M. Park, J. Yeom, S.H. Park, S.W. Kim, J.H. Wang, K. Kim, D.W. Cho, Three-dimensional bioprinting of multilayered constructs containing human mesenchymal stromal cells for osteochondral tissue regeneration in the rabbit knee joint, Biofabrication. 8 (2016). doi:10.1088/1758-5090/8/1/014102.

[99] Y. Yu, K.K. Moncal, J. Li, W. Peng, I. Rivero, J.A. Martin, I.T. Ozbolat, Three-dimensional bioprinting using self-Assembling scalable scaffold-free “tissue strands” as a new bioink, Sci. Rep. 6 (2016). doi:10.1038/srep28714.

[100] X. Cui, K. Breitenkamp, M.G. Finn, M. Lotz, D.D. D’Lima, Direct human cartilage repair using three-dimensional bioprinting technology, Tissue Eng. - Part A. 18 (2012) 1304–1312. doi:10.1089/ten.tea.2011.0543.

[101] G. Gao, X.F. Zhang, K. Hubbell, X. Cui, NR2F2 regulates chondrogenesis of human mesenchymal stem cells in bioprinted cartilage, Biotechnol. Bioeng. 114 (2017) 208–216. doi:10.1002/bit.26042.

[102] T.J. Klein, S.C. Rizzi, J.C. Reichert, N. Georgi, J. Malda, W. Schuurman, R.W. Crawford, D.W. Hutmacher, Strategies for Zonal Cartilage Repair using Hydrogels, Macromol. Biosci. 9 (2009) 1049–1058. doi:10.1002/mabi.200900176.

[103] W. Schuurman, T.J. Klein, W.J.A. Dhert, P.R. van Weeren, D.W. Hutmacher, J. Malda, Cartilage regeneration using zonal chondrocyte subpopulations: A promising approach or an overcomplicated strategy?, J. Tissue Eng. Regen. Med. 9 (2015) 669–678. doi:10.1002/term.1638.

[104] D. Choudhury, H.W. Tun, T. Wang, M.W. Naing, Organ-Derived Decellularized Extracellular Matrix: A Game Changer for Bioink Manufacturing?, Trends Biotechnol. 36 (2018) 787–805. doi:10.1016/j.tibtech.2018.03.003.

[105] S.F. Badylak, D.O. Freytes, T.W. Gilbert, Reprint of: Extracellular matrix as a biological scaffold material: Structure and function, Acta Biomater. 23 (2015) S17–S26. doi:10.1016/j.actbio.2015.07.016.

[106] F. Pati, J. Jang, D.H. Ha, S. Won Kim, J.W. Rhie, J.H. Shim, D.H. Kim, D.W. Cho, Printing three-dimensional tissue analogues with decellularized extracellular matrix bioink, Nat. Commun. 5 (2014). doi:10.1038/ncomms4935.

[107] B. Holmes, W. Zhu, J. Li, J.D. Lee, L.G. Zhang, Development of novel three-dimensional printed scaffolds for osteochondral regeneration, Tissue Eng. - Part A. 21 (2015) 403–415. doi:10.1089/ten.tea.2014.0138.

[108] W. Schuurman, V. Khristov, M.W. Pot, P.R. van Weeren, W.J.A. Dhert, J. Malda, Bioprinting of hybrid tissue constructs with tailorable mechanical properties., Biofabrication. 3 (2011) 021001. doi:10.1088/1758-5082/3/2/021001.

[109] Z. Izadifar, X. Chen, W. Kulyk, Strategic Design and Fabrication of Engineered Scaffolds

for Articular Cartilage Repair, J. Funct. Biomater. 3 (2012) 799–838. doi:10.3390/jfb3040799.

[110] B. Gupta, N. Revagade, J. Hilborn, Poly(lactic acid) fiber: An overview, Prog. Polym. Sci. 32 (2007) 455–482. doi:10.1016/j.progpolymsci.2007.01.005.

[111] C.-Y. Liaw, M. Guvendiren, M. Nowicki, N.J. Castro, R. Rao, Biofabrication Additive manufacturing of polymer melts for implantable medical devices and scaffolds Related content Current and emerging applications of 3D printing in medicine Integrating three-dimensional printing and nanotechnology for musculoskeletal regeneration, (2017). doi:10.1088/1758-5090/aa5766.

[112] L.E. Fitzpatrick, T.C. McDevitt, Cell-derived matrices for tissue engineering and regenerative medicine applications, Biomater. Sci. 3 (2015) 12–24. doi:10.1039/c4bm00246f.

[113] W. Zhang, Y. Zhu, J. Li, Q. Guo, J. Peng, S. Liu, J. Yang, Y. Wang, Cell-derived extracellular matrix: Basic characteristics and current applications in orthopedic tissue engineering, Tissue Eng. - Part B Rev. 22 (2016) 193–207. doi:10.1089/ten.teb.2015.0290.

[114] H. Ragelle, A. Naba, B.L. Larson, F. Zhou, M. Prijić, C.A. Whittaker, A. Del Rosario, R. Langer, R.O. Hynes, D.G. Anderson, Comprehensive proteomic characterization of stem cell-derived extracellular matrices, Biomaterials. 128 (2017) 147–159. doi:10.1016/j.biomaterials.2017.03.008.

[115] H. Lu, T. Hoshiba, N. Kawazoe, G. Chen, Autologous extracellular matrix scaffolds for tissue engineering, Biomaterials. 32 (2011) 2489–2499. doi:10.1016/j.biomaterials.2010.12.016.

[116] M.C. Prewitz, F.P. Seib, M. Von Bonin, J. Friedrichs, A. Stißel, C. Niehage, K. Müller, K. Anastassiadis, C. Waskow, B. Hoflack, M. Bornhäuser, C. Werner, Tightly anchored tissue-mimetic matrices as instructive stem cell microenvironments, Nat. Methods. 10 (2013) 788–794. doi:10.1038/nmeth.2523.

[117] R. Cai, T. Nakamoto, N. Kawazoe, G. Chen, Influence of stepwise chondrogenesis-mimicking 3D extracellular matrix on chondrogenic differentiation of mesenchymal stem cells, Biomaterials. 52 (2015)199–207. doi:10.1016/j.biomaterials.2015.02.033.

[118] E.J. Levorson, P.M. Mountziaris, O. Hu, F.K. Kasper, A.G. Mikos, Cell-derived polymer/extracellular matrix composite scaffolds for cartilage regeneration, part 1: Investigation of cocultures and seeding densities for improved extracellular matrix deposition, Tissue Eng. - Part C Methods. 20 (2014) 340–357. doi:10.1089/ten.tec.2013.0286.

[119] L.A. Hidalgo-Bastida, S.H. Cartmell, Mesenchymal stem cells, osteoblasts and extracellular matrix proteins: Enhancing cell adhesion and differentiation for bone tissue engineering, Tissue Eng. - Part B Rev. 16 (2010) 405–412. doi:10.1089/ten.teb.2009.0714.

[120] J. Li, K.C. Hansen, Y. Zhang, C. Dong, C.Z. Dinu, M. Dzieciatkowska, M. Pei, Rejuvenation of chondrogenic potential in a young stem cell microenvironment, Biomaterials. 35 (2014) 642–653. doi:10.1016/j.biomaterials.2013.09.099.

[121] H. Takashi, M. Katsumi, A. Toshihiro, Hepatocytes maintain their function on basement membrane formed by epithelial cells, Biochem. Biophys. Res. Commun. 359 (2007) 151–156. doi:10.1016/j.bbrc.2007.05.079.

[122] X. Liu, L. Zhou, X. Chen, T. Liu, G. Pan, W. Cui, M. Li, Z.P. Luo, M. Pei, H. Yang, Y. Gong, F. He, Culturing on decellularized extracellular matrix enhances antioxidant properties of human umbilical cord-derived mesenchymal stem cells, Mater. Sci. Eng. C. 61 (2016) 437–448. doi:10.1016/j.msec.2015.12.090.

[123] W.B. Vanwinkle, M.B. Snuggs, L.M. Buja, Cardiogel: A biosynthetic extracellular matrix for cardiomyocyte culture, Vitr. Cell. Dev. Biol. - Anim. 32 (1996) 478–485. doi:10.1007/BF02723051.

[124] T. Hoshiba, N. Kawazoe, T. Tateishi, G. Chen, Development of stepwise osteogenesis-mimicking matrices for the regulation of mesenchymal stem cell functions, J. Biol. Chem. 284 (2009) 31164–31173. doi:10.1074/jbc.M109.054676.

[125] C.Z. Jin, B.H. Choi, S.R. Park, B.H. Min, Cartilage engineering using cell-derived extracellular matrix scaffold in vitro, J. Biomed. Mater. Res. - Part A. 92 (2010) 1567–1577. doi:10.1002/jbm.a.32419.

[126] C. Tang, C. Jin, Y. Xu, B. Wei, L. Wang, Chondrogenic Differentiation Could Be Induced by Autologous Bone Marrow Mesenchymal Stem Cell-Derived Extracellular Matrix Scaffolds Without Exogenous Growth Factor, Tissue Eng. - Part A. 22 (2016) 222–232. doi:10.1089/ten.tea.2014.0491.

[127] C. Tang, Y. Xu, C. Jin, B.H. Min, Z. Li, X. Pei, L. Wang, Feasibility of Autologous Bone Marrow Mesenchymal Stem Cell-Derived Extracellular Matrix Scaffold for Cartilage Tissue Engineering, Artif. Organs. 37 (2013). doi:10.1111/aor.12130.

[128] T. Xiao, W. Guo, M. Chen, C. Hao, S. Gao, J. Huang, Z. Yuan, Y. Zhang, M. Wang, P. Li, J. Peng, A. Wang, Y. Wang, X. Sui, L. Zhang, W. Xu, S. Lu, H. Yin, J. Yang, S. Liu, Q. Guo, Fabrication and In Vitro Study of Tissue-Engineered Cartilage Scaffold Derived from Wharton's Jelly Extracellular Matrix, Biomed Res. Int. 2017 (2017). doi:10.1155/2017/5839071.

[129] C.Z. Jin, S.R. Park, B.H. Choi, K. Park, B.H. Min, In vivo cartilage tissue engineering using a cell-derived extracellular matrix scaffold, Artif. Organs. 31 (2007) 183–192. doi:10.1111/j.1525-1594.2007.00363.x.

[130] C. Tang, C. Jin, X. Du, C. Yan, B.H. Min, Y. Xu, L. Wang, An autologous bone marrow mesenchymal stem cell-derived extracellular matrix scaffold applied with bone marrow stimulation for cartilage repair, Tissue Eng. - Part A. 20 (2014) 2455–2462. doi:10.1089/ten.tea.2013.0464.

[131] R. Nishimura, K. Hata, F. Ikeda, F. Ichida, A. Shimoyama, T. Matsubara, M. Wada, K. Amano, T. Yoneda, Signal transduction and transcriptional regulation during mesenchymal cell differentiation, J. Bone Miner. Metab. 26 (2008) 203–212. doi:10.1007/s00774-007-0824-2.

[132] W.P. Daley, S.B. Peters, M. Larsen, Extracellular matrix dynamics in development and regenerative medicine, J. Cell Sci. 121 (2008) 255–264. doi:10.1242/jcs.006064.

[133] P. Singh, J.E. Schwarzbauer, Fibronectin and stem cell differentiation - lessons from chondrogenesis, J. Cell Sci. 125 (2012) 3703–3712. doi:10.1242/jcs.095786.

[134] T. Assis-Ribas, M.F. Forni, S.M.B. Winnischofer, M.C. Sogayar, M. Trombetta-Lima, Extracellular matrix dynamics during mesenchymal stem cells differentiation, Dev. Biol. 437 (2018) 63–74. doi:10.1016/j.ydbio.2018.03.002.

[135] T. Hoshiba, H. Lu, T. Yamada, N. Kawazoe, T. Tateishi, G. Chen, Effects of extracellular

matrices derived from different cell sources on chondrocyte functions, Biotechnol. Prog. 27 (2011) 788–795. doi:10.1002/btpr.592.

[136] T. Hoshiba, T. Yamada, H. Lu, N. Kawazoe, G. Chen, Maintenance of cartilaginous gene expression on extracellular matrix derived from serially passaged chondrocytes during in vitro chondrocyte expansion, J. Biomed. Mater. Res. Part A. 100A (2012) 694–702. doi:10.1002/jbm.a.34003.

[137] R. Cai, T. Nakamoto, T. Hoshiba, N. Kawazoe, G. Chen, Matrices secreted during simultaneous osteogenesis and adipogenesis of mesenchymal stem cells affect stem cells differentiation, Acta Biomater. 35 (2016) 185–193. doi:10.1016/j.actbio.2016.02.009.

[138] C.W. Cheng, L.D. Solorio, E. Alsberg, Decellularized tissue and cell-derived extracellular matrices as scaffolds for orthopaedic tissue engineering, Biotechnol. Adv. 32 (2014) 462–484. doi:10.1016/j.biotechadv.2013.12.012.

[139] H. Park, H.J. Lee, H. An, K.Y. Lee, Alginate hydrogels modified with low molecular weight hyaluronate for cartilage regeneration, Carbohydr. Polym. 162 (2017) 100–107. doi:10.1016/j.carbpol.2017.01.045.

[140] E. Amann, P. Wolff, E. Breel, M. van Griensven, E.R. Balmayor, Hyaluronic acid facilitates chondrogenesis and matrix deposition of human adipose derived mesenchymal stem cells and human chondrocytes co-cultures, Acta Biomater. 52 (2017) 130–144. doi:10.1016/j.actbio.2017.01.064.

[141] K. Kawasaki, M. Ochi, Y. Uchio, N. Adachi, M. Matsusaki, Hyaluronic acid enhances proliferation and chondroitin sulfate synthesis in cultured chondrocytes embedded in collagen gels, J. Cell. Physiol. 179 (1999) 142–148. doi:10.1002/(SICI)1097-4652(199905)179:2<142::AID-JCP4>3.0.CO;2-Q.

[142] K.L. Spiller, S.A. Maher, A.M. Lowman, Hydrogels for the repair of articular cartilage defects, Tissue Eng. - Part B Rev. 17 (2011) 281–299.doi:10.1089/ten.teb.2011.0077.

[143] J. Gopinathan, I. Noh, Recent trends in bioinks for 3D printing, Biomater. Res. 22 (2018). doi:10.1186/s40824-018-0122-1.

[144] N. Paxton, W. Smolan, T. Böck, F. Melchels, J. Groll, T. Jungst, Proposal to assess printability of bioinks for extrusion-based bioprinting and evaluation of rheological properties governing bioprintability, Biofabrication. 9 (2017). doi:10.1088/1758-5090/aa8dd8.

[145] J.A. Burdick, G.D. Prestwich, Hyaluronic Acid Hydrogels for Biomedical Applications Jason, 23 (2013) 1–31. doi:10.1002/adma.201003963.Hyaluronic.

[146] H. Park, H.J. Lee, H. An, K.Y. Lee, Alginate hydrogels modified with low molecular weight hyaluronate for cartilage regeneration, Carbohydr. Polym. 162 (2017) 100–107. doi:10.1016/j.carbpol.2017.01.045.

[147] I.E. Erickson, A.H. Huang, S. Sengupta, S. Kestle, J.A. Burdick, R.L. Mauck, Macromer density influences mesenchymal stem cell chondrogenesis and maturation in photocrosslinked hyaluronic acid hydrogels., Osteoarthr. Cartil. 17 (2009) 1639–48. doi:10.1016/j.joca.2009.07.003.

[148] I.E. Erickson, S.R. Kestle, K.H. Zellars, M.J. Farrell, M. Kim, J.A. Burdick, R.L. Mauck, High mesenchymal stem cell seeding densities in hyaluronic acid hydrogels produce engineered cartilage with native tissue properties, Acta Biomater. 8 (2012) 3027–3034.

doi:10.1016/j.actbio.2012.04.033.

[149] E. Amann, P. Wolff, E. Breel, M. van Griensven, E.R. Balmayor, Hyaluronic acid facilitates chondrogenesis and matrix deposition of human adipose derived mesenchymal stem cells and human chondrocytes co-cultures, Acta Biomater. 52 (2017) 130–144. doi:10.1016/j.actbio.2017.01.064.

[150] B.S. Kim, H. Kim, G. Gao, J. Jang, D.W. Cho, Decellularized extracellular matrix: A step towards the next generation source for bioink manufacturing, Biofabrication. 9 (2017). doi:10.1088/1758-5090/aa7e98.

[151] J.W. Kuo, Practical aspects of hyaluronan based medical products, CRC Press, 2005. doi:10.1201/9781420037647.

[152] M. Abe, M. Takahashi, A. Nagano, The effect of hyaluronic acid with different molecular weights on collagen crosslink synthesis in cultured chondrocytes embedded in collagen gels, J. Biomed. Mater. Res. - Part A. 75 (2005) 494–499. doi:10.1002/jbm.a.30452.

[153] K. Kawasaki, M. Ochi, Y. Uchio, N. Adachi, M. Matsusaki, Hyaluronic acid enhances proliferation and chondroitin sulfate synthesis in cultured chondrocytes embedded in collagen gels, J. Cell. Physiol. 179 (1999) 142–148. doi:10.1002/(SICI)1097-4652(199905)179:2<142::AID-JCP4>3.0.CO;2-Q.

[154] C. Chung, J. Mesa, M.A. Randolph, M. Yaremchuk, J.A. Burdick, Influence of gel properties on neocartilage formation by auricular chondrocytes photoencapsulated in hyaluronic acid networks, J. Biomed. Mater. Res. - Part A. 77 (2006) 518–525. doi:10.1002/jbm.a.30660.

[155] H.L. Ma, S.C. Hung, S.Y. Lin, Y.L. Chen, W.H. Lo, Chondrogenesis of human mesenchymal stem cells encapsulated in alginate beads, J. Biomed. Mater. Res. - Part A. 64 (2003) 273–281. doi:10.1002/jbm.a.10370.

[156] M.M. Stevens, H.F. Qanadilo, R. Langer, V.P. Shastri, A rapid-curing alginate gel system: Utility in periosteum-derived cartilage tissue engineering, Biomaterials. 25 (2004) 887–894. doi:10.1016/j.biomaterials.2003.07.002.

[157] S.R. Herlofsen, A.M. Küchler, J.E. Melvik, J.E. Brinchmann, Chondrogenic differentiation of human bone marrow-derived mesenchymal stem cells in self-gelling alginate discs reveals novel chondrogenic signature gene clusters, Tissue Eng. - Part A. 17 (2011) 1003–1013. doi:10.1089/ten.tea.2010.0499.

[158] H. Park, K.Y. Lee, Cartilage regeneration using biodegradable oxidized alginate/hyaluronate hydrogels, J. Biomed. Mater. Res. Part A. (2014) n/a-n/a. doi:10.1002/jbm.a.35126.

[159] Y. Anasiz, R.K. Ozgul, D. Uckan-Cetinkaya, A New Chapter for Mesenchymal Stem Cells: Decellularized Extracellular Matrices, Stem Cell Rev. Reports. 13 (2017) 587–597. doi:10.1007/s12015-017-9757-x.

[160] R.O. Hynes, A. Naba, Overview of the matrisome-An inventory of extracellular matrix constituents and functions, Cold Spring Harb. Perspect. Biol. 4 (2012) 1–16. doi:10.1101/cshperspect.a004903.

[161] C. Sanchez, A.C. Bay-Jensen, T. Pap, M. Dvir-Ginzberg, H. Quasnichka, R. Barrett-Jolley, A. Mobasheri, Y. Henrotin, Chondrocyte secretome: a source of novel insights and exploratory biomarkers of osteoarthritis, Osteoarthr. Cartil. 25 (2017) 1199–1209. doi:10.1016/j.joca.2017.02.797.

[162] A. Shakouri-Motlagh, A.J. O'Connor, S.P. Brennecke, B. Kalionis, D.E. Heath, Native and solubilized decellularized extracellular matrix: A critical assessment of their potential for improving the expansion of mesenchymal stem cells, Acta Biomater. 55 (2017) 1–12. doi:10.1016/j.actbio.2017.04.014.

[163] T.J. Keane, I.T. Swinehart, S.F. Badylak, Methods of tissue decellularization used for preparation of biologic scaffolds and in vivo relevance, Methods. 84 (2015) 25–34. doi:10.1016/j.ymeth.2015.03.005.

[164] P.M. Crapo, T.W. Gilbert, S.F. Badylak, An overview of tissue and whole organ decellularization processes, Biomaterials. 32 (2011) 3233–3243. doi:10.1016/j.biomaterials.2011.01.057.

[165] K. Hölzl, S. Lin, L. Tytgat, S. Van Vlierberghe, L. Gu, A. Ovsianikov, Bioink properties before, during and after 3D bioprinting, Biofabrication. 8 (2016). doi:10.1088/1758-5090/8/3/032002.

[166] S.Y. Nam, S.H. Park, ECM based bioink for tissue mimetic 3D bioprinting, in: Adv. Exp. Med. Biol., Springer New York LLC, 2018: pp. 335–353. doi:10.1007/978-981-13-0445-3_20.

[167] J. Vanderburgh, J.A. Sterling, S.A. Guelcher, 3D Printing of Tissue Engineered Constructs for In Vitro Modeling of Disease Progression and Drug Screening, Ann. Biomed. Eng. 45 (2017) 164–179. doi:10.1007/s10439-016-1640-4.

[168] G. Tabilo-Munizaga, G. V. Barbosa-Cánovas, Rheology for the food industry, J. Food Eng. 67 (2005) 147–156. doi:10.1016/j.jfoodeng.2004.05.062.

[169] X. Wang, G. Chen, C. Huang, H. Tu, J. Zou, J. Yan, Bone marrow stem cells-derived extracellular matrix is a promising material, Oncotarget. 8 (2017) 98336–98347. doi:10.18632/oncotarget.21683.

[170] Y. Mao, T. Hoffman, A. Wu, R. Goyal, J. Kohn, Cell type–specific extracellular matrix guided the differentiation of human mesenchymal stem cells in 3D polymeric scaffolds, J. Mater. Sci. Mater. Med. 28 (2017). doi:10.1007/s10856-017-5912-9.

[171] R. Santhakumar, P. Vidyasekar, R.S. Verma, Cardiogel: A nano-matrix scaffold with potential application in cardiac regeneration using mesenchymal stem cells, PLoS One. 9 (2014). doi:10.1371/journal.pone.0114697.

[172] H.W. Cheng, Y.K. Tsui, K.M.C. Cheung, D. Chan, B.P. Chan, Decellularization of chondrocyte-encapsulated collagen microspheres: A three-dimensional model to study the effects of acellular matrix on stem cell fate, Tissue Eng. - Part C Methods. 15 (2009) 697–706. doi:10.1089/ten.tec.2008.0635.

[173] J.M. Ryan, F.P. Barry, J.M. Murphy, B.P. Mahon, Mesenchymal stem cells avoid allogeneic rejection, J. Inflamm. 2 (2005). doi:10.1186/1476-9255-2-8.

[174] S. Aggarwal, M.F. Pittenger, Human mesenchymal stem cells modulate allogeneic immune cell responses, Blood. 105 (2005) 1815–1822. doi:10.1182/blood-2004-04-1559.

X. ANNEXES

X.1 Supplementary data

Supplementary Table 1. Detectable proteins in early chondrogenic matrix derived from MSCs previously and after decellularization process.

PRE	POST
Fibronectin OS=Homo sapiens GN=FN1 PE=1 SV=4	Fibronectin OS=Homo sapiens GN=FN1 PE=1 SV=4
Collagen alpha-3(VI) chain OS=Homo sapiens GN=COL6A3 PE=1 SV=5	Collagen alpha-3(VI) chain OS=Homo sapiens GN=COL6A3 PE=1 SV=5
Transforming growth factor-beta-induced protein ig-h3 OS=Homo sapiens	Transforming growth factor-beta-induced protein ig-h3 OS=Homo sapiens GN
Tenascin OS=Homo sapiens GN=TNC PE=1 SV=3	Tenascin OS=Homo sapiens GN=TNC PE=1 SV=3
Filamin-A OS=Homo sapiens OX=9606 GN=FLNA PE=1 SV=4 - [FLNA_HUMA	Filamin-A OS=Homo sapiens OX=9606 GN=FLNA PE=1 SV=4 - [FLNA_HUMAN]
Collagen alpha-1(XII) chain OS=Homo sapiens GN=COL12A1 PE=1 SV=2	Collagen alpha-1(XII) chain OS=Homo sapiens GN=COL12A1 PE=1 SV=2
Basement membrane-specific heparan sulfate proteoglycan core protein O	Basement membrane-specific heparan sulfate proteoglycan core protein OS=
Fibrillin-1 OS=Homo sapiens GN=FBN1 PE=1 SV=3	Fibrillin-1 OS=Homo sapiens GN=FBN1 PE=1 SV=3
Periostin OS=Homo sapiens GN=POSTN PE=1 SV=2	Periostin OS=Homo sapiens GN=POSTN PE=1 SV=2
Collagen alpha-1(VI) chain OS=Homo sapiens GN=COL6A1 PE=1 SV=3	Collagen alpha-1(VI) chain OS=Homo sapiens GN=COL6A1 PE=1 SV=3
Collagen alpha-2(VI) chain OS=Homo sapiens GN=COL6A2 PE=1 SV=4	Collagen alpha-2(VI) chain OS=Homo sapiens GN=COL6A2 PE=1 SV=4
Vimentin OS=Homo sapiens GN=VIM PE=1 SV=4	Vimentin OS=Homo sapiens GN=VIM PE=1 SV=4
EMILIN-1 OS=Homo sapiens GN=EMILIN1 PE=1 SV=2	EMILIN-1 OS=Homo sapiens GN=EMILIN1 PE=1 SV=2
Matrix-remodeling-associated protein 5 OS=Homo sapiens GN=MXRA5 PE=	Matrix-remodeling-associated protein 5 OS=Homo sapiens GN=MXRA5 PE=2
Collagen alpha-1(V) chain OS=Homo sapiens GN=COL5A1 PE=1 SV=3	Collagen alpha-1(V) chain OS=Homo sapiens GN=COL5A1 PE=1 SV=3
Collagen alpha-1(XIV) chain OS=Homo sapiens GN=COL14A1 PE=1 SV=3	Collagen alpha-1(XIV) chain OS=Homo sapiens GN=COL14A1 PE=1 SV=3
Collagen alpha-2(I) chain OS=Homo sapiens GN=COL1A2 PE=1 SV=7	Collagen alpha-2(I) chain OS=Homo sapiens GN=COL1A2 PE=1 SV=7
Annexin A4 OS=Homo sapiens GN=ANXA4 PE=1 SV=4	Collagen alpha-1(I) chain OS=Homo sapiens GN=COL1A1 PE=1 SV=5
Annexin A7 OS=Homo sapiens GN=ANXA7 PE=1 SV=3	Adipocyte enhancer-binding protein 1 OS=Homo sapiens GN=AEBP1 PE=1 SV=
Collagen alpha-1(I) chain OS=Homo sapiens GN=COL1A1 PE=1 SV=5	Fibulin-2 OS=Homo sapiens GN=FBLN2 PE=1 SV=2
Adipocyte enhancer-binding protein 1 OS=Homo sapiens GN=AEBP1 PE=1	Cartilage oligomeric matrix protein OS=Homo sapiens GN=COMP PE=1 SV=2
Fibulin-2 OS=Homo sapiens GN=FBLN2 PE=1 SV=2	Biglycan OS=Homo sapiens GN=BGN PE=1 SV=2
Cartilage oligomeric matrix protein OS=Homo sapiens GN=COMP PE=1 SV=	EMILIN-1 OS=Homo sapiens OX=9606 GN=EMILIN1 PE=1 SV=3 - [EMIL1_HUM
Biglycan OS=Homo sapiens GN=BGN PE=1 SV=2	Fibulin-1 OS=Homo sapiens GN=FBLN1 PE=1 SV=4
Fibulin-1 OS=Homo sapiens GN=FBLN1 PE=1 SV=4	Cartilage intermediate layer protein 1 OS=Homo sapiens GN=CILP PE=1 SV=4
Cartilage intermediate layer protein 1 OS=Homo sapiens GN=CILP PE=1 SV	Annexin A2 OS=Homo sapiens GN=ANXA2 PE=1 SV=2
Myeloid-derived growth factor OS=Homo sapiens GN=MYDGF PE=1 SV=1	Decorin OS=Homo sapiens GN=DCN PE=1 SV=1
14-3-3 protein eta OS=Homo sapiens GN=YWHAH PE=1 SV=4	Collagen alpha-1(XVI) chain OS=Homo sapiens OX=9606 GN=COL16A1 PE=1 S
Procollagen C-endopeptidase enhancer 1 OS=Homo sapiens GN=PCOLCE P	Collagen alpha-1(III) chain OS=Homo sapiens GN=COL3A1 PE=1 SV=4
Serine protease HTRA1 OS=Homo sapiens GN=HTRA1 PE=1 SV=1	Lumican OS=Homo sapiens OX=9606 GN=LUM PE=1 SV=2 - [LUM_HUMAN]
Annexin A2 OS=Homo sapiens GN=ANXA2 PE=1 SV=2	Versican core protein OS=Homo sapiens GN=VCAN PE=1 SV=3
Decorin OS=Homo sapiens GN=DCN PE=1 SV=1	Annexin A5 OS=Homo sapiens GN=ANXA5 PE=1 SV=2
Collagen alpha-1(III) chain OS=Homo sapiens GN=COL3A1 PE=1 SV=4	Lumican OS=Homo sapiens GN=LUM PE=1 SV=2
Versican core protein OS=Homo sapiens GN=VCAN PE=1 SV=3	Collagen alpha-2(V) chain OS=Homo sapiens GN=COL5A2 PE=1 SV=3
Annexin A5 OS=Homo sapiens GN=ANXA5 PE=1 SV=2	Microfibrillar-associated protein 2 OS=Homo sapiens GN=MFAP2 PE=2 SV=1
Lumican OS=Homo sapiens GN=LUM PE=1 SV=2	Annexin A6 OS=Homo sapiens GN=ANXA6 PE=1 SV=3
Collagen alpha-2(V) chain OS=Homo sapiens GN=COL5A2 PE=1 SV=3	Annexin A1 OS=Homo sapiens GN=ANXA1 PE=1 SV=2
Microfibrillar-associated protein 2 OS=Homo sapiens GN=MFAP2 PE=2 SV=	Collagen alpha-2(IV) chain OS=Homo sapiens GN=COL4A2 PE=1 SV=4
Annexin A6 OS=Homo sapiens GN=ANXA6 PE=1 SV=3	Collagen alpha-1(XI) chain OS=Homo sapiens GN=COL11A1 PE=1 SV=4
Annexin A1 OS=Homo sapiens GN=ANXA1 PE=1 SV=2	Fibrillin-2 OS=Homo sapiens GN=FBN2 PE=1 SV=3
Collagen alpha-2(IV) chain OS=Homo sapiens GN=COL4A2 PE=1 SV=4	EMILIN-2 OS=Homo sapiens GN=EMILIN2 PE=1 SV=3
Collagen alpha-1(XI) chain OS=Homo sapiens GN=COL11A1 PE=1 SV=4	Galectin-1 OS=Homo sapiens GN=LGALS1 PE=1 SV=2
Fibrillin-2 OS=Homo sapiens GN=FBN2 PE=1 SV=3	72 kDa type IV collagenase OS=Homo sapiens GN=MMP2 PE=1 SV=2
EMILIN-2 OS=Homo sapiens GN=EMILIN2 PE=1 SV=3	Protein RRP5 homolog OS=Homo sapiens GN=PDCD11 PE=1 SV=3
Galectin-1 OS=Homo sapiens GN=LGALS1 PE=1 SV=2	Latent-transforming growth factor beta-binding protein 1 OS=Homo sapiens
72 kDa type IV collagenase OS=Homo sapiens GN=MMP2 PE=1 SV=2	Fibromodulin OS=Homo sapiens GN=FMOD PE=1 SV=2
Latent-transforming growth factor beta-binding protein 1 OS=Homo sapier	Dermcidin OS=Homo sapiens GN=DCD PE=1 SV=2
Fibromodulin OS=Homo sapiens GN=FMOD PE=1 SV=2	Cartilage-associated protein OS=Homo sapiens GN=CRTAP PE=1 SV=1
Dermcidin OS=Homo sapiens GN=DCD PE=1 SV=2	Prolargin OS=Homo sapiens GN=PRELP PE=1 SV=1
Cartilage-associated protein OS=Homo sapiens GN=CRTAP PE=1 SV=1	Laminin subunit beta-2 OS=Homo sapiens GN=LAMB2 PE=1 SV=2
Prolargin OS=Homo sapiens GN=PRELP PE=1 SV=1	Microfibrillar-associated protein 5 OS=Homo sapiens GN=MFAP5 PE=1 SV=1
Laminin subunit beta-2 OS=Homo sapiens GN=LAMB2 PE=1 SV=2	SPARC OS=Homo sapiens GN=SPARC PE=1 SV=1
Microfibrillar-associated protein 5 OS=Homo sapiens GN=MFAP5 PE=1 SV=	Collagen alpha-1(IV) chain OS=Homo sapiens GN=COL4A1 PE=1 SV=3
SPARC OS=Homo sapiens GN=SPARC PE=1 SV=1	EGF-containing fibulin-like extracellular matrix protein 1 OS=Homo sapiens G
Collagen alpha-1(IV) chain OS=Homo sapiens GN=COL4A1 PE=1 SV=3	Laminin subunit gamma-1 OS=Homo sapiens GN=LAMC1 PE=1 SV=3
EGF-containing fibulin-like extracellular matrix protein 1 OS=Homo sapiens	Neprilysin OS=Homo sapiens GN=MME PE=1 SV=2
Laminin subunit gamma-1 OS=Homo sapiens GN=LAMC1 PE=1 SV=3	Elastin OS=Homo sapiens GN=ELN PE=1 SV=3
Neprilysin OS=Homo sapiens GN=MME PE=1 SV=2	EGF-containing fibulin-like extracellular matrix protein 2 OS=Homo sapiens G
Elastin OS=Homo sapiens GN=ELN PE=1 SV=3	Matrix metalloproteinase-14 OS=Homo sapiens GN=MMP14 PE=1 SV=3
EGF-containing fibulin-like extracellular matrix protein 2 OS=Homo sapiens	Mimecan OS=Homo sapiens GN=OGN PE=1 SV=1
Matrix metalloproteinase-14 OS=Homo sapiens GN=MMP14 PE=1 SV=3	A disintegrin and metalloproteinase with thrombospondin motifs 4 OS=Homo
Mimecan OS=Homo sapiens GN=OGN PE=1 SV=1	Vitronectin OS=Homo sapiens GN=VTN PE=1 SV=1
A disintegrin and metalloproteinase with thrombospondin motifs 4 OS=Ho	Collagen alpha-1(XXI) chain OS=Homo sapiens GN=COL21A1 PE=2 SV=1
Vitronectin OS=Homo sapiens GN=VTN PE=1 SV=1	Sushi repeat-containing protein SRPX OS=Homo sapiens GN=SRPX PE=1 SV=1
Sushi repeat-containing protein SRPX OS=Homo sapiens GN=SRPX PE=1 SV	Chitinase-3-like protein 1 OS=Homo sapiens GN=CHI3L1 PE=1 SV=2
Collagen alpha-1(XXI) chain OS=Homo sapiens GN=COL21A1 PE=2 SV=1	Tenascin-X OS=Homo sapiens GN=TNXB PE=1 SV=4
Chitinase-3-like protein 1 OS=Homo sapiens GN=CHI3L1 PE=1 SV=2	Cell migration-inducing and hyaluronan-binding protein OS=Homo sapiens GN
Tenascin-X OS=Homo sapiens GN=TNXB PE=1 SV=4	Collagen alpha-1(VIII) chain OS=Homo sapiens GN=COL8A1 PE=1 SV=2
Cell migration-inducing and hyaluronan-binding protein OS=Homo sapiens	Collagen alpha-3(V) chain OS=Homo sapiens GN=COL5A3 PE=1 SV=3
Connective tissue growth factor OS=Homo sapiens GN=CTGF PE=1 SV=2	Galectin-3 OS=Homo sapiens GN=LGALS3 PE=1 SV=5
Collagen alpha-1(VIII) chain OS=Homo sapiens GN=COL8A1 PE=1 SV=2	Collagen alpha-1(XVI) chain OS=Homo sapiens GN=COL16A1 PE=1 SV=2
Collagen alpha-3(V) chain OS=Homo sapiens GN=COL5A3 PE=1 SV=3	Metalloproteinase inhibitor 3 OS=Homo sapiens GN=TIMP3 PE=1 SV=2
Hepatoma-derived growth factor OS=Homo sapiens GN=HDGF PE=1 SV=1	Collagen alpha-1(VII) chain OS=Homo sapiens GN=COL7A1 PE=1 SV=2

Leukocyte elastase inhibitor OS=Homo sapiens GN=SERPINB1 PE=1 SV=1
Mesencephalic astrocyte-derived neurotrophic factor OS=Homo sapiens GI
Guanylate-binding protein 1 OS=Homo sapiens GN=GBP1 PE=1 SV=2
Protein CYR61 OS=Homo sapiens GN=CYR61 PE=1 SV=1
Matrix-remodeling-associated protein 5
Galectin-3 OS=Homo sapiens GN=LGALS3 PE=1 SV=5
Collagen alpha-1(XVI) chain OS=Homo sapiens GN=COL16A1 PE=1 SV=2
Metalloproteinase inhibitor 3 OS=Homo sapiens GN=TIMP3 PE=1 SV=2
Pentraxin-related protein PTX3 OS=Homo sapiens GN=PTX3 PE=1 SV=3
Collagen alpha-1(VII) chain OS=Homo sapiens GN=COL7A1 PE=1 SV=2
Interstitial collagenase OS=Homo sapiens GN=MMP1 PE=1 SV=3
A disintegrin and metalloproteinase with thrombospondin motifs 3 OS=Ho
A disintegrin and metalloproteinase with thrombospondin motifs 2 OS=Ho
Metalloproteinase inhibitor 1 OS=Homo sapiens GN=TIMP1 PE=1 SV=1
Spondin-1 OS=Homo sapiens GN=SPON1 PE=1 SV=2
Lactadherin OS=Homo sapiens GN=MFGE8 PE=1 SV=2
Olfactomedin-like protein 3 OS=Homo sapiens GN=OLFML3 PE=2 SV=1
Sushi repeat-containing protein SRPX2 OS=Homo sapiens GN=SRPX2 PE=1 SV=1
Secretoglobin family 1D member 2 OS=Homo sapiens GN=SCGB1D2 PE=2 SV=1
Collagen alpha-2(VIII) chain OS=Homo sapiens GN=COL8A2 PE=1 SV=2
Stromelysin-1 OS=Homo sapiens GN=MMP3 PE=1 SV=2
Cartilage intermediate layer protein 2 OS=Homo sapiens GN=CILP2 PE=2 SV=2
Semaphorin-3C OS=Homo sapiens GN=SEMA3C PE=2 SV=2
Podocan OS=Homo sapiens GN=PODN PE=1 SV=2
Thyroglobulin OS=Homo sapiens GN=TG PE=1 SV=3
Laminin subunit alpha-4 OS=Homo sapiens GN=LAMA4 PE=1 SV=4
Interstitial collagenase OS=Homo sapiens GN=MMP1 PE=1 SV=3
A disintegrin and metalloproteinase with thrombospondin motifs 3 OS=Homo
A disintegrin and metalloproteinase with thrombospondin motifs 2 OS=Homo
Metalloproteinase inhibitor 1 OS=Homo sapiens GN=TIMP1 PE=1 SV=1
Spondin-1 OS=Homo sapiens GN=SPON1 PE=1 SV=2
Lactadherin OS=Homo sapiens GN=MFGE8 PE=1 SV=2
Olfactomedin-like protein 3 OS=Homo sapiens GN=OLFML3 PE=2 SV=1
Sushi repeat-containing protein SRPX2 OS=Homo sapiens GN=SRPX2 PE=1 SV=
Secretoglobin family 1D member 2 OS=Homo sapiens GN=SCGB1D2 PE=2 SV=
Collagen alpha-2(VIII) chain OS=Homo sapiens GN=COL8A2 PE=1 SV=2
Stromelysin-1 OS=Homo sapiens GN=MMP3 PE=1 SV=2
Cartilage intermediate layer protein 2 OS=Homo sapiens GN=CILP2 PE=2 SV=2
Semaphorin-3C OS=Homo sapiens GN=SEMA3C PE=2 SV=2
Podocan OS=Homo sapiens GN=PODN PE=1 SV=2
Thyroglobulin OS=Homo sapiens GN=TG PE=1 SV=5
Laminin subunit alpha-4 OS=Homo sapiens GN=LAMA4 PE=1 SV=4

XI.2. Curriculum

EDUCATION

Master's Degree in Tissue Engineering

Department of Histology, Faculty of Medicine, University of Granada, Spain. 2015

Graduate in Biomedicine

Faculty of Medicine, University of Barcelona, Spain. 2010-2014

PUBLICATIONS

- Jiménez G, López-Ruiz E, Griñán-Lisón C, Antich C, Marchal JA. Brown adipose tissue and obesity. Libro Obesity: A practical guide. Springer (2015) pp 13-28.

- López-Ruiz E, Jiménez G, García MÁ, Antich C, Boulaiz H, Marchal JA, Perán M. Polymers, scaffolds and bioactive molecules with therapeutic properties in osteochondral pathologies: what's new? Expert Opin Ther Pat. (2016) Aug; 26(8):877-90.

- Jiménez G, López-Ruiz E, Antich C, Chocarro-Wrona C, Marchal JA. Models of Disease. Adv Exp Med Biol. (2018) 1059:331-350

- Jiménez G, Cobo-Molinos J, Antich C, López-Ruiz E. Osteoarthritis: Trauma vs Disease.Adv Exp Med Biol. (2018) 1059:63-83.

- J. Melchor, E. López-Ruiz, J. Soto, G. Jiménez, C. Antich, M. Perán, J.M. Baena, J.A. Marchal, G. Rus, In-bioreactor ultrasonic monitoring of 3D culture human engineered cartilage. Sensors and Actuators B: Chemical,(2018) 266:841-852.

- Juan Melchor, Juan M. Soto, Elena López-Ruiz, Suarez J, Jimenez G, Antich C, Perán M, Marchal JA, Rus G. High-Resolution Strain Measurement for Biomechanical Parameters Assessment in Native and Decellularized Porcine Vessels. Mathematical Problems in Engineering (2019) vol. 2019, Article ID 2402606, 14 pages.

- Baena JM, Jiménez G, López-Ruiz E, Antich C, Griñán-Lisón C, Perán M, Gálvez-Martín P, Marchal JA. Volume-by-volume bioprinting of chondrocytes-alginate

bioinks in high temperature thermoplastic scaffolds for cartilage regeneration. Exp Biol Med (2019) Jan;244(1):13-21.

- López-Ruiz E, Jiménez G, Álvarez de Cienfuegos L, Antic C, Sabata R, Marchal JA, Gálvez-Martín P. Advances of hyaluronic acid in stem cell therapy and tissue engineering, including current clinical trials. Eur Cell Mater. 2019 Mar 19;37:186-213

- Jiménez G, Venkateswaran S, López-Ruiz E, Perán M, Pernagallo S, Díaz-Monchón JJ, Canadas RF, Antich C, Oliveira JM, Callanan A, Walllace R, Reis RL, Montañez E, Carrillo E, Bradley M, Marchal JA. A soft 3D polyacrylate hydrogel recapitulates the cartilage niche and allows growth-factor free tissue engineering of human articular cartilage.Acta Biomater. (2019) May;90:146-156.

- Antich C, Vicente J, Jimenez G, Chocarro C, Carrillo E, Montañez E, Gálvez-Martín P, Marchal JA. Bio-inspired hydrogel composed of hyaluronic acid and alginate as a potential bioink for 3D bioprinting of articular cartilage engineering constructs. Acta Biomater. (2020) In press. https://doi.org/10.1016/j.actbio.2020.01.046

CONTRIBUTIONS TO CONGRESS

- VI Jornadas doctorales internacionales: Avances en la Investigación biomédica y biotecnológica. Jaen, Spain. 2019
  Oral communication: Development of bioink based on cell-derived extracellular matrix for cartilage tissue engineering.

- Wake Forest Institute of Regenerative Medicine (WFIRM) Annual Retreat. Pinehurst, USA. 2019
  Poster: Development of bioink based on cell-derived extracellular matrix for cartilage tissue engineering

- I Jornadas de Jóvenes Investigadores. Granada, Spain. 2018
  Poster: 3D bioprinting of tissue constructs for regenerative medicine applications

- III Jornadas de Investigadores en Formación: Fomentando la interdisciplinariedad. Granada, Spain. 2018
  Póster: 3D printing of hyaluronic acid-based constructs for fabrication of articular cartilage

- III Congress of Young Researchers in Biomedicine. Valencia, Spain. 2018
  Póster: Desarrollo de un nuevo sistema de bioimpresión 3D para la regeneración de tejidos y órganos.

- I Jornadas Científicas del Centro de Investigación Biomédica. Granada, Spain. 2017
  Póster: Desarrollo de un nuevo sistema de bioimpresión 3D para la regeneración de tejidos y órganos

- I Jornadas Científicas del Centro de Investigación Biomédica. Granada, Spain. 2017
  Oral communication: Impresión 3D de constructos bioactivos basados en ácido hialurónico para la formación de neocartílago in vitro

- 2nd Annual Conference and Expo on Biomaterials 2017. Madrid, Spain. 2017
  Póster: Design and characterization of bioink with hyaluronic acid for tissue and bone-3D bioprinting

- ISCT 2017 Annual Meeting. London, UK. 2017
  Oral communication: Design of 3d bioprinted articular cartilage of MSCs-loaded for osteochondral injuries

- VII Jornadas Fundación García Cugat de Investigación Biomédica. Valencia, Spain. 2016
  Oral communication: Bioimpresión de un cartílago artificial 3D para la aplicación en ingeniería tisular de lesiones osteocondrales

- CELLS | Musculoskeletal 2016 Conference. Amsterdam, Holand. 2016
  Oral communication: Novel Bioinks in Hyaluronic Acid Hydrogels-Based for Articular Cartilage 3D Bioprinting

ADDITIONAL DATA

- Silver Winner in Wake Forest Institute of Regenerative Medicine (WFIRM) Annual Retreat, Pinehurst, USA. 2019. Póster: A Novel Cell-derived Extracellular Matrix (ECM) Bioink for Cell-based Cartilage Tissue Bioprinting

- Silver Winner in CELLS | Musculoskeletal 2016 Conference. Amsterdam, Holand. 2016. Oral communication: "Novel Bioinks in Hyaluronic Acid Hydrogels-Based for ArticularCartilage 3D Bioprinting"